ARIEL I
The First
International
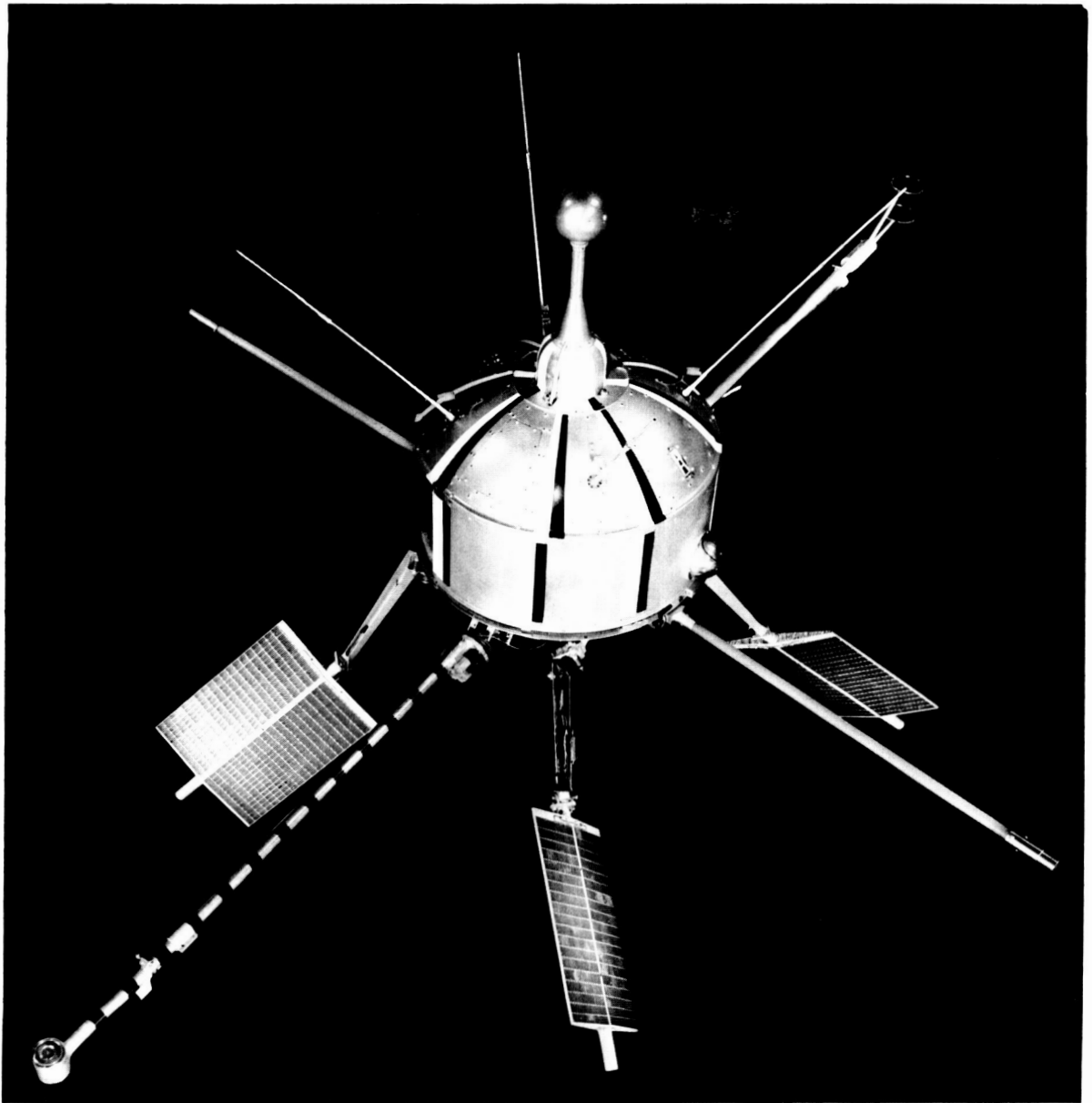# Satellite

NATIONAL AERONAUTICS AND SPACE ADMINISTRATION

ARIE   TIONAL SATELLITE

Ariel I, the International Ionosphere Satellite, in orbit attitude.

ARIEL I

The First

International
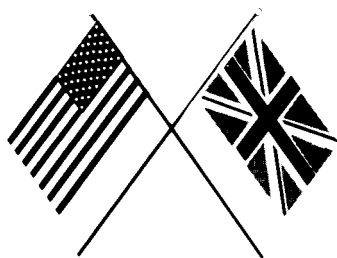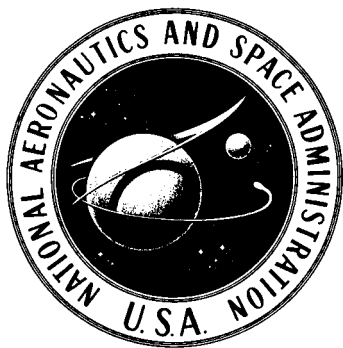
Satellite

The Project Summary

Prepared by
GODDARD SPACE FLIGHT CENTER
Greenbelt, Maryland

FOREWORD

On April 26, 1962, the first international satellite, Ariel I, was successfully launched from Cape Canaveral, Florida. This satellite, designed for ionospheric research, represents two years of cooperative effort between the United Kingdom and the United States. The history of Ariel I and its experiments has been compiled in brief form by members of NASA's Goddard Space Flight Center. This history, consisting of reports and descriptions contributed by the U.K. and U.S. scientists assigned to the Ariel I project, is presented herein as a project summary.

ROBERT C. BAUMANN, *U.S. Ariel I Project Manager*
Goddard Space Flight Center
Greenbelt, Maryland

CONTENTS

Chapter 7

CHAPTER 1

Introduction

PURPOSE OF DOCUMENT

The Ariel I (1962 o1) project summary document has been compiled to record the history of the first international satellite. Herein are described the events leading up to the conception of Ariel I, the technical and management plans used in the project development, the scientific and engineering considerations employed in the design of the satellite and support equipment, and the design details of these components. A list of related documentation containing design information and experimental results is also included.

LIST OF CONTRIBUTORS

This document is a collection of descriptions and reports authored prior to and after the launch of Ariel I (April 26, 1962). These contributions have been edited, revised, and updated to produce continuity. The following list includes the authors who have provided major contributions to this summary.

United Kingdom Contributors

Dr. P. J. Bowen, University College London
Prof. R. L. F. Boyd, University College London
Mr. A. C. Durny, Imperial College London
Prof. H. Elliot, Imperial College London
Dr. K. A. Pounds, University of Leicester
Dr. J. J. Quenby, Imperial College London
Prof. J. Sayers, University of Birmingham
Mr. J. Wager, University of Birmingham
Dr. A. P. Willmore, University College London

United States Contributors

(National Aeronautics and Space Administration, Goddard Space Flight Center)

R. C. Baumann	R. G. Martin
R. E. Bourdeau	W. H. Meyer
A. Buige	M. Schach
P. T. Cole	J. C. Schaffert
C. F. Fuechsel	J. T. Shea
W. H. Hord, Jr.	J. M. Turkiewicz
R. E. Kidwell	C. L. Wagner, Jr.
V. L. Krueger	H. D. White, Jr.
T. J. Lynch	F. C. Yagerhofer

GENERAL INTRODUCTION

Ariel I, the first international satellite, was designed to contribute to man's knowledge of the ionosphere and its complex relation to the sun.

This project developed from proposals made in 1959 to NASA by the British National Committee on Space Research. These proposals were in response to a United States offer to the Committee on Space Research (COSPAR) of the International Council of Scientific Unions to launch scientific experiments or complete satellites prepared by scientists of other nations. The content of the program and the division of responsibility between NASA and the British Committee were agreed during discussions that took place in late 1959 and early 1960. Subsequently, the NASA Administrator assigned project responsibility for the United States to the Goddard Space Flight Center (GSFC).

This assignment included the design, fabrication, integration, and testing of the spacecraft structure, power supply telemetry, command receiver, thermal control, and data storage. GSFC supplied the vehicle, was responsible for launch, performs data acquisition via the worldwide Minitrack network, and provides data processing. The United Kingdom (U.K.) had the responsibility for the design, fabrication, and testing of all flight sensors and their associated electronics up to the telemetry encoder input. The U.K. also is responsible for data analysis and interpretation. The distribution of responsibilities is outlined in Figure 1-1.

A list of the experiments and electronic subsystems follows.
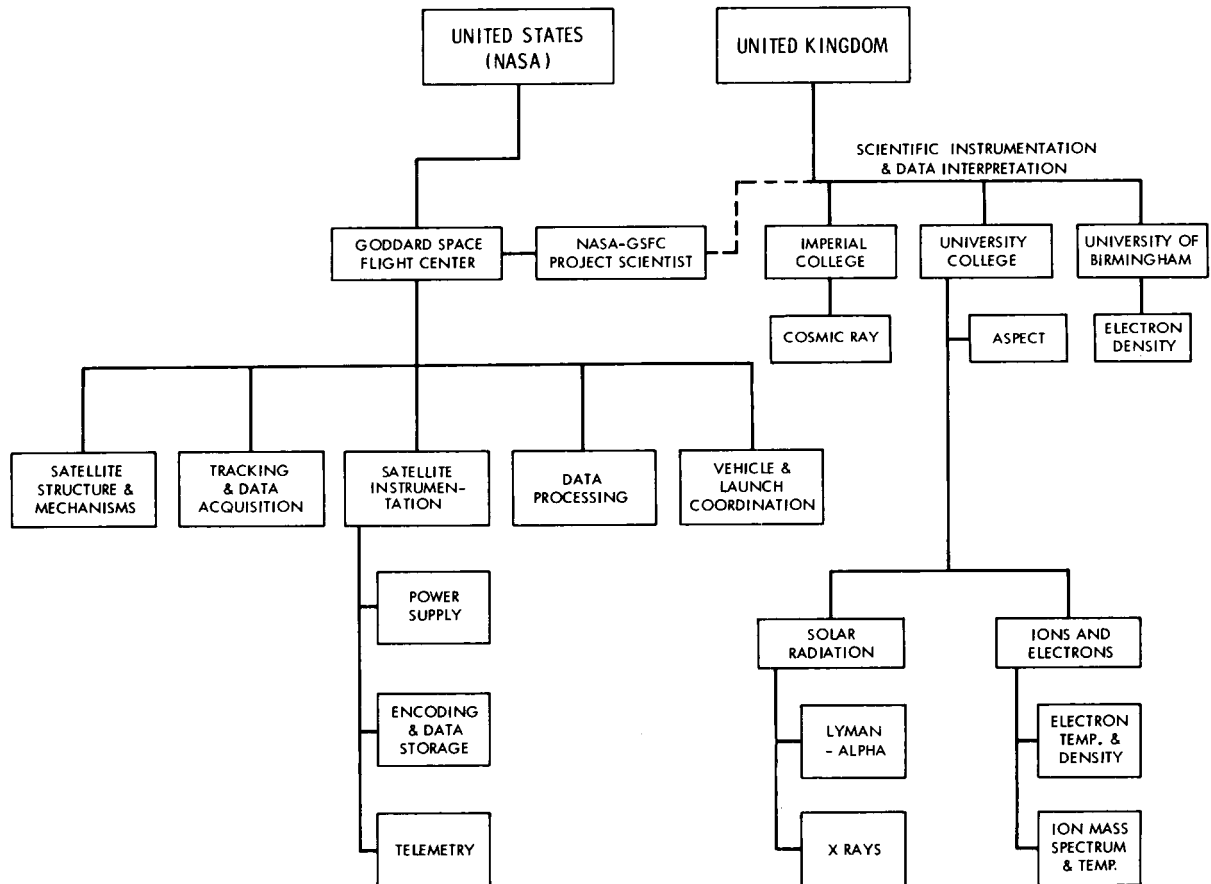
FIGURE 1-1. Prime responsibilities for Ariel I.

Experiments

Electron Temperature and Density—
University College London

This experiment, based on Druyvesteyn's modification of the Langmuir probe, will determine the value of the electron density and temperature near the satellite.

Ion Mass Composition and Temperature—
University College London

This experiment is, basically, the same as the electron temperature experiment. However, the method of measuring the temperature is different.

Solar Lyman-Alpha Emission Measurement—
University College London

Two parts of the solar spectrum were selected for measurement: the Lyman-alpha line of hydrogen, and the rather hard x-ray spectrum. The function of the two solar radiation measurements is to enable simultaneous and nearly

continuous observations of the state of the ionosphere and of the solar atmosphere.

X-Ray Emission—University College London

This experiment provides an indication of solar conditions.

Solar Aspect Measurement—University College London

The solar aspect subsystem provides the latitude and longitude of the sun in the satellite coordinate system. Also, the subsystem provides the satellite spin rate.

Cosmic Ray Analyzer—Imperial College London

The purpose of this experiment is to make accurate measurements of the primary cosmic ray energy spectrum and the effects of interplanetary magnetic field modulation of this spectrum.

Ionosphere Electron Density Measurement—University of Birmingham

The measurement of electron density is performed by this experiment, and by the Langmuir probes of the University College London. However, the two methods of measurement are quite different and therefore complement one another.

Electronic Subsystems

Telemetry—Goddard Space Flight Center
Data Encoders—Goddard Space Flight Center
Tape Recorder—Goddard Space Flight Center
Power System—Goddard Space Flight Center
Spacecraft Parameters (Housekeeping)
 System—Goddard Space Flight Center

Spacecraft and orbital characteristics are detailed in the following list.

Scientific Instrumentation

Electron temperature and density sensors (2)
Ion mass sphere (1)
Solar radiation detectors, Lyman-alpha at 1216A (3)
Solar aspect meter (1)
Electron density sensors (1)
X-ray counters (1)

Spacecraft Characteristics

Size, basic structure—23 inches O.D. by 22 inches high
Weight—136 pounds
Spin rate—36 to 12 rpm throughout life
Lifetime—1 year
Power—p-on-n solar cells and nickel-cadmium batteries
Data Storage—100-minute tape recorder
Antenna—modified crossed dipole
Tracking and data frequency—136.408 Mc nominal

Orbit Parameters

Perigee—390 km (210 nautical miles)
Apogee—1212 km (654 nautical miles)
Inclination—53.86 degrees
Period—100.9 minutes
Eccentricity—0.057

Three complete payloads were constructed: one for prototype testing, a flight model, and a backup in case of malfunction in the first launch attempt. Provision was made for two launching vehicles, including one for backup. Ariel I was launched on April 26, 1962. A cutaway view of the satellite is shown in Figure 1–2.

RELATED WORK

Experiments relating to those in the Ariel I satellite have been performed in sounding rockets and satellites. Future plans include additional experiments in the following fields.

Ion and Electron Studies; Electron Density Measurements

Experiments similar to the ion mass spectrometer, the Langmuir probe, and the electron density experiments were flown successfully by Bourdeau and collaborators on the Explorer VIII satellite (1960 ξ1), which was launched on Nov. 3, 1960. Results have been published in the open literature (References 1 to 5). A spherical ion mass spectrometer was also flown on Sputnik III (1958 δ2) by the USSR (Reference 6).

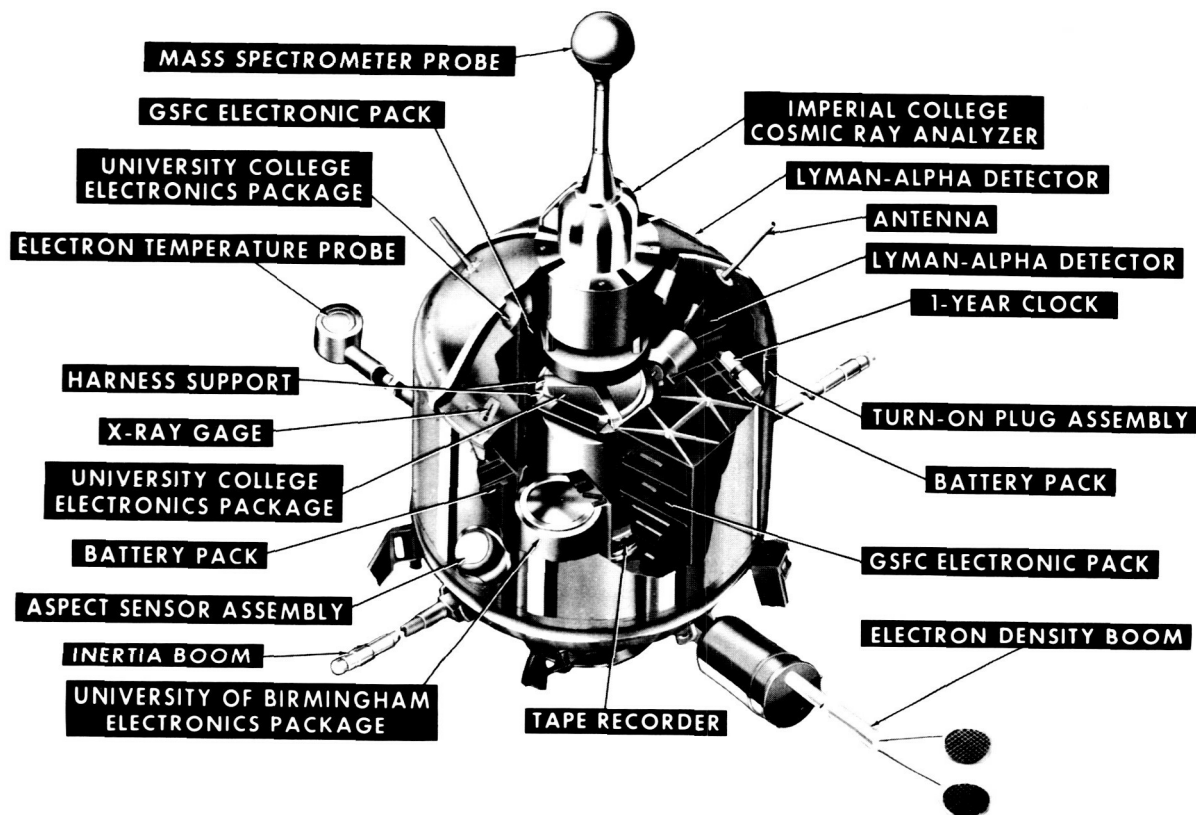NASA plans to use similar experiments on the Atmospheric Structure Satellite and on the EGO and POGO satellites.

MASS SPECTROMETER PROBE

GSFC ELECTRONIC PACK

UNIVERSITY COLLEGE
ELECTRONICS PACKAGE

ELECTRON TEMPERATURE PROBE

HARNESS SUPPORT

X-RAY GAGE

UNIVERSITY COLLEGE
ELECTRONICS PACKAGE

BATTERY PACK

ASPECT SENSOR ASSEMBLY

INERTIA BOOM

UNIVERSITY OF BIRMINGHAM
ELECTRONICS PACKAGE

IMPERIAL COLLEGE
COSMIC RAY ANALYZER

LYMAN-ALPHA DETECTOR

ANTENNA

LYMAN-ALPHA DETECTOR

1-YEAR CLOCK

TURN-ON PLUG ASSEMBLY

BATTERY PACK

GSFC ELECTRONIC PACK

ELECTRON DENSITY BOOM

TAPE RECORDER

FIGURE 1–2. Cutaway view of Ariel I.

Cosmic Ray

The primary purpose of the Ariel I cosmic ray experiment is to carry out a satellite investigation of time variations of heavy nuclei in the primary cosmic radiation with a thin-walled omnidirectional Cerenkov counter. An experiment with a similar objective but using a completely different approach was carried out on Explorer VII (1959 ι1). In this case Pomerantz and Schwed used a thin-walled omnidirectional ionization detector. Again, the primary objective was the satellite investigation of time variation of heavy nuclei. During the eight months of operation of this detector on Explorer VII, significant changes in the spectrum of heavy nuclei were observed.

Detailed accounts of the findings of this satellite can be found in References 7, 8, and 9.

Solar Radiation

The purpose of the x-ray and ultraviolet measurements is to increase knowledge of the sun's ionizing radiations throughout the solar cycle. The measurements of solar radiation are similar to experiments previously performed in space vehicles.

Solar x rays were first quantitively measured in 1949, utilizing thin beryllium-window photocounters in a V-2 rocket flight (Reference 10). The Lyman-alpha line of hydrogen was first detected by Rense in 1952 (Reference 11). Since that time, there have been several dozen measurements of the solar x-ray and hydrogen Lyman-alpha intensities utilizing various rockets: Aerobee-Hi (with solar pointing controls), Nike-Deacon, and Nike-Asps. In addition, experiments have been flown on Explorer VII, the Naval Research Laboratory Greb satellites, and on the Orbiting Solar Observatory (1962 ζ1); these include radiation measurements of both the "quiet" and "active" sun. A survey of the results of measurements of the sun's ionizing radiations is given by Friedman in Reference 12.

The Orbiting Solar Observatory II (OSO II) satellite scheduled for 1963 will continue

measurements of solar x-ray and ultraviolet radiations. This OSO series of satellites will make the most comprehensive coverage of the solar electromagnetic radiations ever attempted. For example, experiments will be flown to measure the 2500 to 3000A band, hydrogen Lyman-alpha line, 400 to 10A band (with 1A resolution), 1 to 8A region, 100 kev to 3 Mev gamma rays (100 kev to 1.5 Mev with 100 kev resolution), and 50 to 500 Mev gamma rays.*

RELATED DOCUMENTS

In addition to the specific reports referenced in the text, there are many reports relating to the design, development, and experimental measurements of Ariel I. The reference and bibliography list at the end of this summary report gives the specific reports referenced herein as well as an additional bibliography of related documents.

*For additional information, refer to the GSFC OSO II Project Development Plan.

CHAPTER 2

Management Plan

APPROACH

The approach of the Ariel I project management utilized a concept of a joint United States–United Kingdom working group with various ad hoc committees named as required. The basic Ariel I working group membership was as follows:

United Kingdom

University of Birmingham   *Electron Density*

Professor J. Sayers   Project Scientist

University College London   *Cosmic Ray*

Dr. H. Elliot   Project Scientist
Dr. J. J. Quenby   Alternate

Imperial College London   *All Other Experiments*

Dr. R. L. F. Boyd   Project Scientist
Dr. A. P. Willmore   Alternate
Mr. M. O. Robins   U.K. Project Manager
Dr. E. B. Dorling   U.K. Coordinator

United States

National Aeronautics and Space Administration
NASA Headquarters:

Dr. J. E. Naugle   U.S. Project Officer
Mr. M. J. Aucremanne   U.S. Project Chief

Goddard Space Flight Center:

Mr. R. C. Baumann   U.S. Project Manager
Mr. R. E. Bourdeau   Project Scientist
Mr. J. T. Shea   U.S. Coordinator
Mr. H. J. Peake   Telemetry RF

Dr. R. W. Rochelle   Telemetry coding
Mr. J. C. Schaffert   Sequence programming
Mr. P. T. Cole   Data storage
Mr. C. L. Wagner   Mechanical design
Mr. F. C. Yagerhofer   Power supply
Mr. M. Schach   Thermal design
Mr. W. H. Hord   Environmental testing
Mr. J. M. Turkiewicz   Electrical systems integration
Mr. C. H. Looney   Tracking systems
Mr. H. E. Carpenter   Tracking operations
Mr. C. J. Creveling   Data reduction
Mr. A. Buige   Operations control

Mr. C. P. Smith   Atlantic Missile Range, Vehicle Coordination
Mr. R. H. Gray   Atlantic Missile Range, Operations and Launch Director

ASSIGNMENTS

Management responsibility for the Ariel I project was assigned as follows.

Project Management

NASA's Goddard Space Flight Center was assigned project management responsibilities for the Ariel I project.

Experiments System Management

The United Kingdom Scientific Mission accepted system management responsibilities for the Ariel I experiments system.

Spacecraft System Management

Goddard Space Flight Center was assigned system management responsibilities for the Ariel I spacecraft system.

Tracking and Data System Management

Goddard Space Flight Center was assigned system management responsibilities for the Ariel I tracking and data system. Acquired data are sent to the United Kingdom after processing (digitizing), and the U.K. is responsible for data reduction and analysis.

NASA Headquarters Direction

The Director, Office of Space Sciences. NASA Headquarters, is responsible for overall direction and evaluation of the performance of the Goddard Space Flight Center as the Ariel I Project Management Center and as the Systems Management Center for the spacecraft and the tracking and data systems.

The Director, Office of International Programs, NASA Headquarters, is responsible for defining and interpreting international agreements relating to the project and for providing the United States (NASA) coordination with the United Kingdom.

Each country has an Ariel I Project Manager, Project Coordinator, and Project Scientist. All working decisions are subject to the approval of the Project Managers. Responsibility for the coordination of the many aspects of the overall program is vested in the Project Coordinators. The Project Scientists are responsible for the ultimate compatibility and integration of the various experiments. Overall policy matters are decided by the NASA Administrator for the United States and by the Chairman of the British National Committee for Space Flight for the United Kingdom.

In the case of subsystems, the work (and contract monitoring) was the responsibility of the individual in charge of the subsystem.

SCHEDULE

The major phases planned and accomplished throughout the program are shown in Figures 2-1 and 2-2. Key milestones in the Ariel I project are reported in the Program Management Plan, described in the next section.

REPORTING PROCEDURES

Reports indicating progress in accomplishing the scheduled milestones and summarizing the project status were furnished by GSFC to NASA Headquarters on a biweekly basis as required by NASA Management Instruction G–2–3, "Program Management Plans." The U.S. Project Manager submitted to the Director, GSFC, each week a written report that described significant events occurring on the project, highlighted problem areas, and indicated any assistance that was required.

Periodic presentations on the Ariel I project are made to the GSFC Executive Council. This group, chaired by the Director of GSFC, is composed of top management officials. The presentations cover all significant aspects, such as funding, procurement, etc. Emphasis is placed on defining problem areas and applying necessary measures to resolve them.

The U.S. Project Manager makes monthly submissions of data for the NASA Administrator's progress report. Such data include the progress made on Ariel I project objectives during the previous month, progress made during current month, and plans for the coming month.

The U.S. Project Manager is responsible for the preparation of semiannual budget reports on his project.

PROCUREMENT

All procurement in the U.S. was handled according to normal GSFC procedures. A singlepoint procurement contract system was used.
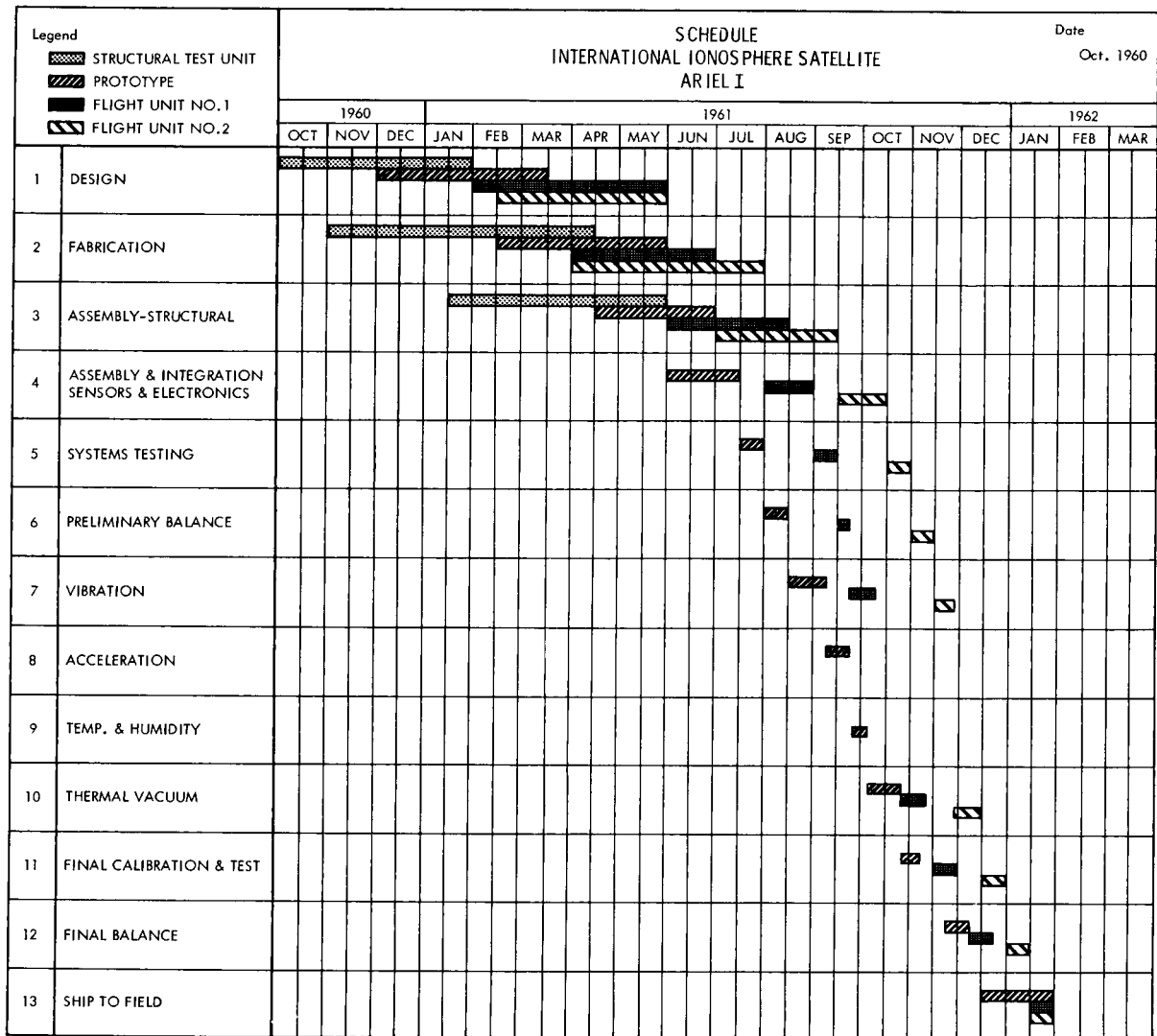
8

FIGURE 2–1. Planned program schedule.

ARIEL I: THE FIRST INTERNATIONAL SATELLITE

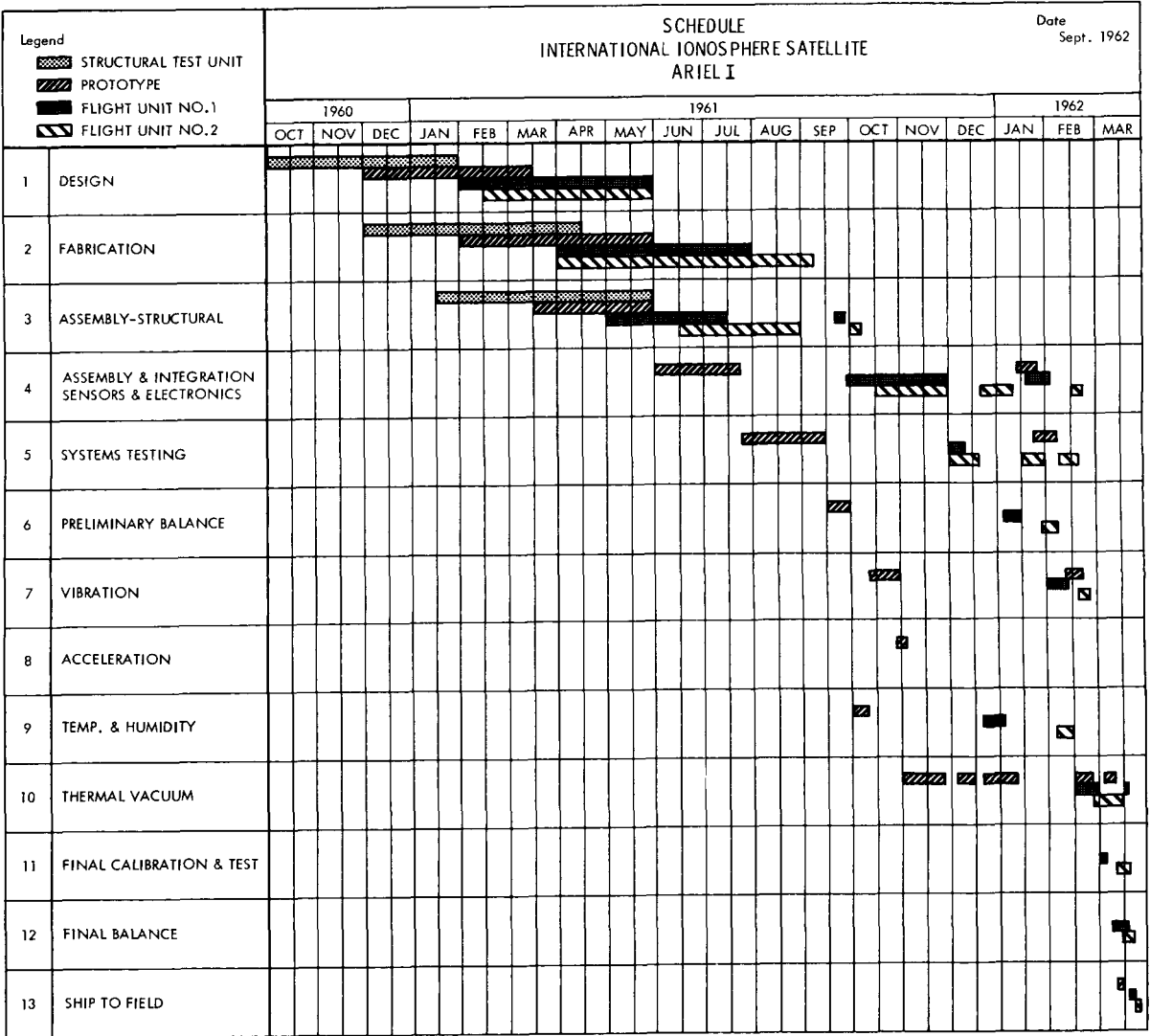| Legend	SCHEDULE INTERNATIONAL IONOSPHERE SATELLITE ARIEL I																		Date Sept. 1962	
▓▓▓ STRUCTURAL TEST UNIT ▨▨ PROTOTYPE ■■ FLIGHT UNIT NO.1 ◪◪ FLIGHT UNIT NO.2																				
	1960			1961												1962				
	OCT	NOV	DEC	JAN	FEB	MAR	APR	MAY	JUN	JUL	AUG	SEP	OCT	NOV	DEC	JAN	FEB	MAR

1	DESIGN
2	FABRICATION
3	ASSEMBLY-STRUCTURAL
4	ASSEMBLY & INTEGRATION SENSORS & ELECTRONICS
5	SYSTEMS TESTING
6	PRELIMINARY BALANCE
7	VIBRATION
8	ACCELERATION
9	TEMP. & HUMIDITY
10	THERMAL VACUUM
11	FINAL CALIBRATION & TEST
12	FINAL BALANCE
13	SHIP TO FIELD

FIGURE 2–2. Actual program schedule.

10

CHAPTER 3

General Technical Plan

BACKGROUND AND PURPOSE

In determining the experiments to be carried out by Ariel I, every effort was made not to duplicate experiments already performed or underway by the U.S. and Russia. Simultaneously, experiments were selected to (1) take advantage of techniques developed in the U.K. as part of the Skylark sounding rocket program, and (2) provide an integrated assault on unknowns connected with the sun-ionosphere relation.

Of the *six* specific experiments carried on board, five are closely interrelated and provide concurrent measurement of two important types of solar emission and the resulting changing states of the ionosphere.

Of these *five*, the three ionospheric experiments measured electron density and temperature as well as the composition and temperature of positive ions. The remaining two experiments monitored the intensity of radiation from the sun in the ultraviolet (Lyman-alpha) and x-ray bands of the solar radiation spectrum. Lyman-alpha radiations originate in the sun's chromosphere (solar surface), while x-rays originate farther out in the area around the sun known as the corona. Previous work has shown that the Lyman-alpha radiation is relatively constant but that x-ray emissions are quite variable with solar conditions.

The *sixth* experiment measured primary cosmic rays by means of a Cerenkov detector carried on board the Ariel I. Simultaneously, measurements of secondary cosmic rays were made by means of ground observation and by means of aircraft, balloons, etc.

ARIEL I CONFIGURATION

Figures 3–1, 3–2, and 3–3 provide essential major component outlines and relative positions for Ariel I. Its basic configuration, which must fit the envelope of the Delta vehicle's payload compartment, is that of a cylinder $10^{1}\!/_{16}$ inches long and 23 inches in diameter. The main element of each closure is a spherical section whose large (inboard) terminator circle is $8\!/_{16}$ inches in diameter. Each spherical section is $5\!/_{4}$ inches long and has an outer surface radius of curvature of $13\!/_{2}$ inches. To this basic 22-inch-high configuration are attached the various elements necessary for the support and conduct of the several experiments incorporated in the system.

The spin axis of the satellite is the central axis of the cylinder, which—for purposes of this description—is also considered as the vertical axis. At the bottom of the satellite is a $9\!/_{8}$-inch-diameter fourth-stage separation flange, within which is mounted the electron temperature gage and the tape recorder.

Extending out horizontally from about midway up the lower spherical section, at 90 degree intervals around the circumference of the satellite, are four solar paddles.

Offset 45 degrees circumferentially from solar paddles, opposite and exactly counterbalancing one another, and extending radially in the same horizontal plane are two booms with nominal lengths of 4 feet. The end of one boom accommodates the two circular capacitor plates of the electron density sensor. Electronics associated with this experiment are housed in a $4\!/_{4}$-inch-diameter by $6\!/_{4}$-inch-long cylinder mounted on the boom close to the main body of the satellite. At the end of the
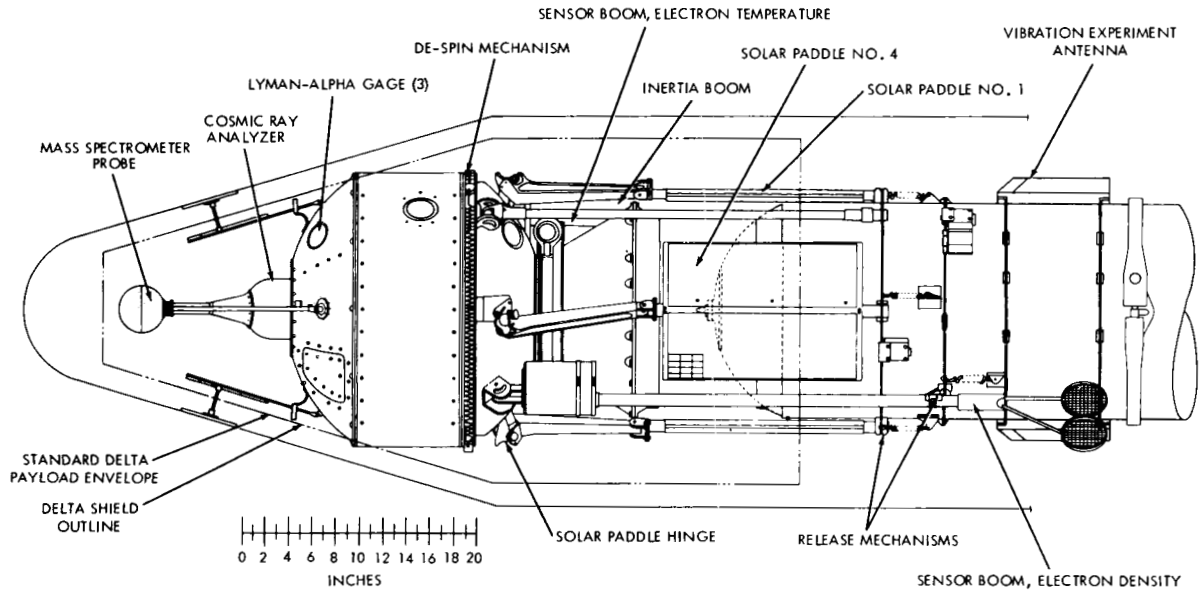
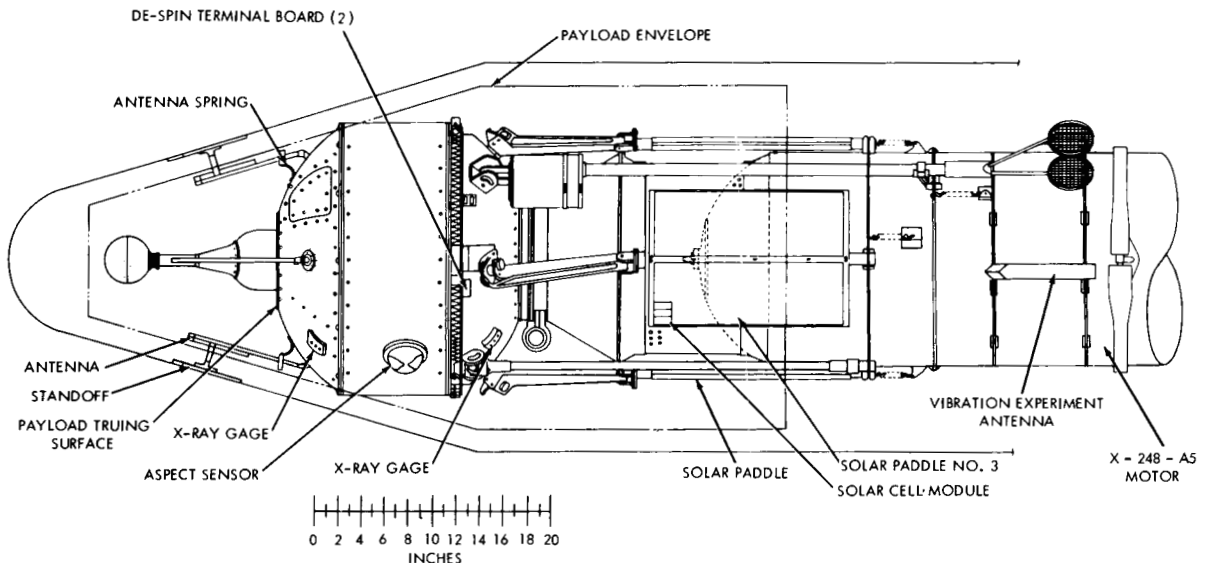FIGURE 3–1. Ariel I satellite—Delta vehicle compatibility, view 1.

FIGURE 3–2. Ariel I satellite—Delta vehicle compatibility, view 2.

other boom is a second electron temperature gage, whose electronics are located inside the satellite.

With the exception of a 3½-inch-diameter hemispherical solar aspect sensor, the central cylindrical section is free of protuberances.

On top of the satellite, in line with the spin axis, is a 5-inch-diameter cylinder containing the cosmic ray Cerenkov detector. Above this,

on an 8-inch-long conical and cylindrical section tapering from a 3-inch to 1-inch diameter, is a 4-inch-diameter ion mass sphere whose center of mass is located 14 inches above the forward face of the main body.

Four turnstile antennas, spaced circumferentially at 90 degrees and angling up at 45 degrees, are mounted on the top spherical section and are perpendicular to the sphere at the interfaces.
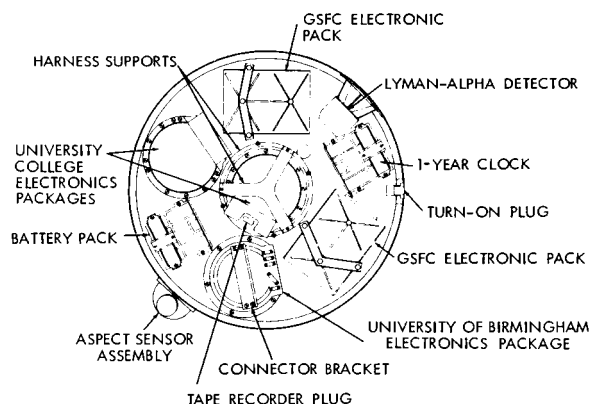
12

FIGURE 3-3. Ariel I satellite main shell, plan view.

There are three flush-mounted solar radiation (Lyman-alpha) detectors on the satellite skin:

two at 60 degrees (one up and one down) from the equator, and one on the equator. All three are in the same vertical plane and in the same 180-degree sector. There are two proportional x-ray counters located 45 degrees up and down from the equator and directly opposite the Lyman-alpha gages.

ARIEL I CIRCUITRY

The electronic circuitry is, in general, covered by the functional diagram of Figure 3-4 and produces the signals described in Figure 3-5. The United Kingdom supplied all equipment listed under the probes and conditioning circuits of Figure 3-4, while GSFC provided all other subsystems.
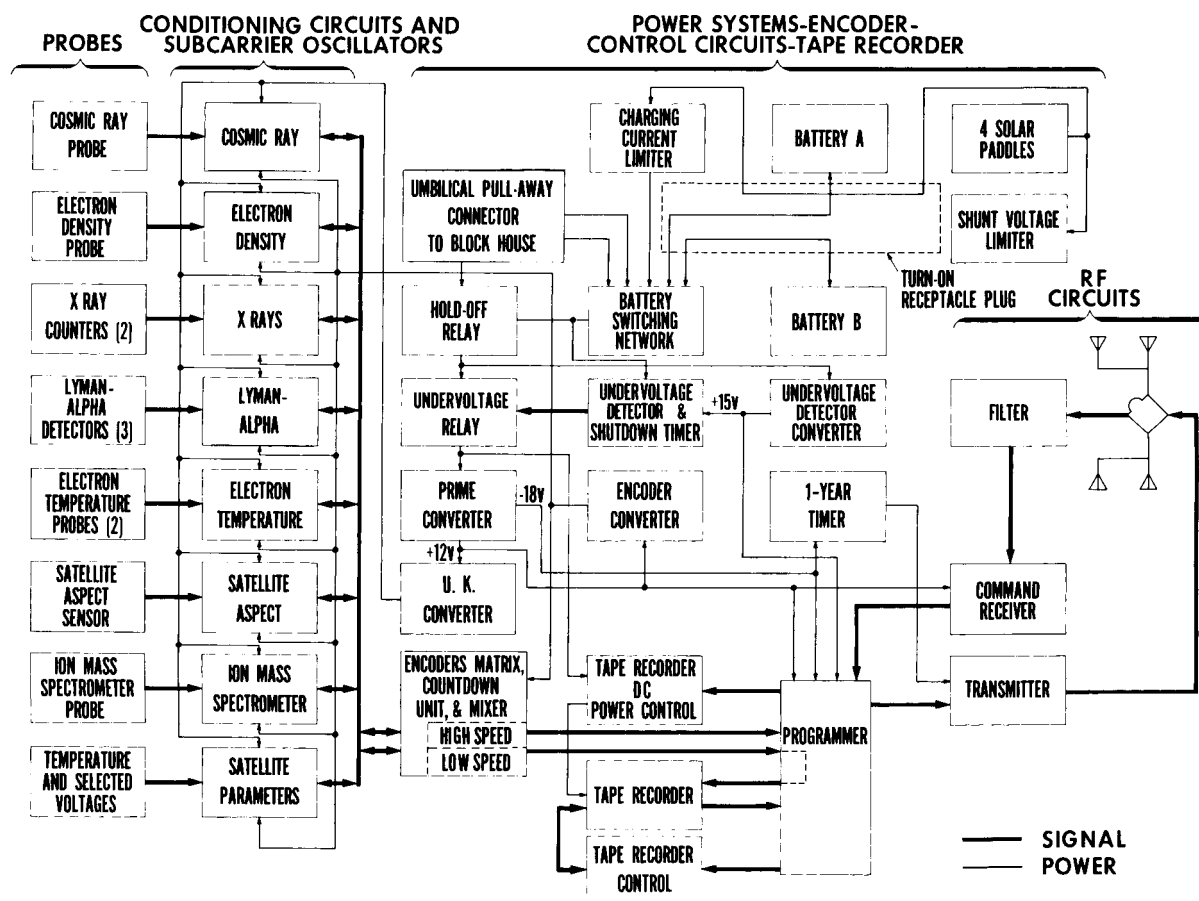

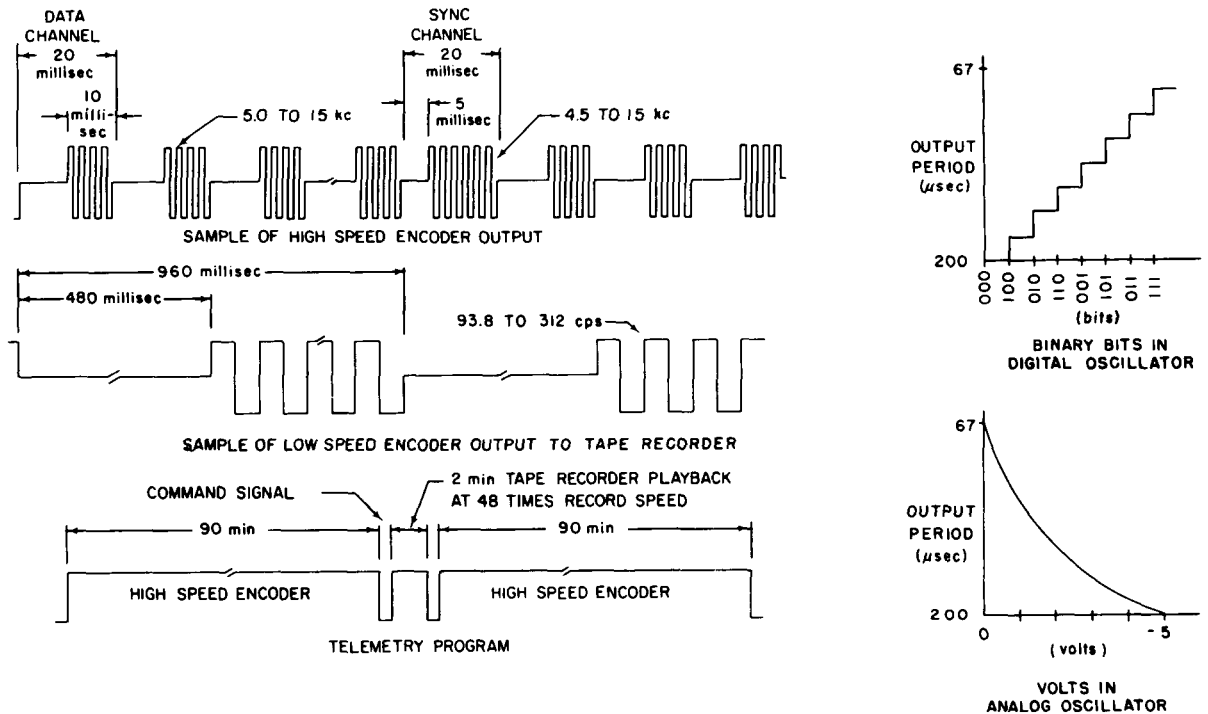FIGURE 3-4. Ariel I functional diagram.

13

FIGURE 3–5. Ariel I telemetry program.

ARIEL I LAUNCH SEQUENCE

The sequence of events from nose cone ejection to satellite separation is:

1. Nose cone ejection

2. Second-stage burnout

3. Second and third-stage coast and yaw until peak of ascent path is reached and vehicle is aligned with its programmed attitude

4. Third-stage spin up to approximately 160 rpm and ignition

5. Second-stage separation and retrorockets fired

6. Burnout of third stage

7. Coast to allow outgassing (thrust) of the third stage to cease

8. De-spin of the third-stage—payload combination (first de-spin) to 76.5 rpm, by releasing "yo-yo" de-spin device

9. Release and erection of experiment booms (second de-spin) and de-spin to 52.4 rpm

10. Release and erection of the inertia booms and paddles, de-spin (third de-spin) to 36.6 rpm

11. Separation of the payload from the third stage at a differential velocity of 7 ft/sec

12. Final rate of spin at the end of 1 year should not be less than 12 rpm

14

CHAPTER 4

United Kingdom Experiments

LANGMUIR PROBE FOR MEASUREMENT OF ELECTRON TEMPERATURE AND DENSITY

Project Scientists

Dr. R. L. F. Boyd, University College London
Dr. A. P. Willmore, University College London

Project Engineers

Dr. P. J. Bowen, University College London
Mr. J. Blades, Pye Ltd., Cambridge
Mr. R. Nettalship, Pye Ltd., Cambridge

The Experiment

This experiment, based on Druyvesteyn's modification of the Langmuir probe, determines the local value of the electron density and temperature near the satellite. At heights well above the F-2 maximum, the ionization is probably in diffusive equilibrium, so that the variation of density with height can be related to the temperature and composition of the plasma. Moreover, it is very probable that temperature equilibrium is closely approximated between the electrons and the positive ions. Thus, the two measurements made in this experiment are related. When they are combined with those from the positive ion mass spectrometer probe—which enables the positive ion temperature and composition to be obtained, it should be possible to study in a comprehensive way the departures from thermal equilibrium and diffusive equilibrium in the atmosphere.

Since the probe is negative with respect to its local ambient atmosphere (potential of which, relative to the vehicle, will be called "space potential"), the density of the electrons is obtained by Boltzmann's relation as:

$$n_e = n_{e0} e^{-\frac{eV_p}{kT_e}},$$

where n_{e0} is the density far from the vehicle, V_p is the magnitude of the probe potential with respect to space, and T_e is the electron temperature.

Thus the current collected by the probe is:

$$i_p = i_0 e^{-\frac{eV_p}{kT_e}},$$

where $i_0 = (2nk/m)\ T_e n_{e0} A$ (A being the probe area).

In order to measure T_e and i_0, from which n_{e0} can also be calculated, a composite sweep wave form consisting of (1) a slow sawtooth wave, (2) a 500-cps sine wave whose amplitude is about kT_e/e, and (3) a 3.5-kc sine wave also of amplitude kT_e/e is applied to the probe.

Because the characteristic is exponential and nonlinear, the probe current contains not only 500-cps and 3.5-kc components, but also harmonics and cross-modulation terms. The cross-modulation component, which is a 3.5-kc wave modulated by 500 cps, is extracted by means of a tuned amplifier; and the carrier and the modulation are separated and measured by phase-sensitive rectifiers. The carrier component is used to derive an AGC feedback voltage that maintains the carrier amplitude at the detector constant. Then the control voltage is a nearly logarithmic function of the carrier amplitude in the probe current. Now it is easy to see that the carrier amplitude is a function of di_p/dV_p and that the rectified 500-cps voltage is a function

of d^2i_p/d^2V_p divided by di_p/dV_p. The latter quantity depends on eV_1/kT_e, where V_1 is the amplitude of the 500-cps modulating voltage, while the former gives i_p (once T_e is known).

The function of the slow sweep, which has an amplitude of several volts, is simply to in-sure that the probe is sometimes a volt or so negative with respect to space. Space potential can be recognized as being very nearly the potential at which $d^2i_p/dV_p{}^2=0$; and thus the value of V_p corresponding to the measurement of i_p is known. This gives i_o and hence n_{eo}.
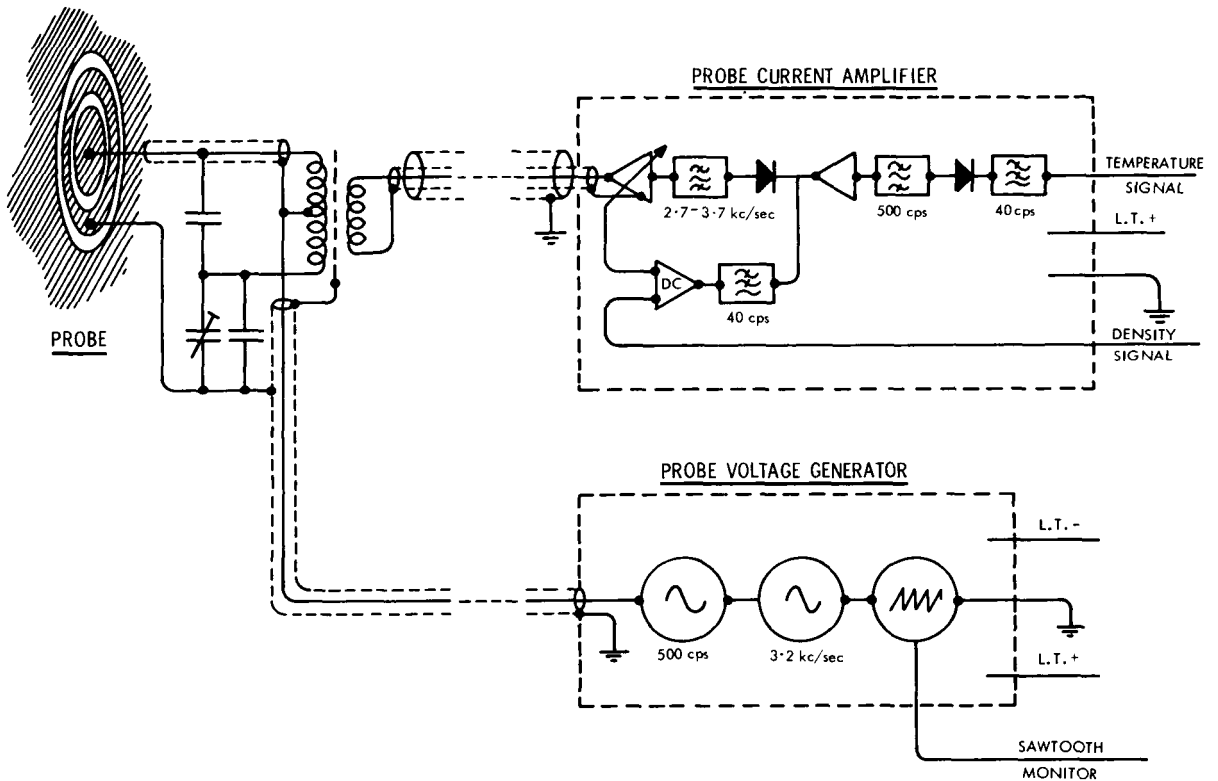

FIGURE 4–1. Electron density and temperature probe, block diagram.

A block diagram of the circuit is shown in Figure 4–1. The probe is a small disk, 2 centimeters in diameter, surrounded by a guard ring. This has the dual purpose of reducing edge effects arising from the fact that the satellite skin is not at probe potential and of reducing the stray capacitance from the probe to ground. (A similar probe constructed for Skylark is shown in Figure 4–2.) The tuned input transformer of the amplifier is mounted behind the probe. The waveform generators and amplifiers are mounted on a 5½-inch card in the interior of the vehicle.

When direct transmission of telemetry data is being used, the modulation depth, carrier amplitude, and a sawtooth voltage are all trans-mitted over the complete probe curve, together with a monitor representing the amplitude V_1. In this case, the complete probe curve can be reconstructed, thus enabling a cross-check of electron temperature to be obtained. The low data rate of the tape store makes it impossible to record the probe curves in this way, so the curves are sampled at two points whose co-ordinates are recorded. The first chosen is the space potential point where $d^2i_p/dV_p{}^2=0$. A trig-ger circuit produces a sampling pulse as the sign of the second derivative reverses (and the phase of the 500-cps wave changes by 180 degrees), and a gate stores the value of the sawtooth and the carrier amplitude in capacitor stores. These values are read out by the telemeter.

16

FIGURE 4–2. Similar electron density probe constructed for Skylark rocket.

Then, when di_p/dV_p reaches a predetermined amplitude, which is set at the lowest value consistent with swamping amplifier noise, a second sampling pulse is generated; and the values of di_p/dV_p, V_p, and the modulation depth are all stored and in due course read out. Thus, there is recorded the space potential, modulation depth or electron temperature, and two points on the first derivative curve.

As there are in all four ionospheric sensors being swept in potential, the effects of mutual interference are being reduced by operating them synchronously. For this purpose, a trigger pulse is obtained from the encoder. The circuitry operates entirely from ± 6.5 volt lines, the total power dissipation being 75 milliwatts.

This experiment is duplicated in the satellite to check the validity of the assumption that the ambient electron density is not greatly affected by the motion of the vehicle. Both probes are mounted with the normal to the probe surface parallel to the spin axis so as to minimize spin modulation of the probe current. One sensor is located inside the separation ring, facing backward from the launch direction, and the other is on the end of the balance boom opposite to that carrying the dielectric experiment, facing forward.

SPHERICAL PROBE FOR MEASUREMENT OF ION MASS COMPOSITION AND TEMPERATURE

Project Scientists

Dr. R. L. F. Boyd, University College London
Dr. A. P. Willmore, University College London

Project Engineers

Dr. P. J. Bowen, University College London
Mr. J. Blades, Pye Ltd., Cambridge
Mr. R. Nettalship, Pye Ltd., Cambridge

The Experiment

The principle of this experiment is somewhat similar to the Langmuir probe. It can be shown that, if the current to a probe immersed in an isotropic plasma is i_p at potential V_p and the energy distribution function of the charged particles is $f(E)$, then

$$\frac{d^2 i_p}{dV_p{}^2} \alpha^e V_p{}^{-1/2} f(E).$$

Thus, by applying a slow sweep voltage V_p and by applying two sine waves of differing frequencies in the manner of the electron energy probe to obtain $d^2 i_p/dV_p{}^2$, the energy distribution function $f(E)$ can be constructed.

If V_p is positive, this distribution function will be that of the positive ions. However, the positive ion current is, in practice, swamped by the electron current; and the probe must be covered with a grid at a negative potential so that these are biased off. If a spherical probe is used, it is no longer necessary that the distribution function be isotropic. In this case it is easy to show from considerations of the conservation of energy and angular momentum that the presence of the grid will not affect the measurements. Thus, with such a probe the energy distribution of the positive ions can be determined.

If the temperature of the positive ions were very low, they would appear at the satellite as a homogeneous stream moving with the satellite speed v_s. Thus, they would have an energy $E = 1/2 m v_s{}^2$. Thus, the energy distribution function consists of peaks corresponding to the mass spectrum of the ions. In fact, the thermal

velocities are not negligibly small; and, in consequence, the peaks are broadened to an easily measurable extent. The result is to degrade the mass resolution but to enable making a measurement of the ion temperature.

The basic problem of this experiment, then, is identical with that of the electron temperature measurement, namely, the determination of d^2i_p/dV_p^2. The principal difference is in the construction of the probe, which is shown in Figure 4–3. The inner electrode is the probe
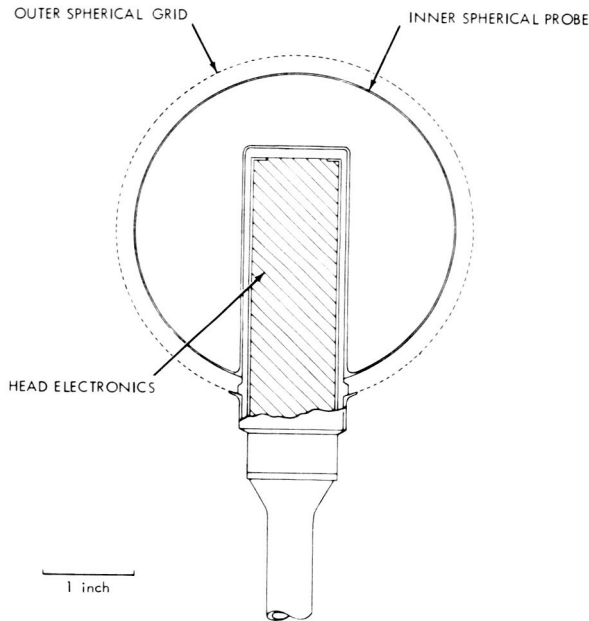

FIGURE 4–3. Sectional view of mass spectrometer probe.

proper, a sphere 9 centimeters in diameter. This is surrounded by a concentric spherical grid of nickel foil 0.1 millimeter in thickness, pierced with 0.5-millimeter holes. The diameter of the grid is 10 centimeters. The grid both serves to repel electrons and acts as an electrostatic shield for the inner electrode. Figure 4–4 is a photograph of this probe as flown on the Black Knight rocket. By making the sphere rather large in comparison with the Langmuir probe, it is possible to obtain probe currents that are not greatly different in the two cases; and in consequence the same circuitry serves for both with only slight modifications, the amplitudes of the sine waves and the input impedance of the tuned amplifier

FIGURE 4–4. Mass spectrometer probe as flown on Black Knight rocket.

being different. The shape of the energy distribution curve is transmitted by direct telemetry but is not recorded.

The probe is mounted on the spin axis, to reduce spin modulation of the probe current. It is carried on a thin tubular support as far from the vehicle as possible—namely, some 10 centimeters in front of the cosmic ray package on which it is supported.

MEASUREMENT OF SOLAR LYMAN-ALPHA EMISSION

Project Scientists

Mr. J. A. Bowles, University College London
Dr. A. P. Willmore, University College London

The Experiment

The function of the two solar radiation experiments is to enable making simultaneous and nearly continuous observations of the state of the ionosphere and of the solar atmosphere, so as to investigate in detail this aspect of the solar-terrestrial relations. To this end, two parts of the solar spectrum have been selected: one where the radiation originates at a low altitude in the chromosphere, and the other in the corona. These are, respectively, the Lyman-alpha line of hydrogen and the rather hard x-ray spectrum. The latter radiation is also emitted from the high-temperature dis-

turbed regions of the corona. The density measurement is made by means of the nitric oxide ionization chambers designed by Dr. H. Friedmann of the U.S. Naval Research Laboratory, Washington, D.C. These chambers are sensitive in the wavelength region 1100 to 1350A, where nearly all the energy in the solar spectrum is concentrated in the Lyman-alpha line. The chambers are mounted, as shown in Figure 4–5, on a molded nylon support cone
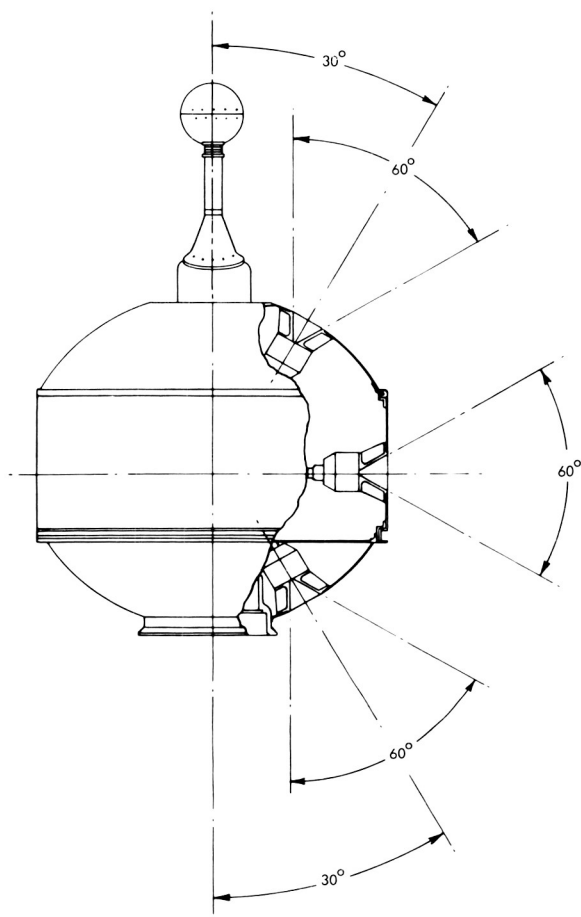

FIGURE 4–5. Mounting of Lyman-alpha detectors.

that restricts the field of view to 60 degrees. Three such chambers are used, mounted at angles of 30, 90, and 150 degrees to the spin axis so that the array covers the whole sky— one in each revolution of the satellite, with nearly constant sensitivity.

The ionization current produced by solar radiation is approximately 5×10^{-8} ampere.

This current is amplified by a transistor chopper amplifier, and the peak value of the current in each revolution is stored in a capacitor having a storage charge time constant of 200 seconds. This store is sampled by both low and high speed encoders. The electronic module card shown in Figure 4–6 operates from -6.5 volts, 1.5 milliamperes, and a bias line of -14 volts.
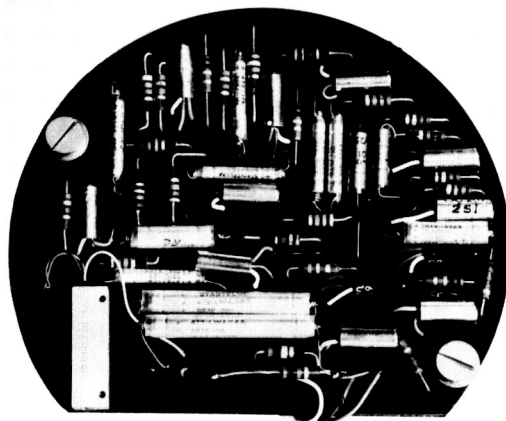

FIGURE 4–6. Electronic card for Lyman-alpha emission experiment.

MEASUREMENT OF THE X-RAY EMISSION FROM THE SUN IN THE 3 TO 12A BAND

Project Scientists

Dr. R. L. F. Boyd, University College London
Dr. K. A. Pounds, University of Leicester
Dr. A. P. Willmore, University College London

Project Engineers

Mr. J. Ackroyd, Bristol Aircraft Company
Dr. P. J. Bowen, University College London
Mr. P. Walker, Bristol Aircraft Company

The Experiment

The wavelength region selected for this observation is 3 to 12A, in which the solar emission is highly variable and is a sensitive indication of solar conditions. The circuitry has been designed, for this reason, to have a wide dynamic range. The radiation detectors are proportional counters, filled with argon and methane as a quenching gas, and using 25μ beryllium windows, which have a high quantum

efficiency in the 3 to 12A region. Each counter has three windows, each 0.5 millimeter in diameter. The windows are spaced at 30 degree intervals round the circumference, giving the counter a field of view of 90 degrees in the plane normal to its axis, without the radiation angle of incidence exceeding 15 degrees. This condition of nearly normal incidence is necessary because, near the cutoff at 13A, the transmission of the window varies rapidly with angle of incidence. Two such counters are used, with matched characteristics, mounted at "latitudes" (reckoned as though the spin axis of the satellite were comparable with that of the earth) of ± 45 degrees, so that the whole sky is covered once in each revolution. Each counter is fitted with a mask that restricts the field of view in the longitudinal direction, so that the two counters together have a field of view which is a sector of 30-degree included angle.

A block diagram of the circuitry is shown in Figure 4–7. The counter is supplied from an extra high tension (EHT) generator, which is a dc to dc converter operating from -6.5 volts and producing 1600 volts; this is stabilized by a corona discharge tube. The counter pulses are fed by a gain-stabilized linear amplifier to a discriminator with a variable bias level. The discriminator output passes through a gate to a 15-stage binary counter capable of counting equally spaced pulses at 1 megacycle.

The gate circuit is operated by a 1-second pulse from the high speed encoder, so timed that the scaler read-out always occurs in the "off" period of the gate. Closing the gate also operates a staircase generator, which produces a waveform of five equal steps used to obtain the discriminator bias level. Thus, the discriminator automatically moves on at the end of each counting period to the next wavelength interval, until the range from 3 to 12A has been covered in five steps of equal quantum energy interval, after which the process is repeated.

In general, the sun is expected to be in the field of view for a time rather shorter than 1
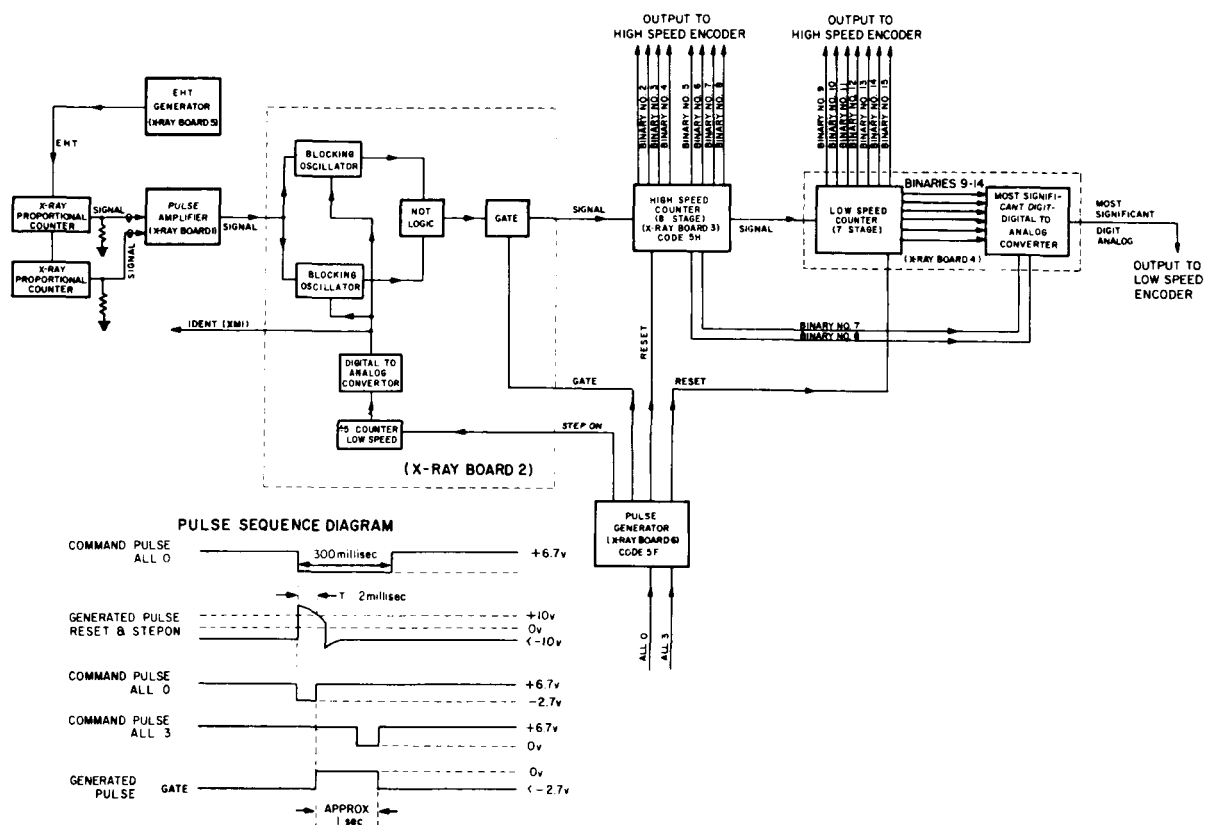

FIGURE 4–7. Block diagram of x-ray spectrometer circuit.

second, so that the effective counting time is less than 1 second. The actual time will be determined from a spin rate measurement. Moreover, there is only a 1:12 chance that the sun will be in the field of view in any given gate period. Thus, the counters do not only observe the sun but also the background radiation from the rest of the sky. On an average, 5×12—or 60—telemeter periods of 5.12 seconds will be required to obtain a complete solar spectrum.

The high speed encoder is used to sample the binary outputs of all 15 scalers. For the low speed encoder the necessary information capacity is not available, so the outputs of the central eight scalers are combined to give an analog voltage representing the logarithm of the stored count to base 2, to one significant digit only, within the range covered by the scalers. In addition, the discriminator bias level is also

FIGURE 4–10. X-ray low speed counter.
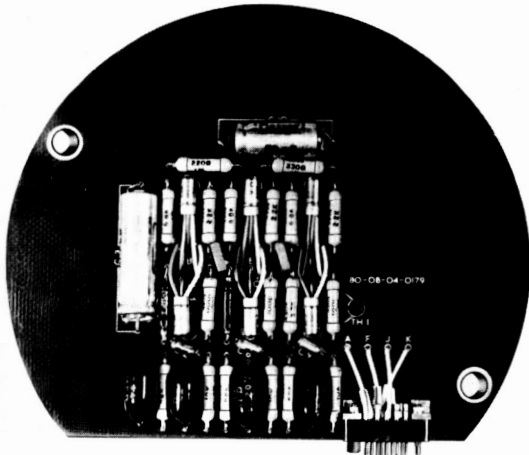
FIGURE 4–8. X-ray linear amplifier.

FIGURE 4–11. X-ray discriminator circuit.

telemetered and, on the high speed encoder only, an EHT monitor.

Figures 4–8 through 4–11 are photographs of the main electronic module elements. These operate from $+6.5$ volt and -6.5 volt lines, with a power consumption of 130 milliwatts.

MEASUREMENT OF SOLAR ASPECT

Project Engineers

Mr. J. Alexander, University College London
Dr. P. J. Bowen, University College London

The Experiment

Both radiation experiments require information on the solar aspect, as their sensitivity is a function of aspect angle and spin rate; and it

FIGURE 4–9. X-ray high speed counter.

was considered that such information would also provide information on the spin rate and the stability of the spin axis which would also be valuable in the interpretation of the ionospheric experiments. In all, it was considered that the necessary information consisted of the solar aspect angle—that is, the latitude of the sun in the satellite system—and of the roll position of the sun or its longitude measured from a reference plane in the vehicle. In fact, the time intervals between telemetry samples of roll position are such as to make possible an ambiguity about the number of complete rolls occurring between measurements; so a spin rate indication has also been included.

The basic method of measurement utilizes a small pyramid of silicon solar cells at the center of a 9-centimeter-diameter hemisphere. The cells are illuminated by the sun through two slits whose shape is defined by the intersection with the hemisphere of a circular cylinder 4½ centimeters in diameter, the axis being parallel to the spin axis. The arrangement is shown in Figure 4–12. The cells are covered by an
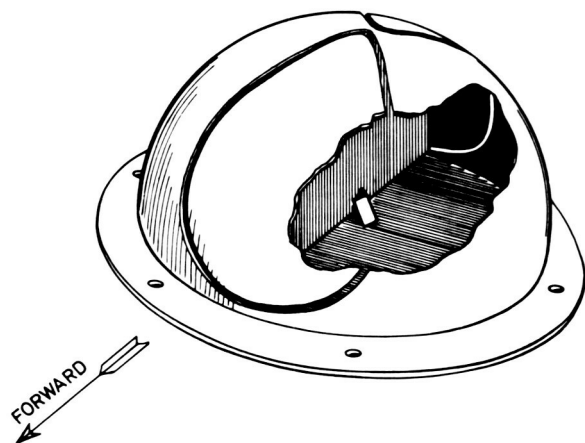

FIGURE 4–12. Satellite aspect slit system.

internal mask so that one cell on each side of the satellite equator is illuminated from one slit, and the outputs from the four cells are combined so that those from the two slits are of opposite polarity. The slit width and cell size are on the order of 1 degree, so that in each revolution of the vehicle one short positive pulse and one short negative pulse are produced. The time interval between positive pulses is then equal to the spin period; the actual time

of their occurrence gives the roll position; and the ratio of the time interval between positive and negative pulses to the interval between positive pulses is a linear function of the aspect angle.

The positive-going pulses are used to supply a simple pulse-rate circuit covering the range 180 rpm to 20 rpm. This will give an indication of the proper operation of the de-spin device and, at the same time, removes the roll position uncertainty. The positive pulses also operate a phase-locked sawtooth generator, which produces a triangular wave of constant amplitude whose commencement is always very close to that of the arrival of the pulse. Thus, this wave represents at any instant the roll position of the sun and is sampled by the telemeter. Finally, the positive pulses are used to turn *on*, and the negative pulses to turn *off*, a bi-stable circuit—thus producing a square wave of constant amplitude whose mean value is proportional to the solar aspect angle. The square wave is passed to a simple averaging circuit whose output is telemetered. The circuitry is supplied with 10 milliwatts from +6.5 volt and −6.5 volt lines.

COSMIC RAY ANALYZER

Project Scientists

Prof. H. Elliot, Imperial College, London
Dr. J. J. Quenby, Imperial College, London
Mr. A. C. Durney, Imperial College, London

Project Engineer

Mr. D. W. Mayne, McMichael Radio, Ltd.

The Experiment

Experimental Objectives

The main purpose of this experiment is to make accurate measurements of the primary cosmic ray energy spectrum and of the way in which this spectrum changes as a result of modulation by the interplanetary magnetic field. There are at present several alternative models of this field; and, to distinguish between the various possibilities, much more refined data are necessary than are now available from the observation of secondary cosmic ray intensity variations deep in the atmosphere and fragmentary information from balloon ascents.

In the present experiment it is proposed to investigate the cosmic ray spectrum by using a Cerenkov detector to measure the intensity of heavy nuclei ($Z \geq 6$) as a function of latitude. The energy spectrum can then be determined from the known values of the minimum energy that a particle must have in order to penetrate the earth's magnetic field at a given latitude. The advantages of measurements carried out in this way are: (1) It avoids the invalidation of cosmic ray measurements by inadvertent detection of Van Allen particles, and (2) it avoids the introduction of uncertainties by albedo particles scattered back from the atmosphere.

The detector will sweep through the cosmic ray energy spectrum four times on each orbit, giving a virtually continuous check on its variation with time. In addition, airplane surveys are to be carried out at the same time so that the intensity distribution in the atmosphere can be uniquely related to the primary spectrum. It is hoped by this means to obtain a sufficiently accurate relation so that the primary spectrum can be determined at any future time simply by an airplane survey.

A large and a small Geiger counter will be included in the instrument package. On those parts of the orbit where the satellite is outside the Van Allen belts the large counter will give a measurement of the energy spectrum of the primary cosmic ray protons, and also bursts of solar protons, in the same way as the Cerenkov detector measures the heavy particle spectrum. Thus, it is hoped that the proton and heavy particle spectra can be compared as a function of time. Inside the Van Allen belts the large Geiger counter will saturate, but the small Geiger counter will be able to count a much higher particle intensity. It is hoped to obtain data on the time variations of the trapped radiation from the small counter rate.

Operation of the Sensor

The Cerenkov detector consists of a hollow perspex sphere, 4 inches in diameter, together with an EMO 6097 photomultiplier 2 inches in diameter, which looks into a hole cut in the surface of the sphere. Cerenkov light flashes produced by cosmic rays in the wall of the sphere are detected by the photomultiplier.

The pulse output of the tube is fed to a discriminator that only accepts pulses corresponding to primary nuclei of $Z \gg 6$ or $Z \gg 8$, rejecting smaller background pulses due to lighter nuclei and the Van Allen particles. Output from the discriminator is fed to a chain of eight binaries, and the contents of this store are sampled by both the data storage and direct telemetry encoders.

An electronic switch that controls the attenuation of the photomultiplier output pulses is coupled to the last binary. There are two levels of attenuation; and, each time the store is completely filled, a pulse is fed into the switch from the last binary, and the switch changes the attenuation to the other value. In this way, the two (effective) levels of the discriminator are obtained.

The complete instrument package is located on the spin axis at the forward end of the satellite, with the perspex sphere protruding outside the satellite surface and the photomultiplier and associated electronics just inside. Primary heavy nuclei can arrive at the sphere from the forward 2π solid angle, where the amount of shielding is in general less than 1 gm/cm², but are absorbed by the satellite structure in the backward 2π solid angle. It is advantageous to locate the Cerenkov detector on the spin axis, since the direction in which it sees cosmic rays changes only slowly in time with respect to the earth's surface and the geomagnetic field. The effect on the cosmic ray intensity of both absorption by the earth and deflection by the geomagnetic field must be taken into account in the analysis of the results.

The Geiger counters are placed in the instrument package with structure shielding on the order of 2 gm/cm² from the outside in the forward direction. The effective length and diameters of the counters are, respectively, 5 and 2 centimeters for the larger and 1 and 0.3 centimeters for the smaller. An additional 1 millimeter of lead is put around the small counter.

Both counters feed in parallel a chain of 13 binaries, and the contents of this store are read periodically by both the data storage and direct telemetry encoders. If the counting rate of the large Geiger tube exceeds capacity of the

binary store, an integrating circuit turns it off with the result that only the smaller counter remains operative—so increasing the dynamic range of the system.

Sensor Structure

A diagram of the sensor is shown in Figure 4–13. The perspex sphere is contained in an
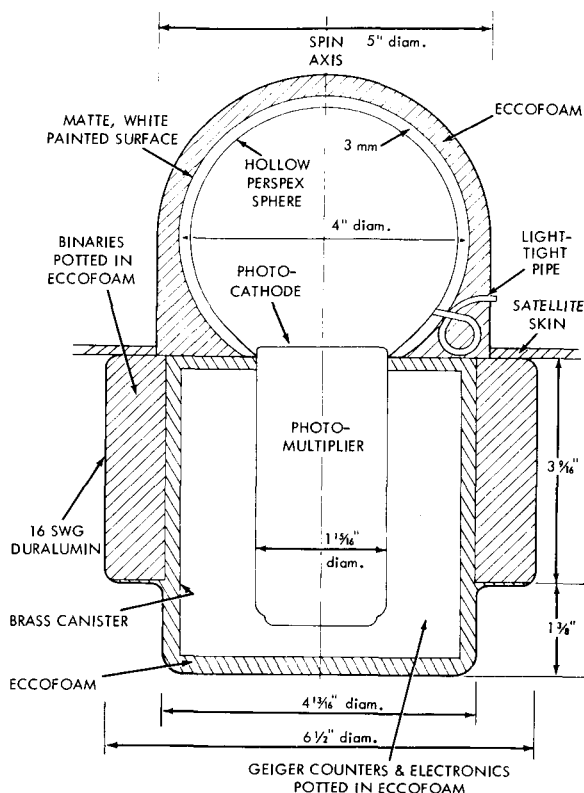

FIGURE 4–13. Cosmic ray analyzer sensor diagram.

aluminium dome, 5 inches in diameter and $4\frac{5}{16}$ inches high, protruding outside the satellite skin, to which the stalk of the University College probe is attached at the top. Eccofoam serves as a packing between the sphere and the aluminium container. The sphere temperature must be kept below 70° C, the softening point of perspex. A light-tight air leak is provided between the interior of the sphere and the outside surroundings.

An aluminium cylinder $6\frac{1}{2}$ inches in diameter and 5 inches deep is attached under the dome inside the satellite and contains the photomultiplier, Geiger counters, and electronics. The photomultiplier is placed along the spin

axis and looks into a 2-inch-diameter hole cut into the wall of the sphere. Some of the electronics, together with the two Geiger counters, are located in an annular space around the photomultiplier; and this whole is potted in Eccofoam and placed in a brass shielding canister. The canister is floated in a foam material to reduce the vibration acting on the photomultiplier. The remainder of the electronics is situated in a further ring surrounding the floating canister, and this also is potted in Eccofoam. Photographs of the sensor are shown in Figures 4–14 and 4–15.

The weight of the potted sensor, including the base of the University College London mass spectrometer, is 5.3 pounds. The center of gravity is on the spin axis, $3\frac{1}{4}$ inches up from the lowest surface on the base of the electronics cylinder. The moment of inertia about the spin axis is 0.2 lb ft^2; and, about an axis through the center of gravity and perpendicular to the spin axis, the mass of inertia is 0.09 lb ft^2.

Sensor Electronics

A block diagram of the electronic circuitry is shown in Figure 4–16. Two input power supply lines are required: 200 milliwatts at -9 ± 1 volts and 100 milliwatts at -6.5 ± 1 volts. The -9 volt line is fed to a dc converter, producing a very stable -6 volt line that is used to supply the EHT converter, the emitter follower, the discriminator, and the gate circuits.

The dc converter incorporating a corona stabilizer supplies the 60-megohm dynode chain of the photomultiplier with -1000 volts, and this EHT voltage was designed to have a ± 4 volt variation for a ± 1 volt variation on the -9 volt input supply. The attenuator is switched to permit measurement of either the cosmic ray rate from $Z \gg 6$ or from $Z \gg 8$.

The discriminator output goes via a gate circuit to the chain of eight binaries. Figure 4–17 shows the circuit of a single binary, together with the size of the output wave form as a function of supply voltage. The outputs of the first six binaries are fed to the input gates of the high speed encoder, while the outputs of the last six binaries are fed to the input gates of the low speed encoder.
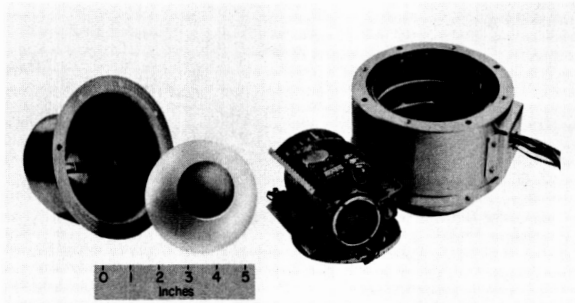
24

FIGURE 4–14. Cosmic ray sensor and electronics.

When a particular information channel is to be sampled, the gate circuits feed three of the binary outputs to a digital oscillator that takes up one of eight different frequency levels, depending on the state of the three binaries. This frequency output is then put on the tape recorder in the case of the low speed encoder, and goes to modulate the telemetry transmitter in the case of the high speed encoder. Thus, to read the binary store, two channels are required on both the data storage and the direct telemetry systems.

While the low speed encoder is sampling the binary store, it is arranged that the gate circuit

FIGURE 4–15. Mass spectrometer probe and cosmic ray experiment assembly.
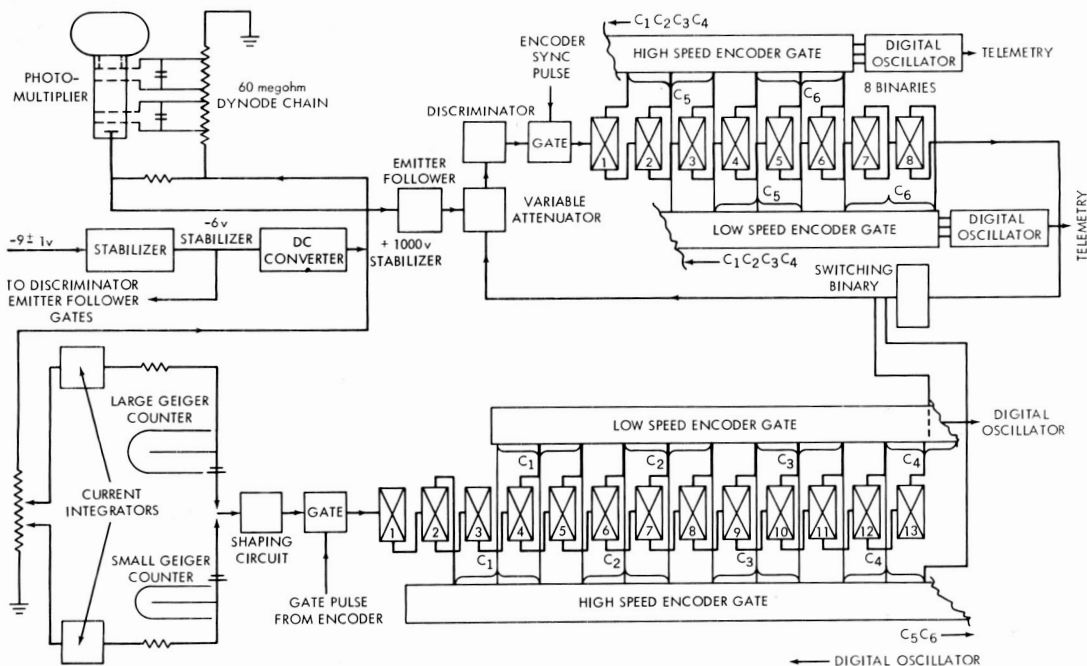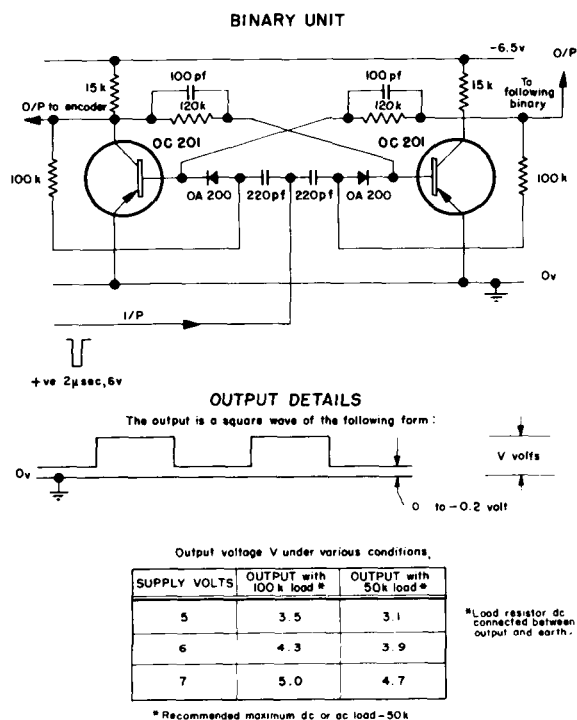

FIGURE 4–16. Block diagram of cosmic ray analyzer circuit.

25

BINARY UNIT

OUTPUT DETAILS

The output is a square wave of the following form:

Output voltage V under various conditions,

SUPPLY VOLTS	OUTPUT with 100 k load *	OUTPUT with 50k load *
5	3.5	3.1
6	4.3	3.9
7	5.0	4.7

*Load resistor dc connected between output and earth.

* Recommended maximum dc or ac load – 50k

(Note: The binary units will be operated from the unstabilized – 6.5v (±1v) supply.)

FIGURE 4–17. Circuit of a single binary unit with output details.

placed after the discriminator prevents any output reaching the first binary. This is done because the state of the binaries may change during the time taken to sample both binary sets. The gate circuit is driven by a pulse from the low speed encoder, which has a quiescent level of +6.7 volts and goes to −2.7 volts during the period when the state of the two sets of binaries is read by the digital oscillator. Zero current is drawn from the encoder at +6.7 volts, and 10μ amp at −2.7 volts.

An electronic switch working from the output of the last binary will change the value of the two-position attenuator and successively feed the two cosmic ray counting rates into the telemetry systems. When the binary store is filled, the flipover of the last binary changes the state of a switching binary, the output of which determines the value of the attenuation. To tell which attenuation value is being used, the switching binary output is also fed to both the low and high speed encoders as one of the three binary elements in information channel C4, the

other two elements being taken from the Geiger counter store.

Appropriate voltages for the Geiger counters are tapped off the dynode chain. The anode-to-cathode voltage of the larger counter is made to fall below the working voltage at counting rates, in excess of that which the data encoder can handle. Pulse outputs from the two counters are mixed and fed via a gate circuit to a chain of 13 binaries. Numbers 2 to 12 are read by the high speed encoder, and numbers 3 to 13 are read by the low speed encoder. The design of the binaries and the method of sampling by the encoders are similar to the case of the Cerenkov channel. Thus, four channels of both the data storage and the direct telemetry systems are required. The gate circuit stops extra pulses being fed to the store, while the low speed encoder samples the four sets of binaries and works from similar pulses to the Cerenkov channel gate.

The digital oscillators and the associated input gate circuits for both encoders are located on a card held below the sensor by extensions to the bolts that locate the sensor on the satellite skin.

Plugs and Connections

About twenty-six leads are required between the gate and oscillator circuitry in the sensor and the encoder modules. Two power leads at −6.5 and −9 volts are also required. About eight further output leads are necessary if the sensor performance during environmental testing is to be monitored independently of the telemetry system.

Thermal Design

The following temperature restrictions are requested:
1. Perspex sphere, 70°C (this is the softening temperature of the plastic);
2. Electronics, 0° to 40°C;
3. Photomultiplier, 0° to 30°C (if possible).
Relevant information about materials:
1. The outer shell of the unit is made of 16 swg aluminium alloy (BS1470) and weights an estimated 16 ounces; it has a surface finish similar to duralumin.
2. The inner shielding canister is made of brass and weights about 16 ounces.

26

3. An estimated 23 ounces of Eccofoam is used in potting.

4. The remaining 2.3 pounds of sensor weight is made up of electronic components, circuit boards, photomultiplier, Geiger counters, etc.

PLASMA DIELECTRIC CONSTANT MEASUREMENT OF IONOSPHERIC ELECTRON DENSITY

Project Scientist

Prof. J. Sayers, University of Birmingham

Project Engineer

Mr. J. Wager, University of Birmingham

The Experiment

The measurement of electron density is performed both by this experiment and by the Langmuir probes of University College London. However, the two methods are quite different in principle and, being subject to different errors in general, therefore complement one another. Two circular disks of wire mesh, 3.5 inches in diameter and separated by 3.5 inches, form a parallel-plate capacitor (mesh is used in order to allow free passage of electrons into the capacitor). The capacitor is at the outer end of a boom 49.5 inches long, so that the electron density will not be greatly affected by the presence of the satellite.

The capacitor forms one arm of an RF capacitance bridge, operating at 10 megacycles. From a knowledge of the capacitance at 10 megacycles, and of the capacitance in vacuo, the dielectric constant k of the ionospheric plasma can be found; this is related to the electron density by the expression

$$k = 1 - \frac{N_e e^2}{\pi m \omega^2},$$

where N_e is the electron density, e and m are respectively the electronic charge and mass, and ω is the angular frequency of operation of the bridge (here $2\pi \times 10^{-7}$ rad/sec). However, N_e in the equation will be equal to the ambient electron density only if the potential of the capacitor plates is the same as the space potential. In general, there will be a potential difference between the satellite and space. To insure that at some times the capacitor plates

are at space potential, a sawtooth wave with an amplitude of about 4 volts is applied to them; N_e is then taken to be the maximum value obtained during the sweep. Immediately before the start of each sweep a rather large negative potential (-5 volts) is applied to the plates to denude them of electrons and to provide a check on the in-vacuo capacitance.

Block diagrams of the circuitry are shown in Figure 4–18. To avoid a possible interaction with the University College London probe experiments, the experiment is turned on only for 10 seconds in each 61.42-second period. This is controlled by trigger pulses from the low speed encoder binary sequence. A gating unit then supplies power to the VF bridge circuitry and the bridge potential waveform generator—all of which are located at the hinge end of the boom—for this period. The output from the bridge is amplified, separated into in-phase and quadrative components (corresponding to the real and imaginary parts of the dielectric constant, respectively), and telemetered through the high speed encoder. Also, the maximum values in each sweep are selected by peak reading circuits and are stored in capacitors until they are read out by the low speed encoder.

The temperature of the boom electronics, the voltage supply levels, and the variable frequency (VF) amplitude are also measured and telemetered by both encoders.

DUTCHMAN EXPERIMENTS

Project Scientist

Dr. A. P. Willmore, University College London

Project Engineer

C. L. Wagner, Jr., Goddard Space Flight Center

The Experiment

The payload-supporting Dutchman contains two experiments directly connected with the spacecraft instrumentation. The first of these is designed to measure solar aspect and spin rate during the period before separation occurs, while the second is designed to detect contamination of the spacecraft thermal coatings and sensors as a result, for example, of evaporation from the nose fairing following aerodynamic heating. Each of these experiments receives
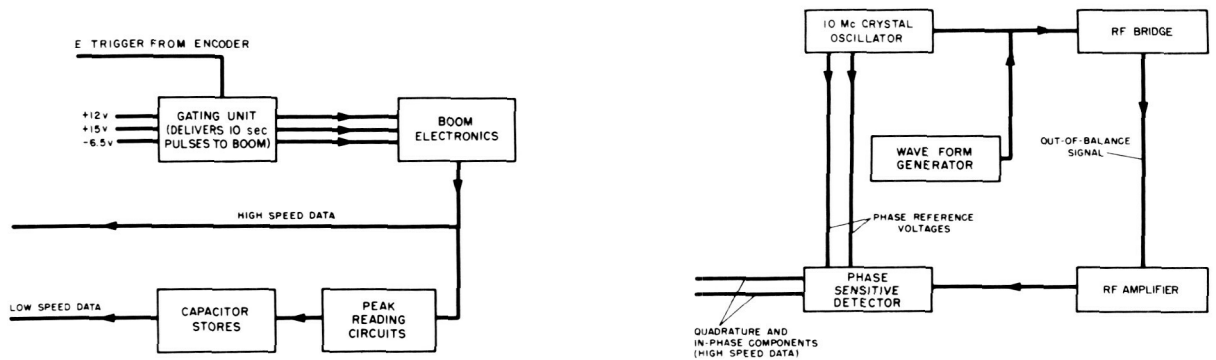
FIGURE 4-18. Electron density circuit, block diagram.

power from the regulated +6 volt supply provided for the vibration experiment, and the signals from the two are combined for transmission over a single telemetry channel. In addition, an indication of the operation of a third-stage pressure switch is provided on this channel.

The aspect sensor is of the same pattern as that used in the spacecraft, but the aspect computer has been omitted. The pulse sequence from the solar cells is telemetered directly. The advantage of this procedure is that the rather long time delays associated with the aspect computer are eliminated, thus enabling third-stage spin and nutation to be calculated.

A diagram of the contamination experiment is shown in Figure 4-19. A small, focused lamp is used with a filter to produce an approximately parallel beam of suitably colored light. A small sample of this beam is obtained by reflection from an unsilvered glass surface, and its intensity is measured by means of a photodiode.
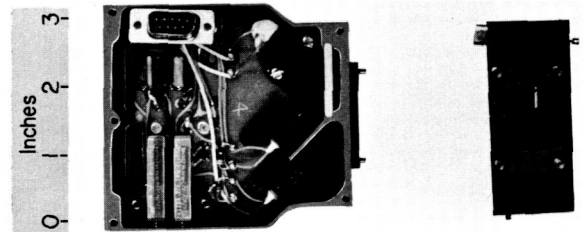
FIGURE 4-19. Contamination experiment.

The remainder of the light is incident on another glass slide, the intensity of the reflected light being monitored by means of a second photodiode. The second glass slide is exposed to contamination by the fairing, such contamination being revealed by the change in reflectivity of the glass.

A simple gating circuit is used to switch between the reference and sample slides at a rate of 1 cps. The output from the photodiodes is superimposed on the photocell pulses of the aspect sensor.

CHAPTER 5

United States Satellite and Subsystems

STRUCTURE AND MECHANICAL DESIGN

Introduction

The Ariel I structure and mechanisms design encompasses two separate major areas of endeavor: (1) The satellite itself requires structure and mechanisms; and (2) just as important to the total payload is the development of a separation and release system interface structure and associated mechanisms.

The satellite itself relies heavily on the use of epoxy-bonded filaments of fiber glass for much of its structure, used in combination with machined wrought aluminum alloys. The ancillary interface system (Dutchman and separation structures) is largely composed of magnesium thin-wall castings.

Satellite Structure

General

The spacecraft structure should properly be divided into two main groups: the basic structure, and the appendages. The basic structure must then be further divided into the following subcomponents:
1. Upper dome,
2. Mid-skin,
3. Shelf and base assembly,
4. Lower dome.

The appendages are as follows:
1. Four solar paddles,
2. Two inertia booms,
3. Electron density experiment boom,
4. Electron temperature experiment boom,
5. Telemetry antennas.

Design Parameters

Several design considerations were paramount in the development of the structure:

The Scout 25.7-inch-diameter heat shield limited the payload size to 23 inches in diameter by 2 feet in length, not including certain experiments.

The aft appendages must be folded into the space described by a hollow cylinder 23 inch O.D. x 18 inch I.D. x 4 feet 8 inches long.

The structure should be manufactured of non-metals and/or nonmagnetic materials, so that the effects of magnetic spin damping are reduced to a degree that the half-life of the satellite's spin rate be 1 year.

The total satellite weight should not exceed 135 pounds.

The structure must withstand accelerations and vibrations of the launch vehicle. In this case the ABL-X248-A5 motor (last stage) governs.

Outer Structure

General: As a result of the above considerations the material chosen for the skin of the Ariel I was epoxy-bonded fiber glass. The domes were constructed from monofilament glass fibers cross-woven into cloth laminations that were molded into a spherical shell of 13½-inch radius by 5⅝ inches high. Shell Epon 828 with a CL hardener was used as the bonding agent. The top dome is $\frac{1}{16}$ inch thick, and the bottom dome—basically used only as a thermal shield—is $\frac{1}{32}$ inch thick. The mid-skin was made from a cylinder of epon-bonded,

monofilament-wound fiber glass $\frac{1}{16}$ inch thick x 23 inches in diameter x 10.7 inches long.

Upper Dome (Figure 5–1): Into the top of the

(a)

(b)
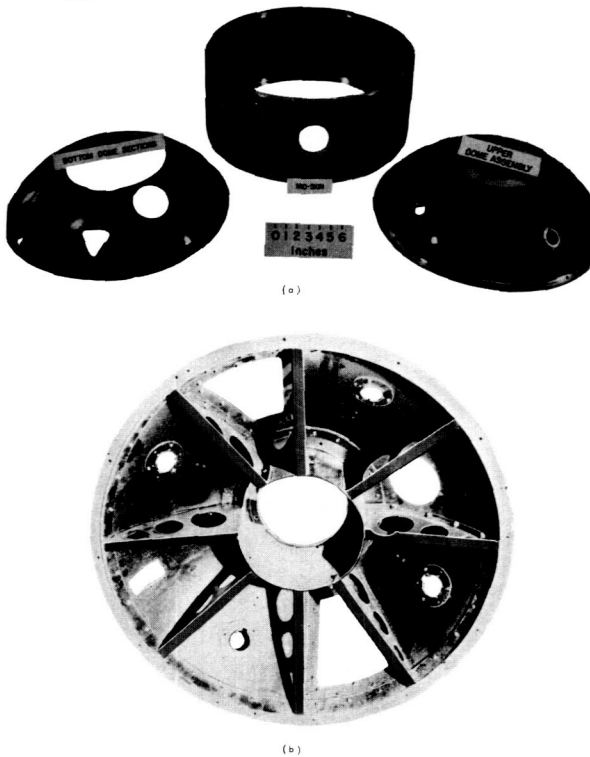
(a) Uncoated upper and lower domes and mid-skin
(b) Interior view of upper dome
FIGURE 5–1. Domes and mid-skin.

upper dome skin was bonded and riveted an aluminum disk 8½ inches in diameter x 0.2 inch thick. Machined integrally with, and centrally located on, the disk is a 7-inch-I.D. thin-walled cylinder extending internally 3.7 inches. This hat-shaped structure supports the cosmic ray—ion mass sphere experiments and the eight radial fiber glass ribs, which are also attached to the dome skin—thus giving stiffness and strength to the dome. A machined aluminum ring was bonded and riveted to the base of the dome to allow the assembly to be bolted to the top of the 23-inch-diameter mid-skin. Holes were cut in the proper places of the dome to allow attachment of experiments and antenna mounts.

Mid-Skin (Figure 5–1a): The mid-skin fiber glass is bonded and riveted to two end flanges, machined from AISI 6061-T6 aluminum, which are shaped to provide nonshifting attachment to the upper structure and the shelf-base assembly. In detail, shear lips prevent radial movement, pins prevent rotational displacement, and machine screws tie the components together.

Lower Dome (Figure 5–1a): The lower dome is segmented and fitted with doublers for installation of sensors and the segments themselves. Gold-plated aluminum machine screws hold these components in position.
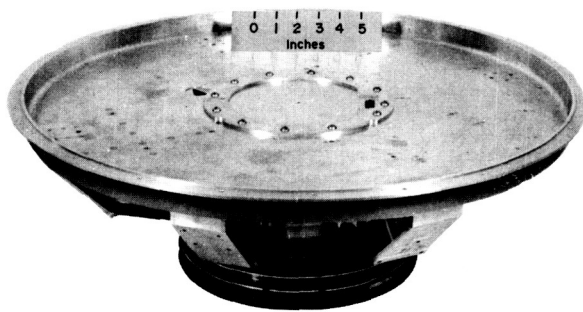
Shelf and Base Assembly (Figure 5–2)

General: The instrument shelf and base assembly is made from AISI 6061-T6 aluminum plates, bars, and billets machined into shape and semipermanently affixed into the assembly condition. The separate parts are as follows.

Shelf: The shelf is basically a 21-inch-diameter plate 0.08 inch thick with eight integral stiffening ribs leading radially from a 7½-inch-diameter integral cylinder to the outer periphery. This undercarriage of ribbing tapers from 0.7 inch at the cylinder to 0.3 inch at the 21-inch-diameter periphery. The top of the shelf at the 21-inch diameter is dished upwards 1 inch and then again extends radially until the shelf is 23 inches in diameter. This step is machined to supply room for the de-spin system and to provide a mating surface for the mid-skin.

Base: The base is a cylinder of 7 inches I.D. and fits into the 7½-inch-diameter short-shelf cylinder, extending aft 6½ inches. The aft 2 inches is machined to an 8½-inch I.D. to provide proper view angles for the spin-axis-mounted electron temperature sensor. The forward 7-inch-diameter x 4½-inch-long space is provided for containing the above sensor, the satellite's tape recorder, and the boom escapement mechanism. The outer diameter is machined to provide (1) a mounting surface for the separation adapter ring, (2) a mounting surface for the bottom dome segments, and (3) a key for six support struts.

Struts: The six struts are each machined from solid stock and take the shape of a modified "I" beam. Each strut serves to support the shelf and to supply the mount for a paddle arm or experiment boom hinge. The struts are keyed to the base and, after being fastened into position with machine screws, are keyed to the shelf by shrink-fit shear pins.

(a) Viewed from above
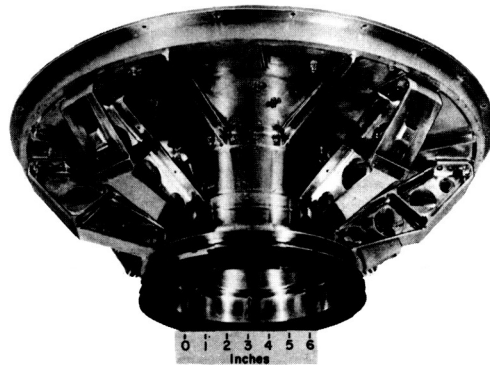
(b) Viewed from below

FIGURE 5-2. Electronic shelf and base assembly.

Appendages

General (Figure 5-3): The eight appendages should be considered in three separate group-
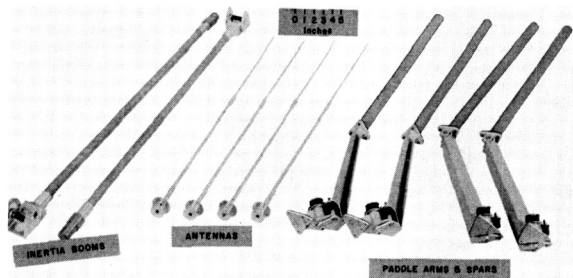

FIGURE 5-3. Satellite appendages.

ings: paddle arms; inertia arms; and sensor, or experiment, booms.

Paddle Arms: The paddle arm and hinge design was suggested by that used on Explorer XII (1961 *v1*); however, space considerations dictated by the Scout heat shield and paddle location restrictions required by the experiments complicated the design considerably. The arms themselves are long slender channels machined from AISI 7075 aluminum. One pair of arms lead directly from their hinges to the paddle interface; but space and positional requirements for the other pair of solar paddles required a secondary folding hinge at the outboard end of each arm. From this secondary hinge extends the paddle interface of these two arms.

Inertia Booms: The inertia booms, when extended, provide a proper moment of inertia ratio so that the longitudinal axis remains the

spin axis of the spacecraft. These booms are made of thin-walled tubes of epon-bonded fiber glass cloth, rolled into cylindrical shape. Each boom is attached to the shelf by a detent-locking, spring-loaded hinge; and at the outboard end of its 30 inches is a 0.7-pound steel weight that is 4 inches long. Both the inertia booms and the paddles are erected at 52.4 rpm, reducing spin to 36.6 rpm.

Experiment Booms: The sensor booms are made by the experimenters, but the method of erection is part of the structure's responsibility. The hinge valves are machined from solid stock and use a double detent lock and a torsion-spring positive force to assure opening in the event of no payload spin-up. (This consideration is true in all appendage extension.)

Escapement (Figure 5-4)

Boom erection rotation speed of the normal experiment is 76.5 rpm, which would produce large shocks to the experiments if these booms were allowed to open without restraint. As a result, an escapement device was designed to reduce these forces by controlling erection speed.

The clock escapement principle is employed in the design of the timing mechanism. Since the primary interest in the application is to reduce shock—and not the accuracy or timing, the less sophisticated mechanism, called a "run-away-escapement," is used. It consists of a gear train coupled to an escape wheel, and a pallet fitted over the escape wheel to control its rotation rate. The two booms are required
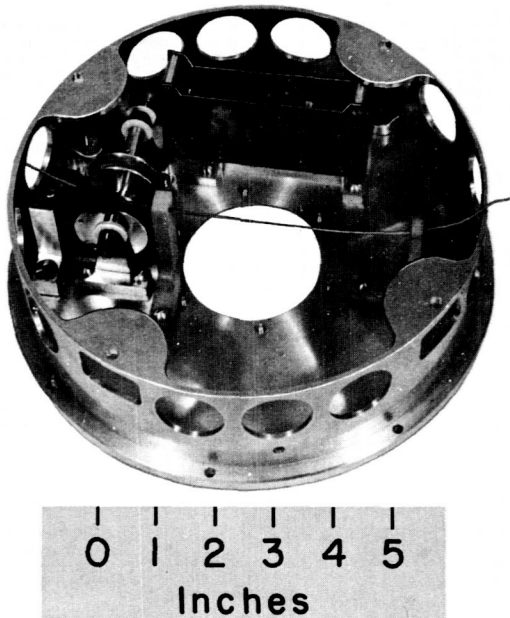
31

FIGURE 5–4. Escapement mechanism.

tension springs wound one-half turn about the payload. The weights were released by pyrotechnique guillotine cutters, and the weight-spring combinations unhook themselves when in a radical attitude from the spacecraft. By this system the payload is despun from 160 to 76.5 rpm.

Antennas (Figure 5–5)

The four turnstile-type antennas are of the double-fold design, so that they can fit into the
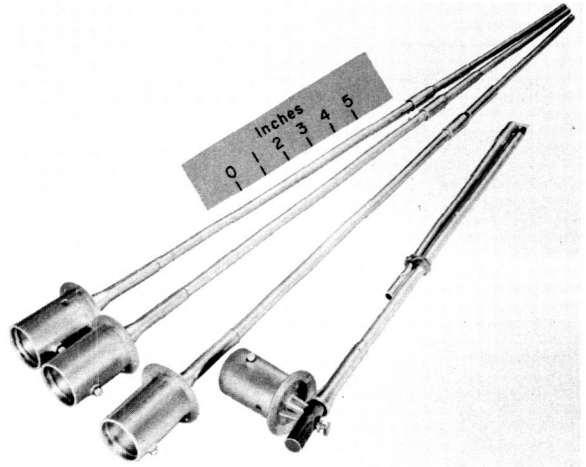
FIGURE 5–5. Flight antennas.

heat shield. These antennas are located on the top dome equispaced 90 degrees apart, and in their erected position make an angle of 40 degrees with the spin axis. Upon ejection of the heat shield, the antennas are erected to their length of 21¾ inches.

Battery Containers

The two containers for the spacecraft battery power supply were designed to withstand the force of expanding gas generated internally in the sealed batteries, which could result from a partial power system malfunction. The container can withstand loadings of 50 pounds from each of two stacks of batteries without significant expansion—thus preventing rupture of the batteries and subsequent contamination of the payload. These containers are mounted on the instrument shelf and supply rigidity in the area of the inertia boom hinge.

to be simultaneously controlled; thus a double pulley mounted on a common shaft is coupled to the free end of the gear train. A doubled nylon cord, with one end attached to the boom and the other end to the pulley, serves as the control links. The rotation rate of the escapement is a function of the satellite acting torque and the moment of inertia of the part. The pallet's moment of inertia is adjusted to allow the booms to erect in 2 to 3 seconds. This escapement will successfully control the boom erection when the satellite spin rate is between 60 and 90 rpm.

The booms are also tied together by this mechanism, so that they erect simultaneously and thus prevent any unbalance that would cause coning of the payload. (The other appendages open too quickly to create this problem.)

De-Spin Device

The de-spin system is built in a self-contained ring fitting in the space provided at the periphery of the shelf. It is of the "stretch yo-yo" design (Reference 13), which will de-spin a system having a ±20 percent nominal spin rate error to ±2 percent of the required final value. The basic components are a pair of equal weights attached to a matched pair of long

Miscellany

The above-mentioned components plus a wealth of miscellaneous supports, adapters, and bracketry make up the structures and mechanisms of the orbiting spacecraft, accounting for 51.6 pounds of its weight.

Separation and Release Systems

Although not a part of the spacecraft, the separation and release system (Figure 5–6) is
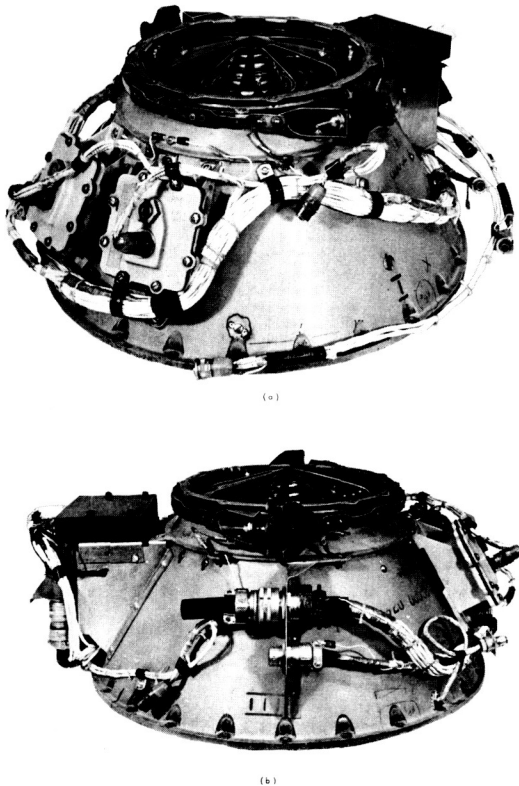
(a) View 1
(b) View 2

FIGURE 5–6. Separation and release mechanism.

responsible for programming proper de-spin of the system, erection of the appendages, and separation of the payload. The system was designed originally to adapt the spacecraft directly to the fourth stage of the Scout vehicle. A thin-walled, machined magnesium casting in the shape of a hollow, truncated cone forms the basic transition unit from the satellite to the last stage. At the satellite interface is the separation spring, segmented marman clamp, and separation bolts. Here, too, are found the

two 3-pin feed-through connectors that carry into the satellite the de-spin signal, battery charge, and turn-on, turn-off circuitry. The wide base of the cone fits over the forward shoulder of the vehicle interface and is bolted to studs protruding from that surface. Fastened to the cone itself are two 12-volt battery supplies and an electronic release sequencer. Bonded to the cylinder of the X-248 motor are brackets and supports holding the release cords and pin pullers—which, when retracted, release the cords and allow erection of the appendages. Total balanced weight of this system is 18.3 pounds.

Delta Dutchman

When the Ariel I was transferred to the Thor-Delta vehicle, an adapter ring was required to move the folded payload forward some 12 inches so that the pedal-leaf second- to third-stage separation skirt would not damage the sensor booms during stage separation. This Dutchman (Figure 5–7) is a fabrication of cast magnesium end rings separated by a 16-inch-diameter cylinder of rolled and welded 0.09-inch-thick magnesium sheet. The riveted fabrication is 13.0 inches long.

Since the Thor-Delta can carry a heavier payload than the Scout, the available space in the Dutchman cylinder is utilized to contain the electronics and sensors of a vibration and contamination experiment. The total weight of this composite is 17.0 pounds; the Dutchman accounts for 7.3 pounds of this total.

Detailed Data on Structure and Mechanical Design

Physical measurements of the structures and mechanisms of the Ariel I payload are presented as Appendix A.

THERMAL DESIGN AND COATINGS
Thermal Design

For a given solar absorptance–thermal emittance (a/e) ratio, a variation in mean orbital temperature of 35° C can be expected in the main structure over a period of 1 year. This total variation may be subdivided as follows: (1) 0 to 6 watts internal power, 5° C; (2) 63 to 100 percent sunlight orbits, 20° C; and (3) variation in sun, spin-axis angle—including
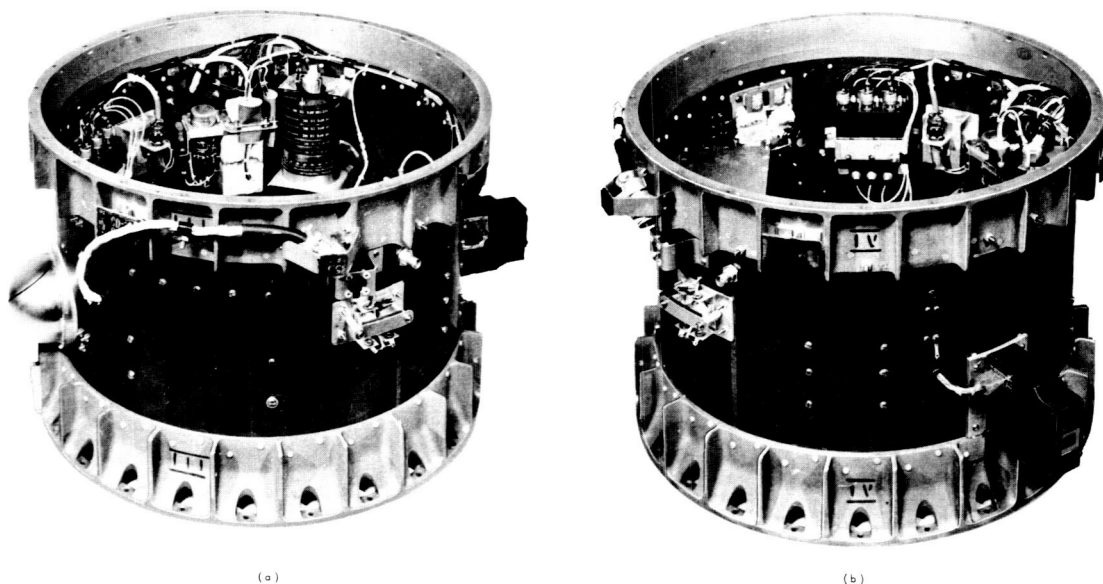
(a) View 1   (b) View 2

FIGURE 5-7. Dutchman adapter cylinder and experiments.

shading by paddles and booms, 10° C. A ±10 percent tolerance for achieving the design a/e would result in a tolerance of about ±7° C in mean orbital temperature for a given orbit, sun angle, and internal power. Skin temperature gradients can vary from about 20° to 60° C, depending on sun—spin-axis angle. The variation in mean orbital temperatures of the boom-mounted components due to sun—spin-axis angle changes will be somewhat greater than the corresponding temperature predictions for the main structure because of the nonspherical geometry and greater shading effects. Solar paddle temperatures should remain between +33° and −63° C, the temperatures corresponding to the hottest and coldest combinations of spin axis, orbital plane, and orbital position locations with respect to the sun.

Thermal Coatings

The thermal coating are evaporated gold with not more than 25 percent of the total surface area covered with a combination of black and white paints. This represents a compromise of the experimenters' requirement for a conducting surface with a preference for gold or rhodium over other metals and a thermal requirement for maximizing the painted areas to minimize the tolerances on a/e ratio.

The following process has been developed for applying the thermal coatings so that mirrorlike gold surfaces which have good adhesion to the substrate and which can withstand without damage aerodynamic heating to 250°F are obtained. First, the surfaces are sanded, cleaned, and baked at 310°F for 1 hour. Then layers of varnish, lacquer, paint, and metals are applied in the following sequence and are baked at the temperatures and for the time intervals indicated:

1. Sealing varnish, 300°F for 20 minutes,
2. Clear lacquer, 290°F for 30 minutes,
3. Conducting silver paint, 280°F for 18 hours,
4. Electroplated copper, 1.5 mil thickness,
5. Lacquer, 275°F for 30 minutes,
6. Evaporated gold, 0.00004 inch thick,
7. Four coats of black paint in eight longitudinal stripes, 250°F for 30 minutes.

Steps 3 and 4 are applied only to the cylindrical section and the forward dome to provide a ground plane for the antennas. The lacquer is the type used for providing a proper substrate for evaporative films. The combination of the varnish plus the repeated baking at decreasing temperatures with each successive step is used to protect the evaporated gold

34

from damage by outgassing of the substrate. Final adjustment of a/e was made by the application of white paint over part of the black paint areas. The black and white paints are carbon black and zinc sulfide pigments, respectively, in a silicone vehicle.

DESCRIPTION OF ELECTRONIC SYSTEM

Electronic Subsystem

A typical electronic subsystem of the spacecraft is a printed circuit card, which is completely encapsulated in Eccofoam (Figure 5–8).
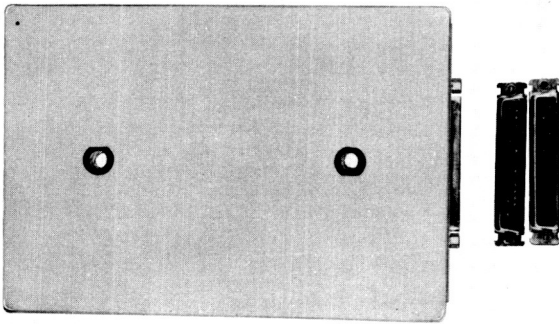
FIGURE 5–8. Printed circuit card, completely encapsulated for space flight.

These printed circuit cards are of three types. One type of circuit card provides for mounting individual electronic components as shown in Figure 5–9. Medium component density is
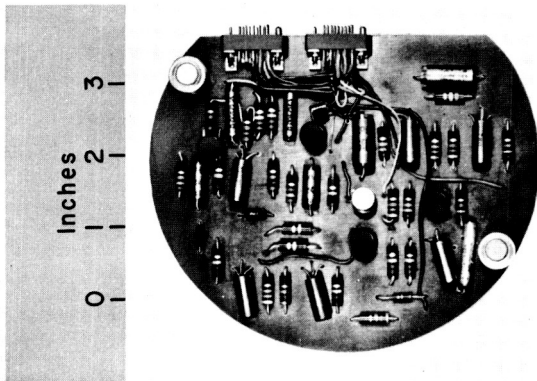
FIGURE 5–9. Printed circuit card, mounting individual components.

achieved by mounting the components vertically on the record type of printed circuit card shown in Figure 5–10. Maximum component
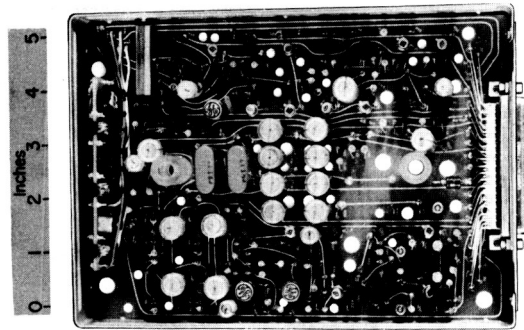
FIGURE 5–10. Printed circuit card, mounting component of medium density.

density is achieved by mounting modules on the printed circuit cards as shown in Figures 5–11 and 5–12.

FIGURE 5–11. Printed circuit card, mounting unencapsulated modules.
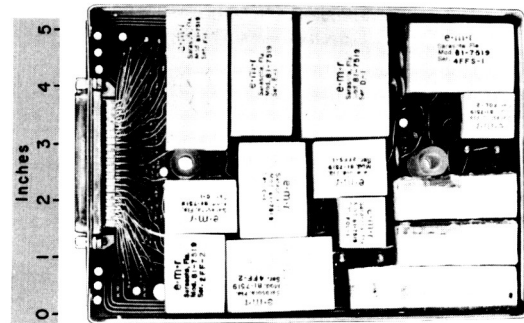
FIGURE 5–12. Printed circuit card, mounting encapsulated modules.

Block Diagram Discussion

A block diagram of the spacecraft's electronic system is given in Figure 5–13. Eight probes are shown with their data outputs processed
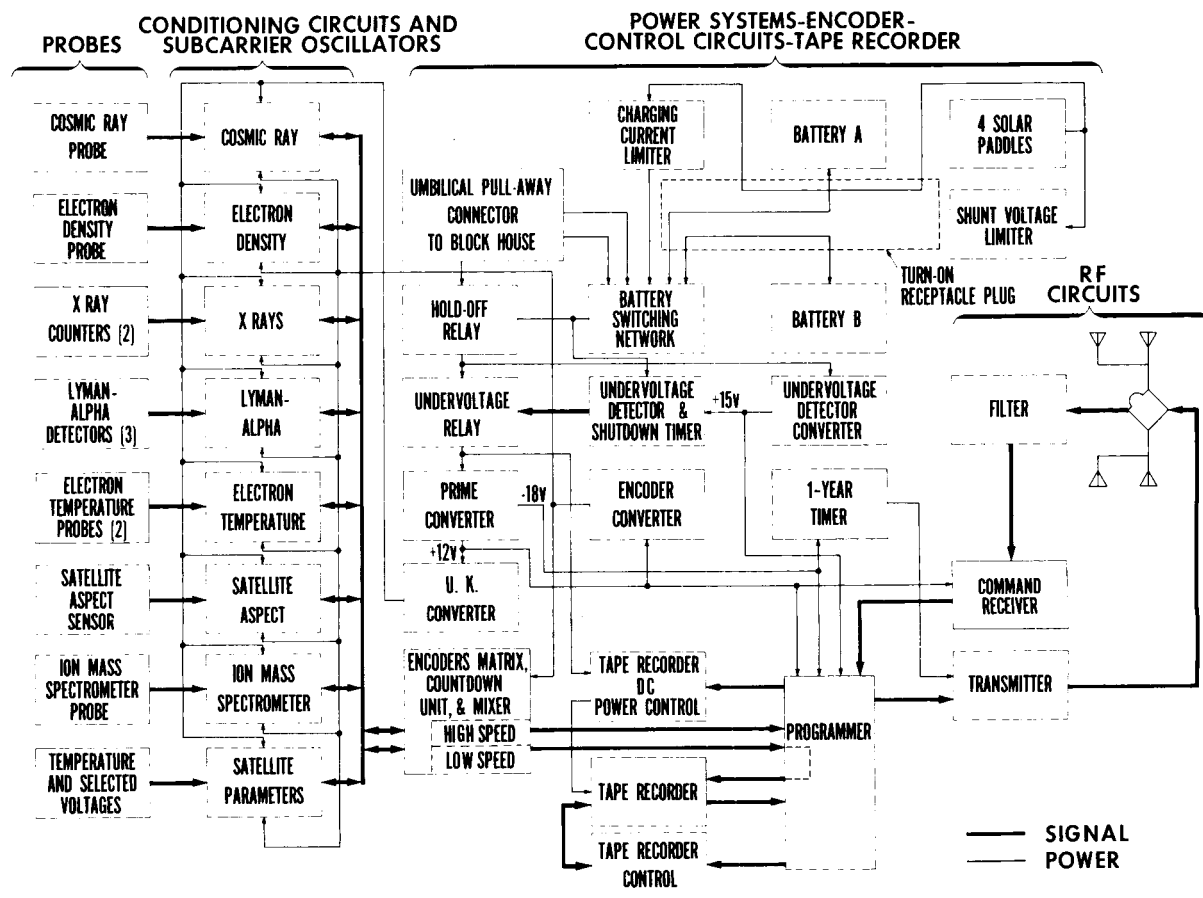
FIGURE 5-13. Ariel I electronic function diagram.

by signal conditioning circuits. The outputs of the signal conditioning circuits are connected to subcarrier oscillators (analog and digital). The subcarrier oscillators convert analog and digital data to representative ac signals. The frequencies of these signals are dependent on the value of the input analog voltage and/or digital data, Figure 5-14. The outputs from the subcarrier oscillators are sequentially gated as high speed (HS) or low speed (LS) data outputs by the respective encoder matrices. The encoder assignments of experimental data outputs are listed in Table 5-1.

The high speed encoder data are transmitted in real time, whereas the low speed encoder data are recorded on magnetic tape. There is a speed reduction between the two encoders of 48:1. By playing back the recorded data 48 times faster than it was recorded, the low speed

data are transmitted at the same bandwidth as the high speed data.

Playback of the magnetic tape recorder is initiated by a ground station command to the Command Receiver in the spacecraft. The Command Receiver in turn commands the Programmer to switch the Tape Recorder from Record to Playback.

The output format of the high speed and low speed encoders is shown in Figure 5-14; also shown is the telemetry program for almost two complete orbits.

The power system for the spacecraft consists of solar paddles, two battery packs, shunt voltage limiter, battery charging current limiter, battery switching network, and undervoltage detector system.

The *four solar paddles* are mounted with silicon solar cells and together are capable of
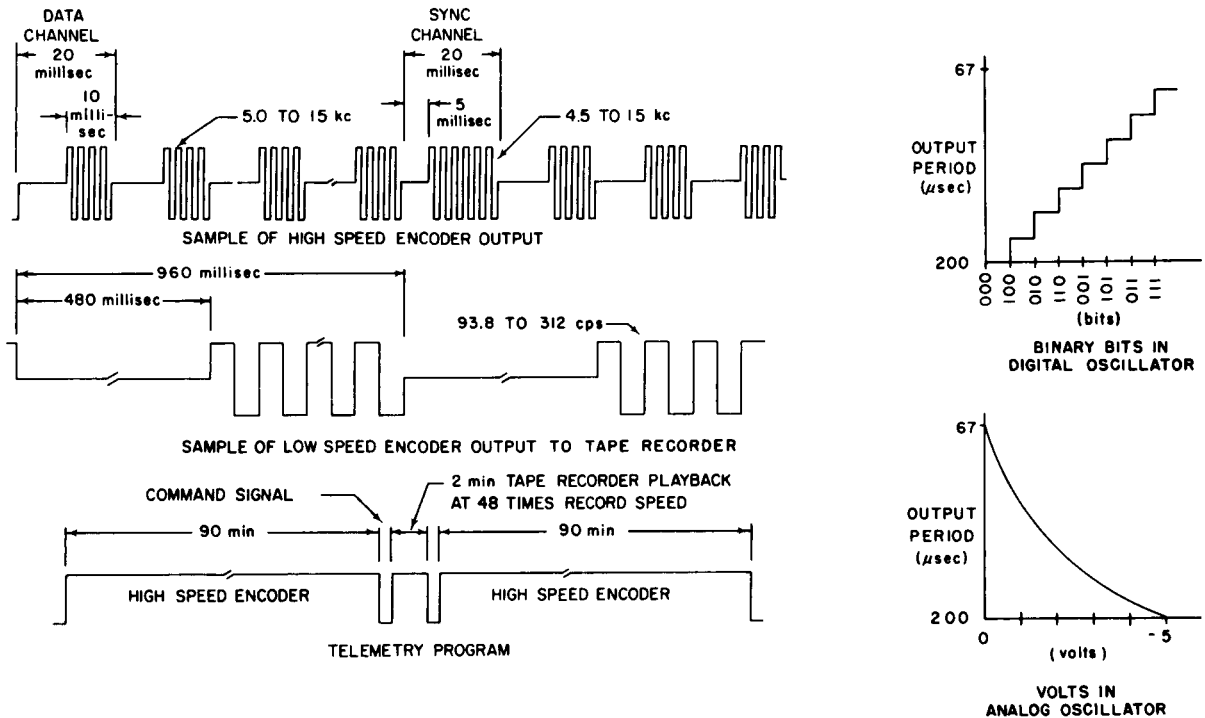
FIGURE 5–14. Telemetry system.

providing 0.5 to 2 amperes at 15 volts, depending on the spacecraft aspect to the sun. The *shunt voltage limiter* regulates the solar paddle output voltage to 14.5 volts. The *battery charging current limiter* regulates the battery charging current to a value not in excess of 0.5 ampere. The *battery switching network* selects the battery with the highest voltage to operate the spacecraft. The *undervoltage detector system* includes an undervoltage detector, converter, relay, and shutdown timer. Operation of this system turns off the entire spacecraft to provide maximum charging current to the batteries.

The hold-off relay is operated from the block house and is used to turn the power system *on* and *off* after the turn-on plug has been installed in the spacecraft.

The four converters are dc to dc converters that supply regulated voltages to the spacecraft's electronic subsystems.

Encoder

The encoder (Figure 5–15) is operated by a crystal-controlled clock. The clock frequency is divided to produce a 50-cps signal for the high speed (HS) encoder data rate. The 50 cps is divided by 48 to produce the low speed (LS) encoder data rate of 50/48 cps.

The HS encoder format consists of 256 channels arranged in 16 frames (16 channels per frame). A complete set of 256 channels is referred to as a HS encoder sequence. The LS encoder format contains 2 frames, also with 16 channels per frame. A complete set of 32 channels is referred to as a LS encoder sequence. The channel allocation for both formats is given in Figures 5–16 and 5–17. These figures may be compared with the notations on Table 5–1 for identification of channels.

Operation of the HS encoder is independent of the operation of the LS encoder for increased reliability. However, a loose type of synchronization between the two encoders is provided. Synchronization is defined as being achieved when both encoders start their respective sequences within 20 milliseconds of each other. If the time difference is greater than 20 milliseconds, a "blipper" circuit shortens the LS sequence by 20 milliseconds, causing the next

TABLE 5-1

Encoder Input Data

Experiment	Nomenclature of Each Output	Experiment	Nomenclature of Each Output
Electron temperature no. 1	U_1—HS U_2—HS U_3—HS U_m—HS U_1—LS U_2—LS U_3—LS	X-ray counter—Con.	X_4—HS X_5—HS X_{m1}—HS X_{m2}—HS X_1—LS X_{m1}—LS
Electron temperature no. 2	T_1—HS T_2—HS T_3—HS T_m—HS T_1—LS T_2—LS T_3—LS	Cosmic ray	C_1—HS C_2—HS C_3—HS C_4—HS C_5—GS C_6—HS C_1—LS C_2—LS C_3—LS C_4—LS C_5—LS C_6—LS
Mass spectrometer	I_1—HS I_2—HS I_3—HS I_{m1}—HS I_{m2}—HS		
Lyman-alpha	L—HS L—HS	Electron density	E_1—HS E_2—HS E_3—HS E_4—HS E_{m1}—HS E_{m2}—HS E_{m3}—HS E_{m4}—HS E_1—LS E_2—LS E_3—LS E_4—LS E_{m1}—LS E_{m2}—LS E_{m3}—LS E_{m4}—LS
Aspect	A_1—HS A_2—HS A_3—HS A_3—LS		
Performance parameters	P—HS PV_1—HS PV_2—HS Pt_1—HS		
X-ray counter	X_1—HS X_2—HS X_3—HS		

LS encoder sequence to begin 20 milliseconds earlier. This "blipper" operates once for each LS encoder sequence until synchronization is achieved between the two encoders.

Programmer and Tape Recorder

The main function of the programmer is to control the transmission of LS and HS encoder data to the ground station. A block diagram of the programmer is shown in Figure 5-18.

To transmit the data stored by the tape recorder, an RF command is sent to the satellite from a ground station. The command receiver sends a pulse to the programmer, at which time the programmer (1) disconnects the HS encoder from the transmitter, (2) disconnects the tape recorder input from the LS encoder, and (3) gates a 320.83-cps signal for 2 seconds to the transmitter and tape recorder. The 2 seconds of 320.83 cps is thus transmitted and, at the
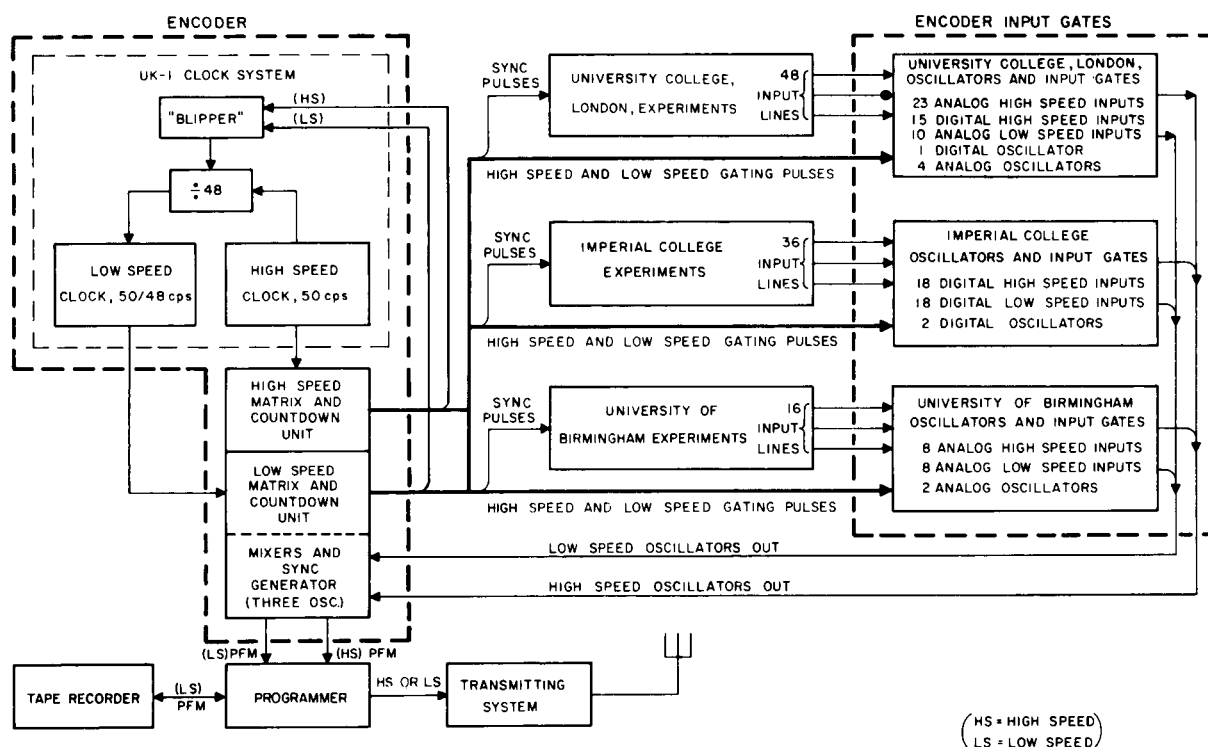
38

ENCODER

UK-I CLOCK SYSTEM

"BLIPPER" (HS) (LS)

÷ 48

LOW SPEED CLOCK, 50/48 cps

HIGH SPEED CLOCK, 50 cps

HIGH SPEED MATRIX AND COUNTDOWN UNIT

LOW SPEED MATRIX AND COUNTDOWN UNIT

MIXERS AND SYNC GENERATOR (THREE OSC.)

SYNC PULSES — UNIVERSITY COLLEGE, LONDON, EXPERIMENTS — 48 INPUT LINES

HIGH SPEED AND LOW SPEED GATING PULSES

SYNC PULSES — IMPERIAL COLLEGE EXPERIMENTS — 36 INPUT LINES

HIGH SPEED AND LOW SPEED GATING PULSES

SYNC PULSES — UNIVERSITY OF BIRMINGHAM EXPERIMENTS — 16 INPUT LINES

HIGH SPEED AND LOW SPEED GATING PULSES

LOW SPEED OSCILLATORS OUT

HIGH SPEED OSCILLATORS OUT

ENCODER INPUT GATES

UNIVERSITY COLLEGE, LONDON, OSCILLATORS AND INPUT GATES
23 ANALOG HIGH SPEED INPUTS
15 DIGITAL HIGH SPEED INPUTS
10 ANALOG LOW SPEED INPUTS
1 DIGITAL OSCILLATOR
4 ANALOG OSCILLATORS

IMPERIAL COLLEGE OSCILLATORS AND INPUT GATES
18 DIGITAL HIGH SPEED INPUTS
18 DIGITAL LOW SPEED INPUTS
2 DIGITAL OSCILLATORS

UNIVERSITY OF BIRMINGHAM OSCILLATORS AND INPUT GATES
8 ANALOG HIGH SPEED INPUTS
8 ANALOG LOW SPEED INPUTS
2 ANALOG OSCILLATORS

(LS) PFM (HS) PFM

TAPE RECORDER — (LS) PFM — PROGRAMMER — HS OR LS — TRANSMITTING SYSTEM

(HS = HIGH SPEED, LS = LOW SPEED)

FIGURE 5–15. Ariel I encoder function diagram.

FIGURE 5-16

FRAME	CHANNEL 0	1	2	3	4	5	6	7	8	9	10	11	12	13	14	15
0	S	C_1	C_2	C_3	E_3	E_4	E_1	E_2	T_1	T_2	U_1	U_2	I_1	I_2	E_1	E_2
1		C_4	C_5	C_6												
2		T_3	L	E_{m_1}												
3		T_m	A_1	E_{m_2}												
4		U_3	A_2	E_{m_3}												
5		U_m	R_2	P												
6		I_3	X_{m_1}	X_{m_2}												
7		I_{m_1}	I_{m_2}	R_1												
8		C_1	C_2	C_3												
9		C_4	C_5	C_6												
10		T_3	L	E_{m_1}												
11		T_m	A_1	E_{m_2}												
12		U_3	A_3	E_{m_4}												
13		P	R_1	P												
14		I_3	X_1	X_2												
15		X_3	X_4	X_5												

FIGURE 5–16. High speed encoder telemetry channel allocation.

FIGURE 5-17

FRAME	CHANNEL 0	1	2	3	4	5	6	7	8	9	10	11	12	13	14	15
0	S	X_1	X_{m_1}	E_4	E_1	E_2	E_3	X_1	C_1	C_2	C_3	C_4	X_1	A_3	C_5	C_6
1	S	X_1	X_{m_1}	E_{m_4}	E_{m_1}	E_{m_2}	E_{m_3}	X_1	T_1	T_2	T_3	L	X_1	U_1	U_2	U_3

FIGURE 5–17. Low speed encoder telemetry channel allocation.

same time, recorded on the tape recorder. The transmitted pulse signals receipt of the command, and the tape recorder playback follows immediately.

At the end of the 2 seconds of 320.83 cps the programmer (1) switches the tape recorder from record to playback and simultaneously shifts the tape speed to 48 times its record speed, and (2) connects the transmitter to the tape recorder.

Transmission of tape recorder playback for a period of 125 to 134 seconds is controlled by a timer in the tape recorder. This period of time is sufficient to play back all stored data. This includes a 15.4-kc pulse, approximately 42 milliseconds long, which is the 2 seconds of the 320.83-cps signal recorded immediately prior to tape recorder playback. This pulse indicates the end of LS encoder data and also serves as a time reference for correcting data from both encoders.

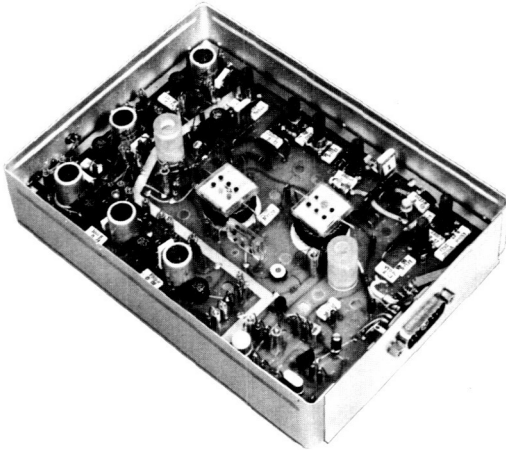The programmer also generates a 140-second

FIGURE 5–22. The command receiver.

FIGURE 5–23. Phase modulation transmitter prior to encapsulation.

Transmitter

The phase modulation transmitter is transistorized and delivers 260 milliwatts of power to the antenna system at a frequency of 136.410 megacycles. Frequency stability is ± 0.002 percent or less over a temperature range of $-20°$ to $+60°$ C. Peak deviation from the square-wave modulation is ± 1 radian, with less than 2.5-cps incidental frequency modulation and less than 3-percent amplitude modulation. Harmonic frequencies are 60 decibels below the carrier power. Total power drain from the -18 volt power supply is about 900 milliwatts. The transmitter consists of a crystal-controlled oscillator operating at a frequency of 68.205 megacycles; a buffer stage to isolate the oscillator from the phase modulator; a phase modulator that employs voltage variable capacitors to shift the phase of the carrier (the instance phase excursions are controlled by the LS and HS encoder output data); a doubler stage that multiplies the output frequency of the modulator to 136.410 megacycles; a driver stage that amplifies the doubler output power to about 60 milliwatts; a final amplifier that delivers 250 milliwatts to an antenna load impedance of 50 ohms; and a harmonic filter to prevent radiation of unwanted harmonics of the carrier frequency. (See Figures 5–23, 5–24, and 5–25.)

RF Antennas

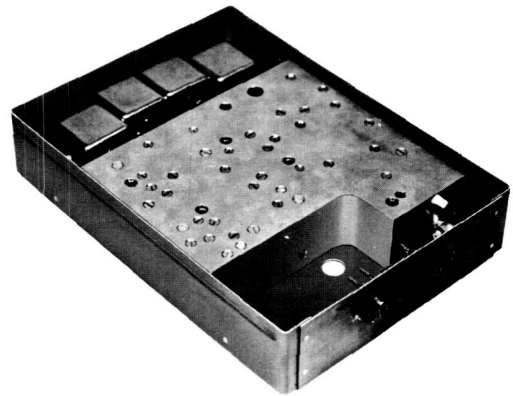The Ariel I spacecraft RF antenna system includes a coaxial hybrid power divider, coaxial
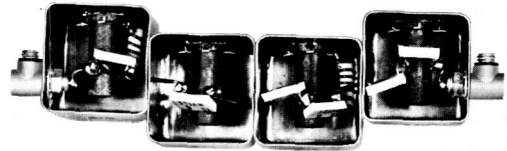

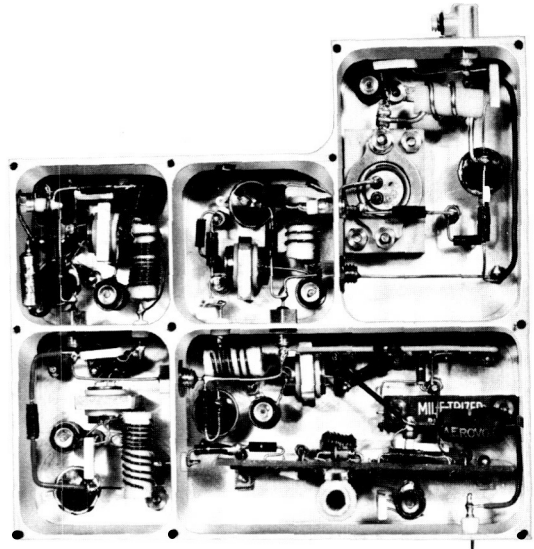
FIGURE 5–24. Transmitter RF filter.

FIGURE 5–25. Transmitter subassembly.

phasing lines, and a canted turnstile antenna. The hybrid power divider and filter provides about 20-decibel isolation between the command receiver and the transmitter. The antennas are driven from the base, each pair acting as a dipole, with the dipole pairs in

42

phase quadrature. Radiation in the plane of the turnstile is essentially linear, while circular polarization is obtained along the spin axis. The total power radiated varies with satellite aspect from +2 to −4 decibels relative to an isotropic radiator. Spacecraft commands are received through the same antenna system and have about the same pattern, but see an additional 2-decibel loss because of mismatch at the command frequency.

Power System

Power to the spacecraft electronics is provided by a solar cell array and two battery packs. Power control and regulator circuits include a shunt voltage limiter, a battery charging current limiter, a battery switching network, an undervoltage detector, a hold-off relay and turn-on plug, and several dc to dc converters.

Solar Cell Array

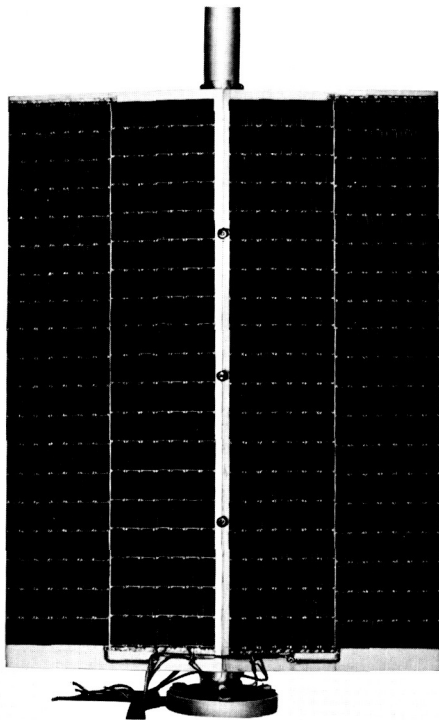The solar cell array consists of four solar paddles (Figure 5–26) arranged in a series-

FIGURE 5–26. Solar cell array.

parallel matrix and furnishes 0.5 to 2 amperes at 15 volts, depending on the spacecraft aspect

to the sun. The solar cells are p-n type silicon cells that perform as photoelectric converters. The cells are flat mounted, of gridded construction, and exhibit a high efficiency. While the spacecraft is orbiting in sunlight, the solar cells power all electronic subsystems on board the spacecraft and supply a charging current to the two battery packs.

Battery Packs

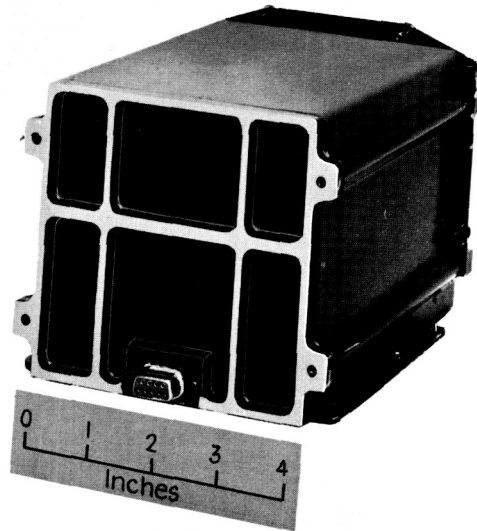Each battery pack (Figure 5–27) consists of

FIGURE 5–27. Battery pack.

ten individual cells connected in series. The cells are nickel-cadmium, sintered-plate type, hermetically sealed in a stainless-steel case. Each cell has a nominal potential of 1.3 volts. All ten cells have a nominal output of 13 volts.

Shunt Voltage Limiter

The shunt voltage limiter regulates the solar paddle output voltage to 14.5 volts. Excess power from the solar paddles is dumped through a pair of power resistors located on the arms that extend the solar paddles; the dumping is controlled by a pair of power control transistors.

Battery Charging Current Limiter

The battery charging current limiter (Figure 5–28) regulates the battery charging current to a value not in excess of 0.5 ampere. This circuit prevents the generation of hydrogen in the batteries due to excessive charging currents.
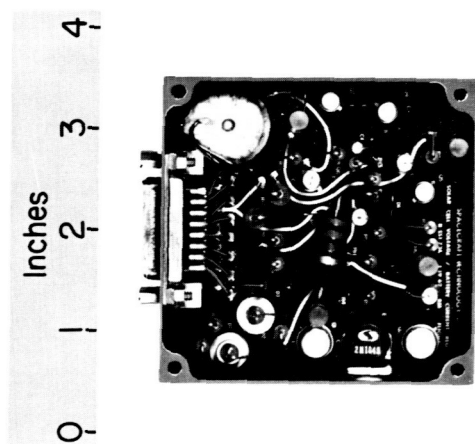
43

FIGURE 5–28. Battery current regulator.

Battery Switching Network

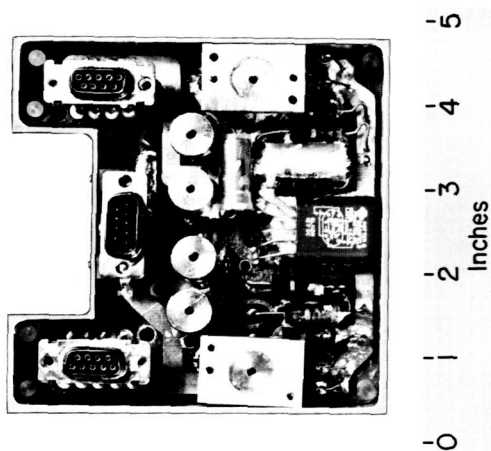The battery switching network (Figure 5–29)

FIGURE 5–29. Battery selector.

connects the battery with the highest voltage to operate the spacecraft. The other battery is connected to the solar cell array and receives a trickle charge from the array. When the voltage difference between the two batteries exceeds 1.2 volts, the standby battery is connected to operate the spacecraft.

Undervoltage Detector

The undervoltage detector (Figure 5–30) disconnects both battery packs from the spacecraft electronics when the output voltage of both batteries falls below the minimum acceptable level. The detector also activates a
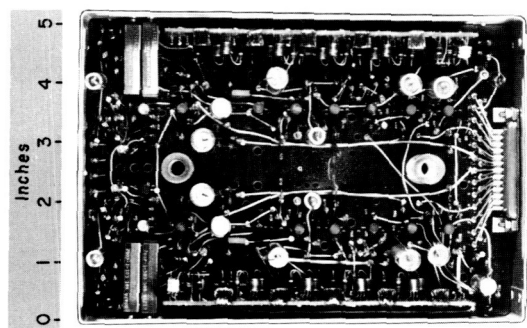

FIGURE 5–30. Undervoltage detector.

recycling timer which, after 18 hours, connects the battery output to the spacecraft electronics. During the 18 hours, the batteries are connected to the solar cell array and are charged. At the end of the 18-hour charging period, the batteries are connected to the spacecraft electronics. If, after this charging period, the batteries are still below the minimum acceptable level, the charging cycle is repeated.

Hold-Off Relay

The hold-off relay is controlled from the blockhouse and provides for turning the spacecraft power system *on* and *off* when the turn-on plug has been installed in the spacecraft. When the spacecraft is launched, the hold-off relay connects the battery to operate the spacecraft.

Dc to Dc Converters

The dc to dc converters supply the different dc voltage levels required to operate the spacecraft electronics. There are four converters in the power system: the prime converter, encoder converter, U.K. converter, and undervoltage detector converter.

The prime converter (Figure 5–31) is connected to the main powerline at the output of the undervoltage relay. The outputs of this converter are +12 and −18 volts, regulated to ±1 percent at 80-percent efficiency. This converter supplied power to the transmitter, command receiver, programmer, encoder converter, and U.K. converter.

The encoder converter (Figure 5–32) furnishes the +1.9, −4.0, −6.2, −2.7, and +6.7 volts to the encoder. The −2.7 volts is regulated to 0.25 percent; all the remaining voltages are
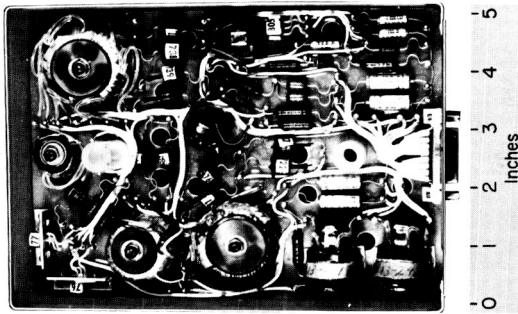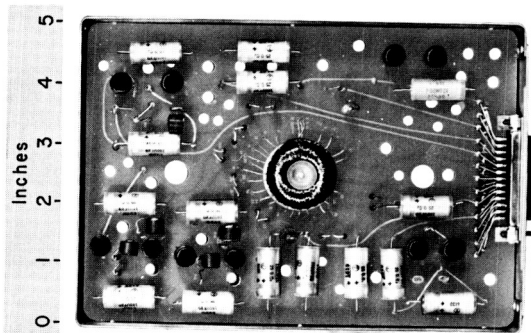
FIGURE 5–31. Prime converter.

FIGURE 5–32. Encoder converter.

regulated to ±5 percent. This converter has an efficiency of about 30 percent.

The U.K. converter (Figure 5–33) supplies all power to the experiments. The output voltages are +6.5, +15, and −6.5 volts—all at ±5 percent; −9.0 volts at ±10 percent; 12 volts at −8 percent; −15 volts at ±7 percent; and 24 volts at ±8 percent. The overall efficiency is about 60 percent.
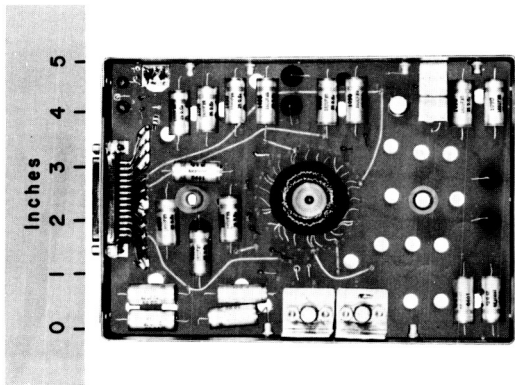
The undervoltage detector circuit converter

FIGURE 5–33. U.K.-1 converter.

(Figure 5–34) is connected to the main power-line; this converter furnishes 15 and −18 volts,
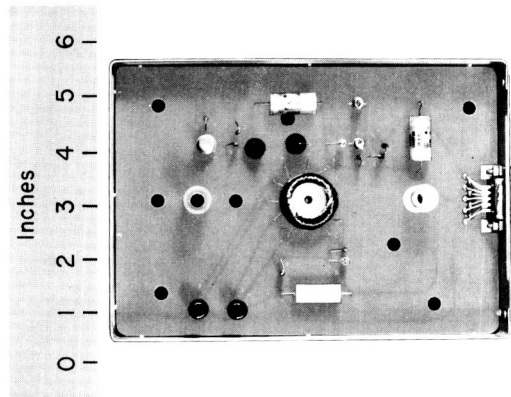
FIGURE 5–34. Undervoltage detector circuit converter.

both at ±5 percent and at an efficiency of approximately 50 percent. This converter is disconnected from the batteries only when the hold-off relay is actuated.

One-Year Timer

A 1-year timer (Figure 5–35) incorporated in the spacecraft removes power from the trans-
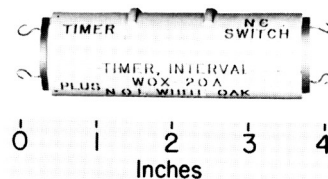
FIGURE 5–35. One-year timer.

mitter at the end of 1 year. Two timers are used in a parallel redundant hookup. The timers employ an electrochemical de-plating process having a timing accuracy of ±10 percent.

Orbital Injection Programmer

The orbital injection programmer consists of a battery-operated electronic timing system. Its function is to program the events associated with the ignition and separation of the third stage. The orbital injection programmer is activated when the third-stage motor is ignited. At this time two pressure switches provide

signals to start a 900-second timer. At the end of this timing period two pulses are applied to the silicon-controlled rectifier circuit, which in turn fires one pair of squibs. This time is designated t_1. The t_1 output from the 900-second timer starts a 60-second timer. At intervals of 60 seconds from time t_1, pulses are provided to the silicon-controlled rectifier circuit to fire three additional pairs of squibs. The times of these firings are designated t_2, t_3 and t_4. The orbital injection programmer is redundant throughout and is operated from two separate batteries. Failure of either programmer will not prevent the squib firing sequence from being completed. Accuracy of the timing cycles is 5 percent or better. The events at the squib firing times are: despin (t_1), boom release (t_2), paddle release (t_3), and separation (t_4). The three modules that make up this timer are shown in Figure 5–36.

WIRE HARNESS

One of the early steps of the integration process was to plan the construction of the wire harness. The wire harness design was based on information from both the U.K. and the U.S. (GSFC) experimenters. This information included a wiring table listing the origin, function, and destination of each wire and the size, type, and color of each wire. All pin assignments were made by the individual experimenters and electronic subsystems designers.

Teflon-insulated wire was chosen for the harnesses on the basis that its outgassing properties were negligible. For all shielded leads, no. 22 shielded Teflon insulated wire was used. Test points were brought out to the turn-on plug to eliminate the need for separate test points. The number of test points brought out was limited to only those that were absolutely essential for checkout of the spacecraft. The solar paddle interconnections were facilitated by a mating 37-pin connector pair, with the common voltages bussed together on connectors at the solder-pot end of the contacts. This made it possible to remove the harness when the satellite was disassembled
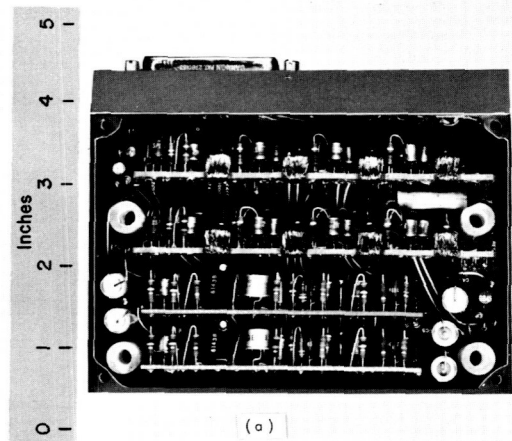
(a)
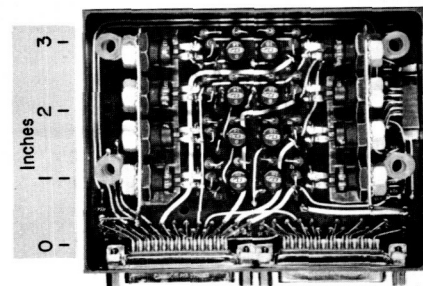
(b)
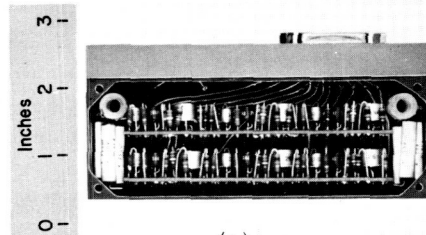
(c)

(a) 900-second timer
(b) Silicon-controlled rectifier circuit
(c) 60-second timer

FIGURE 5–36. Orbital injection programmer.

for inspection after tests. Also, the high voltage lines for the x-ray experiment were soldered and the joint encapsulated to eliminate the corona problem. To disassemble the x-ray detector from its associated printed circuit card, it was necessary to cut off the encapsulated solder joint in the high voltage (1600 volt) line.

CHAPTER 6

Systems Integration

ELECTRONIC INTEGRATION TASK

Electronic integration of the subsystems was the responsibility of the Electronic Integration Group of NASA's Goddard Space Flight Center.

The task of integrating the subsystem included the molding of the subsystems into a compatible system, testing the system and evaluating the results, solving interface problems, and monitoring the spacecraft's signals until launch.

To successfully execute these tasks, the integration group had to (1) have a thorough knowledge of all subsystems (mechanical and electronic), (2) design and fabricate a wiring harness, (3) design and fabricate a test stand for evaluating the performance of the spacecraft's electronics, and (4) originate test procedures for each electronic subsystem as well as for the integrated system.

ELECTRONIC INTEGRATION PLAN

Integration of the electronic subsystems required the cooperation and assistance of the experimenters in the United Kingdom and of many departments and branches at NASA's GSFC. Directly involved are the Project Managers (United Kingdom and United States), the U.K. experimenters, GSFC support subsystem designers, the GSFC Systems Integration Branch personnel, GSFC Data Systems personnel, the GSFC Environmental Test Facility personnel, and the vendors and suppliers.

The step-by-step plan for the integration of the Ariel I spacecraft subsystems was as follows:

1. To collect design and performance specifications for all electronic subsystems of the spacecraft.

2. To evaluate the subsystem specifications with the dual purpose of gaining knowledge of the subsystem operation and of designing a data processing system capable of monitoring the performance of all the electronic subsystems as an integrated electronic system within a reasonable time of 1 to 3 hours.

3. To obtain electronic subsystem wiring information for building a spacecraft wiring and test harness.

4. To build a power control panel to be used with the spacecraft wiring and test harness for integration and interference testing.

5. To design and build test panels for bench-testing the electronic subsystems as required.

6. To work out with the mechanical engineers, who assemble the spacecraft, any problems that may arise from wiring requirements (e.g., accessibility of connectors, holes in the spacecraft structure for routing of wires, supports, and tiedown fixtures for the wires).

7. To write a test procedure for the complete electronic system of the spacecraft from information and experience gained with electronic subsystems operated individually on the test bench.

8. To detect and assist in resolving problems due to electrical interference or incompatibilities between electronic subsystems as they are connected into the spacecraft.

9. To arrange with Test and Evaluation (T&E) Division, GSFC, to supply the exciters for the experiment sensors.

10. To arrange with T&E Division, GSFC, for the necessary wiring connections through the walls of the environmental test chambers.

11. To monitor the spacecraft performance as it undergoes all phases of integration testing, environmental testing, and launch site testing.

12. To report to the project coordinator and the subsystem designers all failures observed in an electronic subsystem during the three test phases specified in step 11.

PERFORMANCE EVALUATION

General

The task of the Ariel I Integration Group (GSFC) was to weld the electronic subsystems into an operational spacecraft. To accomplish this task, the Integration Group tested each subsystem to determine normal operating parameters, tested the integrated system for compatibility, and monitored the spacecraft performance during the environmental tests and launching.

For the convenience of presentation, the various test phases will be referred to as *integration* testing, *environmental* testing, and *launch site* testing.

Integration Testing

Integration testing consisted of developing bench test procedures for each subsystem, developing an overall system test procedure, connecting all subsystems to the wire harness, and testing the spacecraft subsystems both individually and as an integrated operational spacecraft.

To develop and perform bench tests, the Ariel I Integration Group had to gather specifications information on operating characteristics and input-output data for each subsystem. This was accomplished by using a wiring and test procedure checklist, which was distributed to the experimenters. The experimenters completed the checklists and returned them to the Integration Group. A bench test procedure for the cosmic ray experiment was developed from the data received from the experimenter. After approval by the experimenter, the procedure was circulated among all concerned as a guide for the development of the remaining bench test procedures.

Each subsystem, after proper bench testing, was installed in the spacecraft. Test points were incorporated in the wiring harness, and test cables connected these to a test stand. The test stand was used to check the compatibility of the integrated subsystems. Transients, power consumption, automatic controls, and operation of each subsystem were checked. If the results of any test were unsatisfactory, the Integration Group reported and sometimes recommended changes to correct the incompatibility. After much testing, redesign, and effort, the Integration Group developed a completely integrated electronic system. During this time the Integration Group developed the system test procedure.

Samples of spacecraft data sheets used during integration and environmental testing are shown in Figures 6–1 and 6–2.

Environmental Testing

The major objectives of the test program are twofold: (1) to determine the ability of the design to meet all performance requirements, and (2) to demonstrate the quality and dependability of the flight hardware. The first of these objectives is accomplished by qualification testing of prototype hardware. The reliability program and acceptance testing are directed toward the achievement of the second objective.

Qualification testing is conducted on the prototype spacecraft complete with simulated or prototype experiment, on the individual prototype experiments, and on prototype subassemblies. Qualification tests include environmental tests as well as tests that are entirely functional in nature. An environmental test has the following essential features: (1) pre-exposure examination and functional check, (2) exposure to environment, (3) functional check during or after exposure, and (4) post-exposure examination.

Environments to which prototype items are subjected are sinusoidal and random vibration, acceleration, shock, static loading, humidity, temperature, and thermal vacuum. Hermetically sealed items are given a leak-detection test. The environments simulated by this series of tests are those expected to be imposed by storage, handling, transportation, prelaunch, boost, separation, and orbital flight.

In mechanical tests, the test levels are 1.5 times the maximum levels expected during transportation, handling, and launch.

In prototype temperature tests at atmospheric pressure and in thermal vacuum tests, temperatures above the maximum and below the minimum orbital operating temperatures are imposed on operating prototype items. In the thermal vacuum test, these temperature conditions are combined with space simulations at a vacuum of at least 1×10^{-5} mm Hg. Prototype items, while nonoperative, are exposed during the atmospheric temperature test to the maximum and minimum temperatures to which they could be subjected during storage and transportation. Humidity tests are performed as applicable. Equipment is designed to be operable between 0° and +50°C in orbital environment.

Acceptance testing, conducted on flight items, is limited to the environments of vibration, temperature, and thermal vacuum. The levels of test environment are no greater than the environments expected during launch and orbit.

Performance data developed throughout the course of the test program are used to the extent applicable for verification of reliability. Additional testing of components and subassemblies is conducted for the specific purpose of supporting the reliability program (References 14 through 17).

Launch Site Testing

Two complete ground stations, each consisting of two special telemeter radio receivers, were used to monitor the spacecraft performance at the launch site. The main station was trailer-mounted, and the backup station was placed in hangar AE at the Atlantic Missile Range. The backup station was operated in parallel with the main station during testing.

The special telemeter radio receivers were fed by two 136-megacycle preamplifiers connected to a nine-element yagi antenna. A frequency counter and signal generator were used to measure the spacecraft transmitter frequency.

Launch site testing included a complete system test of the spacecraft in the trailer upon arrival at Cape Canaveral, Florida. All other tests were exclusively by RF link from the spin facility and launch pad gantry. Each test or checkout included a complete analysis of test data.

Several practice runs of the final pre-launch countdown were performed.

DESCRIPTION OF TEST STAND

The performance evaluation test stand is pictured in Figure 6–3 and is shown in block diagram form in Figure 6–4. This equipment can be classified into functional groups as follows: (1) power control system, (2) RF system, (3) sensor exciter panel, (4) data reduction system, and (5) data recorders.

Power Control System

This system simulates the power output, internal impedance of the solar array, and the sunlight/darkness cycling that the spacecraft will experience in orbit. The internal impedance and power output of the solar array is simulated by a 17.5-ohm resistor in series with a 30-volt power source, arranged as shown in Figure 6–5. The resistor and power supply form the Thevenin equivalent of the solar array and produce the same voltage and current as that of the array. The diode, connected between the resistor and the timer, prevents reverse current from flowing through the power supply from the spacecraft battery system should the power supply voltage accidentally fall below the battery voltage. Throughout the testing phase, the spacecraft was powered electrically by the solar array simulator.

The recycling timer is on for 60 minutes and off for 40 minutes; this simulates the least favorable sunlight-to-darkness ratio expected during the 100-minute orbit.

During the prototype tests a meter panel was used to measure the voltages and currents used by each subsystem (Figure 6–4). Each current meter is shunted by a shorting switch; this enables the operator to insert or remove the meter from the circuit. Individual current meters were used for each line that was monitored. A single voltmeter was switched to the voltage point to be measured. The voltage readings were normalized by placing a miniature potentiometer at each voltage test point, and the potentiometers were adjusted so that the

TELEMETERED DATA OF EXPERIMENTS AND PARAMETERS

FIGURE 6-1. Spacecraft data sheet used during integration and testing.

CONTINUOUS MONITOR OF GODDARD ELECTRONICS DURING TESTING

TEST				PAYLOAD ___ DATE ___ TIME ___ TEST CONDITIONS ___ PERFORMED BY ___	PAYLOAD ___ DATE ___ TIME ___ TEST CONDITIONS ___ PERFORMED BY ___	PAYLOAD ___ DATE ___ TIME ___ TEST CONDITIONS ___ PERFORMED BY ___	PAYLOAD ___ DATE ___ TIME ___ TEST CONDITIONS ___ PERFORMED BY ___	PAYLOAD ___ DATE ___ TIME ___ TEST CONDITIONS ___ PERFORMED BY ___	PAYLOAD ___ DATE ___ TIME ___ TEST CONDITIONS ___ PERFORMED BY ___
POWER SYSTEM CHECK	VOLTAGE	BATTERY A	CHARGE						
			DISCHARGE						
		BATTERY B	CHARGE						
			DISCHARGE						
	SYSTEM VOLTAGE (DUMPING RESISTORS)								
	CURRENT	BATTERY A	COMMAND						
			NON-COMMAND						
		BATTERY B	COMMAND						
			NON-COMMAND						
	POWER DRAIN ON BATTERIES		COMMAND						
			NON-COMMAND						
	VOLTAGES	U R CONVERTER	+6.5 v						
			-6.5 v						
			-9 v						
			+12 v						
			-15 v						
			+24 v						
		PRIME CONVERTER	+12 v						
			-18 v						
		PROGRAMMER CONVERTER	+15 v						
TRANSMITTER CHECK	TRANSMITTER POWER								
	TRANSMITTER FREQUENCY								
ENCODER CHECK	CHECK IF PAYLOAD IS IN SYNC								
	A - HS COUNT								
	B - LS COUNT								
	HS DIGITAL OSCILLATOR PERIODS CHANNEL 0	FRAME 0 (191.4 - 197.6)							
		FRAME 1 (220.9 - 223.4)							
		FRAME 2 (175.6 - 181.6)							
		FRAME 3 (220.9 - 223.4)							
		FRAME 4 (157.8 - 163.6)							
		FRAME 5 (220.9 - 223.4)							
		FRAME 6 (140.9 - 467.1)							
		FRAME 7 (220.9 - 223.4)							
		FRAME 8 (122.2 - 127.4)							
		FRAME 9 (220.9 - 223.4)							
		FRAME 10 (105.6 - 110.6)							
		FRAME 11 (220.9 - 223.4)							
		FRAME 12 (86.7 - 92.1)							
		FRAME 13 (220.9 - 223.4)							
		FRAME 14 (68.5 - 72.9)							
		FRAME 15 (220.9 - 223.4)							
	LS DIGITAL OSCILLATOR PERIODS CHANNEL 0	FRAME 0 (220.9 - 223.4)							
		FRAME 1							
		FRAME 0 (220.9 - 223.4)							
		FRAME 1							
BATTERY SWITCHING TEST	INITIAL VOLTAGE ON EXT POWER SUPPLY A								
	INITIAL VOLTAGE ON EXT POWER SUPPLY B								
	VOLTAGE ON A TO SWITCH TO B								
	VOLTAGE ON B TO SWITCH TO A								
	BATTERY SWITCHING DIFFERENTIAL (VOLTS)								
SHUNT REGULATOR TEST	VOLTAGE AT BATTERY TO CAUSE DUMPING								
	CURRENT IN RIGHT RESISTOR (ma)*								
	POWER DISSIPATION IN RIGHT RESISTOR (mw)								
	CURRENT IN LEFT RESISTOR (ma)*								
	POWER DISSIPATION IN LEFT RESISTOR (mw)								
	TOTAL CURRENT IN DUMPING CIRCUIT (ma)								
	TOTAL POWER DISSIPATED IN DUMPING CIRCUIT (mw)								
	TOTAL CURRENT INPUT TO SATELLITE (ma)								
TAPE RECORDER PLAYBACK	PROGRAMMER BACK UP TIMER COUNT								
	PLAYBACK BLANK PERIODS 1638 - 6531								
UNDER VOLTAGE TEST	VOLTAGE AT BATTERY CAUSING UNDER VOLTAGE								
	UNDER VOLTAGE COUNT (SPEED UP)								
	UNDER VOLTAGE COUNT (NORMAL 18 HOURS)								

* RESISTOR VALUES ARE 10 OHMS

FIGURE 6–2. Sample spacecraft data form.

voltmeter would show a midscale indication if the voltage was correct—which permits rapid voltage checking. Each power line to a subsystem was switch-controlled from the meter panel; this facilitated deactivation of individual subsystems. Also, each power converter was monitored at the input and switch-controlled at the output; this made it possible to remove any converter from its load and switch in external power. These switching arrangements greatly simplified many tests.

RF System

The RF system receives and demodulates the RF signal from the transmitter, measures transmitter power and frequency, and presents an RF load to the transmitter and the command receiver. The RF system consists of a simulated command transmitter, an RF power monitor, a UHF counter, and a special-purpose telemeter radio receiver. The simulated command transmitter consists of a crystal oscillator followed by an amplitude-modulated RF stage.
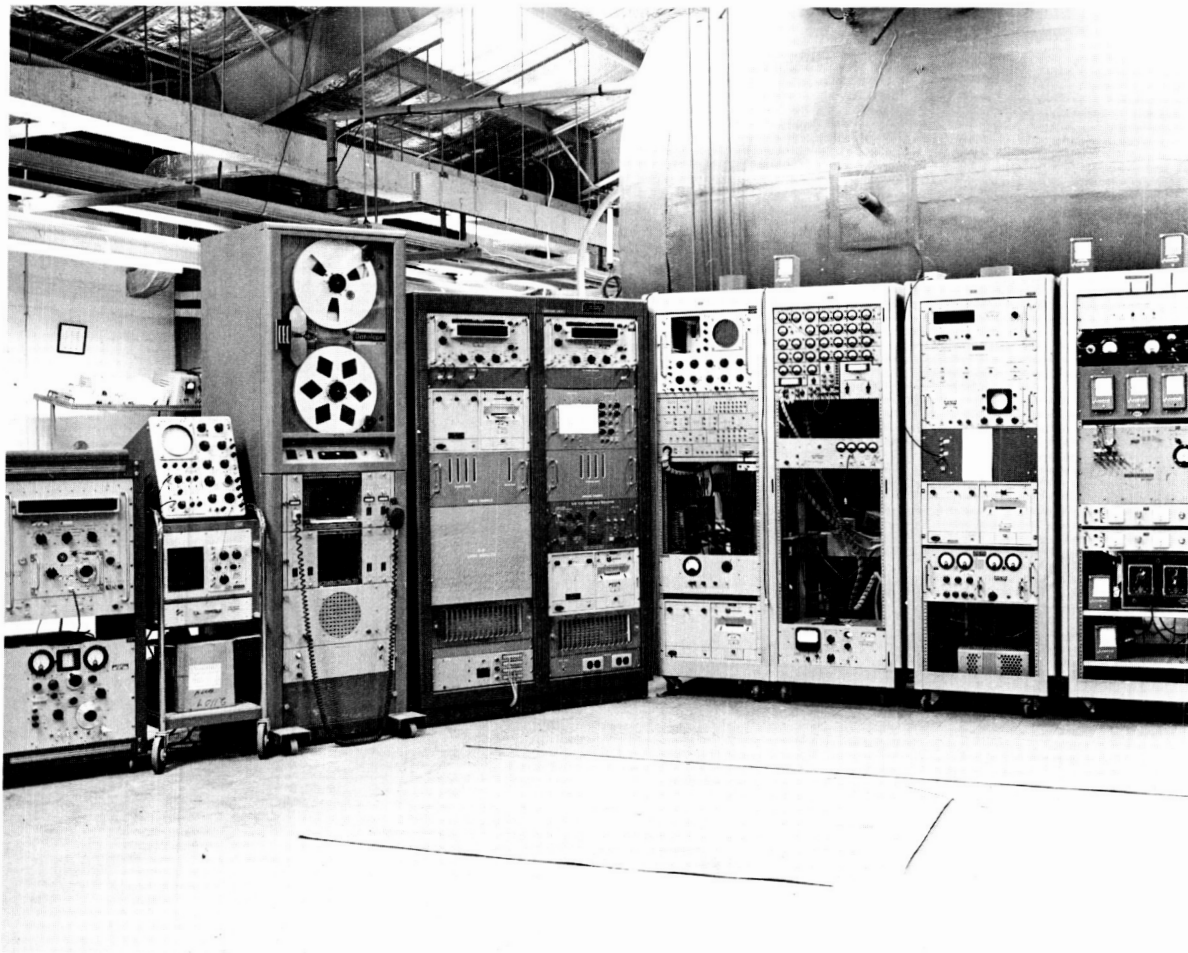
FIGURE 6–3. Ariel I test stand, front view.

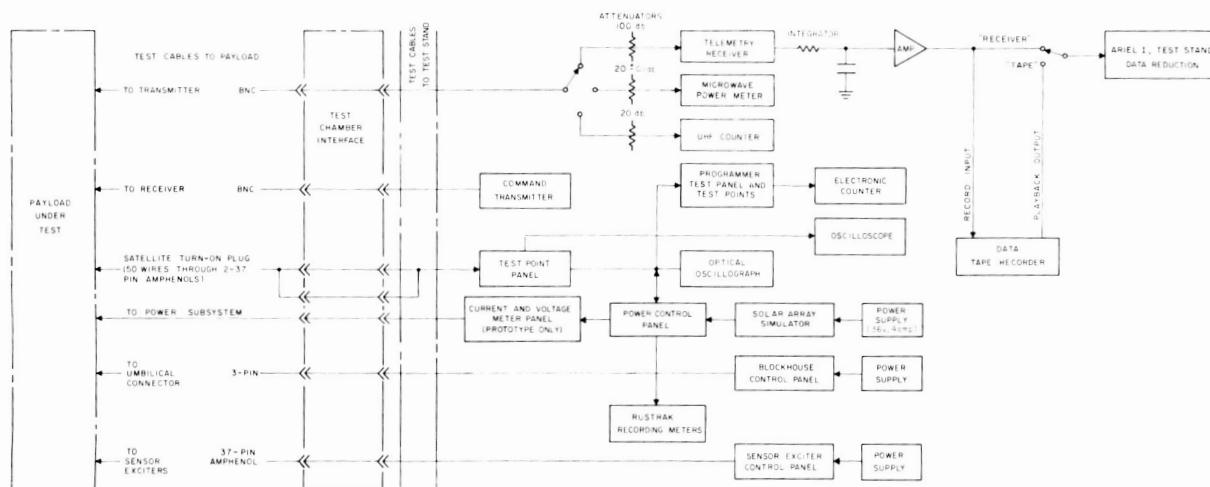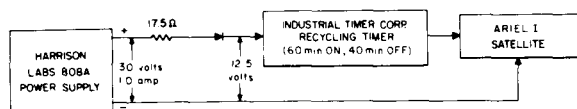FIGURE 6-4. Block diagram of test stand.

53

FIGURE 6–5. Block diagram of solar cell array simulator.

The modulating signal is generated from an L-C audio oscillator, adjusted to the command subcarrier frequency. The total power output from the transmitter is about 80 milliwatts. At the launch site it was necessary to build a power amplifier (low decibel gain) to boost the power output, because the spacecraft was several miles from the test stand.

Sensor Excitor Panel

This panel provides artificial stimulation to the aspect sensor, the electron density sensor, and the Lyman-alpha sensors. The aspect stimulator is a transistor driver relay circuit that intermittently illuminates three flashlight bulbs. The flash rate and flash separation of the bulbs corresponds to a specific spin and aspect angle. The electron-density stimulator consisted of an 8-inch plastic disk with a pie-shaped piece of brass shim stock attached to it; this was mounted on the electron density boom and rotated by a 1-rpm synchronous motor. Two notches on the rim of the disk enabled a microswitch, with a roller-cam follower, to position the disk in one to two positions: (1) maximum proximity between brass and plates, and (2) minimum proximity between brass and plates. This is illustrated in Figure 6–6.

The Lyman-alpha sensor excitor consists of a hydrogen-discharge tube and a high-voltage power supply. The discharge tube was used in the vacuum chamber and illuminated one of the Lyman-alpha sensors. The Lyman-alpha line (for ultraviolet light) is readily absorbed in
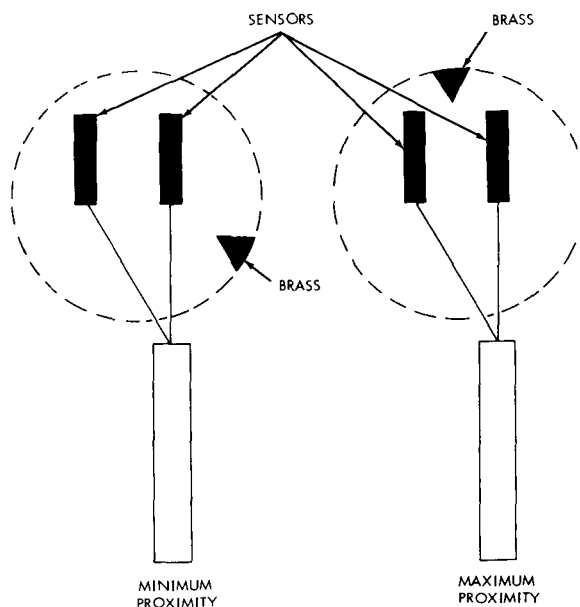

FIGURE 6–6. Electron density boom excitor.

air by water vapor and can travel only a few millimeters.

The x-ray sensor, the cosmic ray sensor, and the electron temperature probes were not excited from the sensor excitor panel. A 50-millicurie source of iron (Fe55) was used to provide 5-kilo volt x rays. A radioactive source was used to excite the cosmic ray experiment.

A diode-resistor dummy load was applied to the electron temperature probe sensors to simulate free electrons with a specific average energy.

Data Recorders

An instrumentation data magnetic tape recorder was used to record the complete demodulated RF from the spacecraft.

Printers in the Ariel I test stand data reduction system provided printed records of test stand data output.
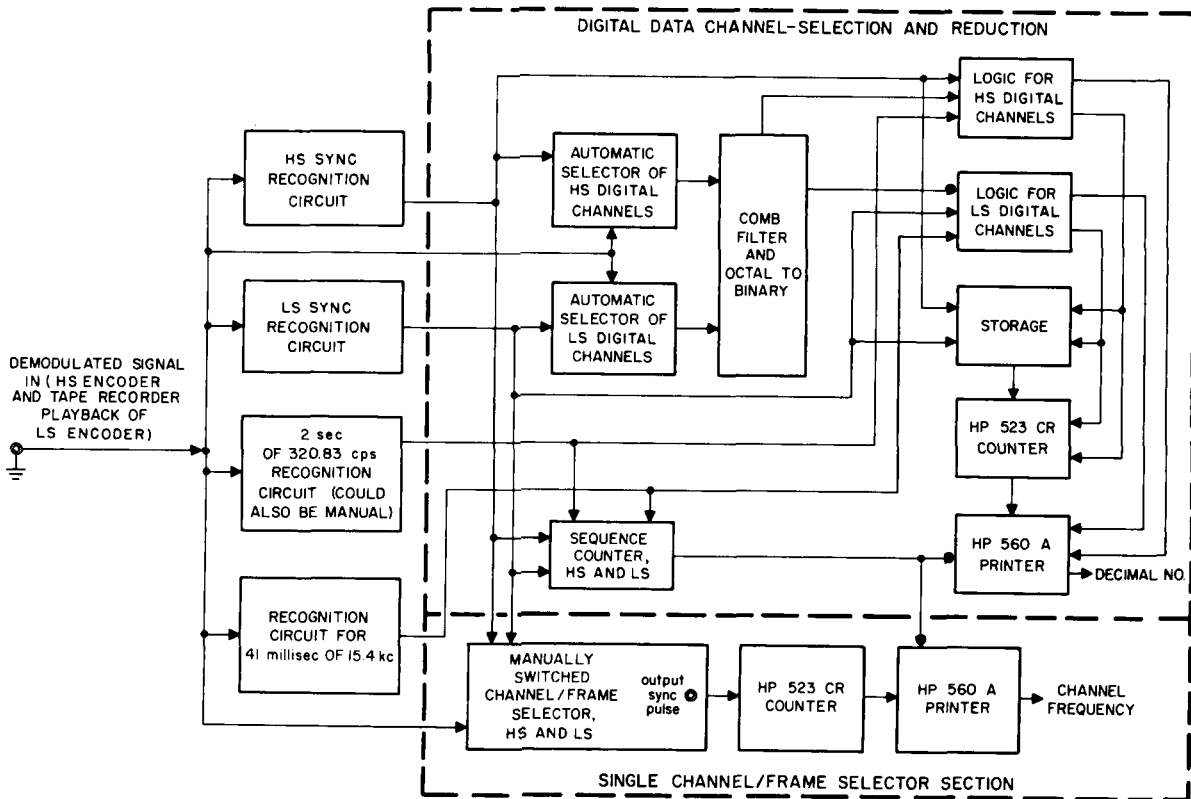
FIGURE 6–7. Test-stand data reduction system.

TEST-STAND TELEMETER DATA REDUCTION SYSTEM

The Ariel I Integration Group (GSFC) performed a study on the decoding equipment requirements. The Data Instrumentation Division of GSFC developed and supplied the system (Figure 6–7). The requirements and development of this system are discussed herein.

The telemetered RF signal goes through a phase modulation receiver, a tracking filter, and into the PFM decoder, etc.

The input to the decoder is a series of pulses in the frequency range from 4.5 to 15.4 kilocycles. The length of the pulses is 10-millisecond duration, and the pulses are separated by 10 milliseconds except for the frame sync pulses, which last for 15 milliseconds and are preceded by a space of 5 milliseconds. The frame sync pulses, in addition to being coded by an additional millisecond of pulse width, are also coded in frequency as listed in the following charts.

Frame Sync Pulses			
High Speed Encoder		Tape Recorder Playback of Low Speed Encoder	
Channel 0, Frame	Frame Sync Pulse Frequency (cps)	Channel 0, Frame	Frame Sync Pulse Frequency (cps)
0	4, 500	0	4, 500
1	5, 140	1	--------
2	4, 500		
3	5, 600		
4	4, 500		
5	6, 230		
6	4, 500		
7	6, 960		
8	4, 500		
9	8, 015		
10	4, 500		
11	9, 250		
12	4, 500		
13	11, 190		
14	4, 500		
15	14, 120		

55

Channel zero in each frame for both HS and LS encoders is used for frame sync pulses. All the remaining channels are either digital data channels or analog data channels. The pulse frequency of the analog data channels varies from 5 to 15 kilocycles. The pulse frequency for the digital data channels will be one of the following eight values.

Digital Data Channel Pulses from HS Encoder and Tape Recorder Playback of LS Encoder

Binary Bit Input to Digital Oscillator	Frequency (cps)
0 0 0	5,140
0 0 1	5,600
0 1 0	6,230
0 1 1	6,960
1 0 0	8,015
1 0 1	9,250
1 1 0	11,190
1 1 1	14,120

General Requirements for Test-Stand Data Reduction Equipment

The HS and LS encoders are synchronized, and the data from the two encoders are related. Since the data from the two encoders are transmitted at different times, it is necessary to reconstruct the time relation.

It was therefore required that, in addition to other requirements, the test-stand data reduction equipment have a four-place decimal counter to count each encoder sequence (HS or LS), independently of whether or not a data print-out occurred during the sequence.

Significance of Digital Data Channels and the Required Reduction and Presentation of Their Data

The cosmic ray and x-ray experiments have HS encoder digital data channels.

Cosmic Ray Experiment

The cosmic ray experiment has two separate binary counters. Binary counter no. 1 has HS encoder channels $C_1(1-0)$ $(1-8)$; $C_2(2-0)$ $(2-8)$; $C_3(3-0)$ $(3-8)$; and $C_4(1-1)$ $(1-9)$, which represent binary bits $(2^1, 2^2, 2^3)$; $(2^4, 2^5, 2^6)$; $(2^7, 2^8, 2^9)$; and $(2^{10}, 2^{11})$ respectively. This is shown in Figure 6–8a.

In particular it should be noted that the most significant binary bit of C_4, called "Sensitivity Indicator 0 or 1," does not come from counter no. 1 and thus should be treated as a separate piece of data. In addition, the binary number stored in counter no. 1 is two times the number represented by C_1, C_2, C_3, and C_4 because binary 2^0 is not one of the digital data inputs.

Binary counter no. 2 has HS encoder channels $C_5(2-1)$ $(2-9)$ and $C_6(3-1)(3-9)$, which represent binary bits $(2^0, 2^1, 2^2)$ and $(2^3, 2^4, 2^5)$ respectively. This is shown in Figure 6–8b.

In the experiment, "Sensitivity Indicator 0 or 1" indicates the sensitivity of the discriminator that sends pulses to counter no. 2, and so it is desirable to print "Sensitivity Indicator 0 or 1" and the number stored in counter no. 2 adjacent to each other.
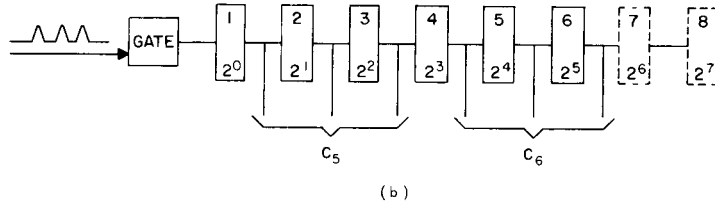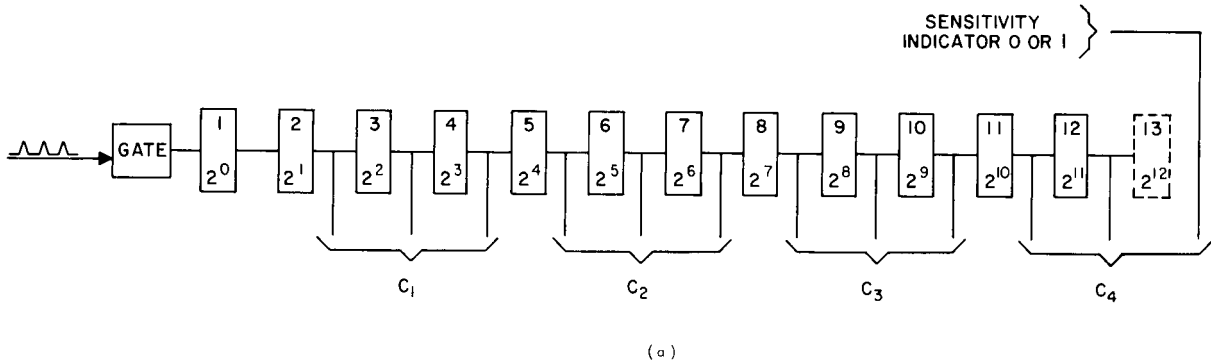
Binary counter no. 1 also has LS encoder digital data channels $C_1(8-0)$, $C_2(9-0)$, $C_3(10-0)$, and $C_4(11-0)$, which represent binary bits $(2^3, 2^4, 2^5)$; $(2^6, 2^7, 2^8)$; $(2^9, 2^{10}, 2^{11})$; and $(2^{12}, 2^{13})$ respectively. This is shown in Figure 6–9a.

In particular it should again be noted that the most significant binary bit of C^4, called "Sensitivity Indicator 0 or 1," does not come from counter no. 1 and thus should be treated as a separate piece of data. In addition, the binary number stored in counter no. 1 is four times the number represented by C_1, C_2, C_3, and C_4 because binaries 2^0 and 2^1 are not used as digital data inputs.

Binary counter no. 2 has LS encoder channels $C_5(14—0)$ and $C_6(15—0)$, which represent binary bits $(2^3, 2^4, 2^5)$ and $(2^6, 2^7, 2^8)$ respectively. This is shown in Figure 6–9b.

In the experiment, "Sensitivity Indicator 0 or 1" indicates the sensitivity of the discriminator that sends pulses to counter no. 2, and so it is desirable to print "Sensitivity Indicator 0 or 1" and the number stored in counter no. 2 adjacent to each other.
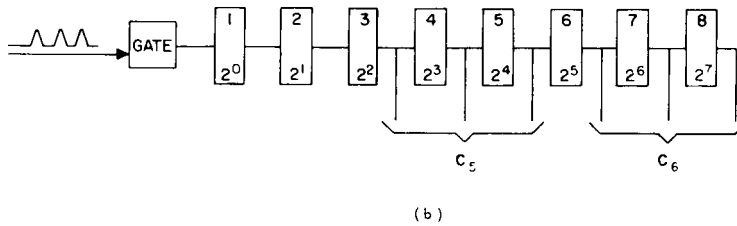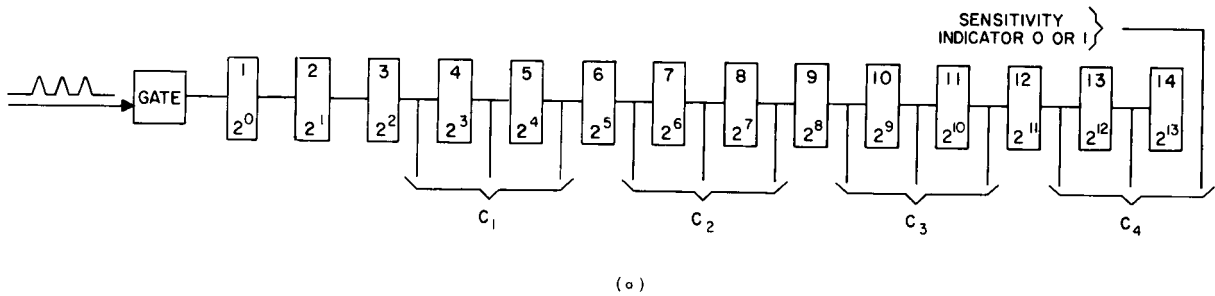
(a) Binary counter no. 1
(b) Binary counter no. 2
FIGURE 6-8. HS encoder digital data channel connections.

(a) Binary counter no. 1
(b) Binary counter no. 2
FIGURE 6–9. LS encoder digital data channel connections.

X-Ray Experiment

The x-ray experiment has one 15-stage binary counter. HS encoder channels $X_1(2—14)$ $X_2(3—14)$, $X_3(1—15)$, $X_4(2—15)$, and X_5- (3—15) represent binary bits $(2^0, 2^1, 2^2)$, $(2^3, 2^4, 2^5)$, $(2^6, 2^7, 2^8)$, $(2^9, 2^{10}, 2^{11})$, and $(2^{12}, 2^{13}, 2^{14})$ respectively. This is shown below in Figure 6–10.
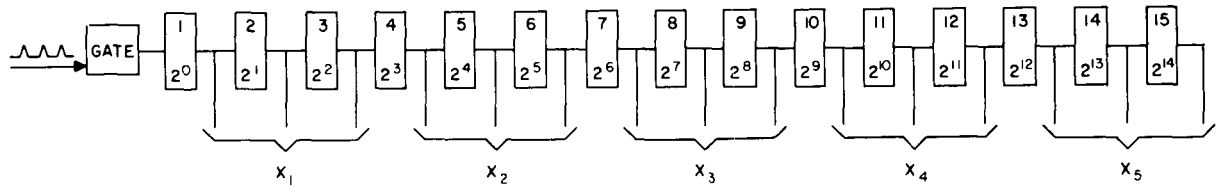

FIGURE 6–10. X-ray binary counter.

General Requirements

All numbers are to be converted to decimal before print-out. Each decimal number is to be identified as to the experimental data it represents. It will be sufficient to print out the number stored in one counter of one experiment for each HS or LS encoder sequence and to have a switch that will select which counter store will be printed. This means it would be sufficient to print $C_1(1—0)$, $C_2(2—0)$, $C_3(3—0)$, $C_4(1—1)$ as one number per HS encoder sequence; $C_5(2—1)$, $C_6(3—1)$, and "Sensitivity Indicator 0 or 1" of $C_4(1—1)$ as one number per HS encoder sequence; $C_5(2—9)$, $C_6(3—9)$, and "Sensitivity Indicator 0 or 1" of $C_4(1—9)$ as one number per HS encoder sequence; $X_1(2—14)$, $X_2(3—14)$, $X_3(1—15)$, $X_4(2—15)$, and $X_5(3—15)$ as one number per HS encoder sequence; and $C_1(8—0)$, $C_2(9—0)$, $C_3(10—0)$, and $C_4(11—0)$ as one number per LS encoder sequence. Each encoder sequence is to be counted and its number printed whenever a decimal number is printed from any of its channels.

Significance of HS and LS Encoder Analog Data Channels and the Required Reduction and Presentation of Their Data

Analog data channels are exactly what their name implies. The only reduction required for these channels is to count the frequency of the pulse. The presentation required is a print-out of pulse frequency, data channel identification, and number of encoder sequence during which the frequency pulse occurred.

It would be sufficient if the selectivity of the "Single Channel/Frame Selector Section" were limited to selecting 1 of 16 channels to be printed once for every frame of the encoder sequence. The fact that this arrangement would print the pulse frequency of any digital data channels that happen to be in the column of selected channel "X" is not a drawback, since it will allow for checking the digital oscillator pulse frequency for any drift that might begin to occur. The same considerations apply equally well to frame sync channel 0.

For channels 1, 2, and 3 the channel of interest may occur only once per HS encoder sequence, and the rest of the print-out is an inconvenience. However, for channels 0 and 4 through 15 the print-out for each frame is a distinct advantage. In the case of the LS encoder data this type of selection is acceptable with no particular advantages or disadvantages.

It was also required that an "output sync pulse" be made available on one "Output Sync Pulse" terminal. It has one distinct output at the time of Channel 0, frame 0 (0—0) at the beginning of each encoder (HS or LS) sequence. It also has another distinct output that will occur during the time of telemetering of the channel selected for print-out.

These pulses are for marking one channel of a strip chart recorder. Another channel of the strip chart recorder is connected by a wire to a test point in the satellite that monitors the voltage input to the encoder oscillator. The "Output Sync Pulses" will thus (1) identify the beginning of each encoder sequence and (2) mark that portion of the test point trace during which telemetering took place. Thus, the performance of the encoder oscillator may be checked at the same time

that performance of an experiment parameter is being checked.

Correlation of HS Encoder Data with LS Encoder Data

If an auxiliary tape recorder is used to record the demodulated playback of the satellite tape recorder, the matter of correlation of HS and LS encoder data becomes a "straightforward" procedure. It consists of the following steps:

1. Operate the satellite for a little over 1½ hours while the HS encoder digital channel data on one printer and the selected channels "X" on the other printer are being recorded.

2. Arrange for the switch that initiates the RF command signal to the satellite to also put the auxiliary tape recorder into the record mode. Operate the switch, and record the 2 seconds of 320.83-cps signal and the full playback of the tape recorder, which must include the 41 milliseconds of 15.4-kilocycle time marker.

3. Rewind the auxiliary tape recorder and play it back while obtaining digital data on one printer and selected channel "X" data on the other printer. Repeat 16 times, once for each column of channels.

4. Correlate the data by counting back six sequences from the 320.83-cps time mark on the HS encoder data records for each sequence counted back from the 15.4-kilocycle time mark on the LS encoder data records.

59

CHAPTER 7

Tracking and Data Acquisition

The Ariel I International Ionosphere Satellite was launched from Cape Canaveral, Florida, by a Thor-Delta vehicle and was placed into a near-earth elliptical orbit having an apogee of 1214 kilometers (754 statute miles, 655 nautical miles), a perigee of 390 kilometers (242 statute miles, 210 nautical miles), an inclination of 55 degrees, and an anomalistic period of 99 minutes. (On board the satellite is a single PFM–PM telemeter with a power output of 250 milliwatts. This telemetry system is being used by the Minitrack network for tracking and data acquisition.)

TRACKING

Tracking is the sole responsibility of the South Atlantic and Singapore Stations and the Minitrack network, during the active lifetime of the satellite, with the exception of the early orbit determination phase. A preliminary orbit was computed, based on nominal radius and velocity injection vectors; and an analysis of this orbit indicated that insufficient Minitrack tracking data would be obtained during the first 12 hours of operation to define the satellite's orbit. For this reason, outside tracking support was required.

The overall tracking picture is very good. An analysis of the first two weeks of operation for the Ariel I satellite has shown that sufficient tracking will be available to accurately compute and continually update the orbit. Ariel I is tracked by the following stations under GSFC control:

> Antofagasta, Chile, S.A.
> Blossom Point, La Plata, Md., U.S.A.
> Lima, Peru, S.A.

> Quito, Ecuador, S.A.
> Santiago, Chile, S.A.
> Johannesburg, South Africa
> Woomera, Australia
> Fort Myers, Fla., U.S.A.
> St. Johns, Newfoundland
> East Grand Forks, Minnesota, U.S.A.
> Winkfield, England

In addition, the South Atlantic and Singapore stations track and record the satellite telemetry.

DATA ACQUISITION

The Ariel I satellite utilized a PFM-PM telemetry system having a power output of 250 milliwatts. A signal-to-noise analysis of the telemetry system had shown that it could be adequately handled by the Minitrack Mod I Telemetry Acquisition System. Performance of the Mod I system with Ariel I has substantiated this investigation.

A block diagram illustrating the acquisition system is shown in Figure 7–1. The following system parameters were utilized:
1. Antenna polarization—linear
2. Dual channel preamplifiers—136.500 Mc
3. Mod I telemetry receivers
   Frequency:
      Receiver A—136.410 Mc
      Receiver B—136.410 Mc
   Inputs:
      Receiver A—output of vertically polarized antenna system
      Receiver B—output of horizontally polarized antenna system
   Operation—AGC mode

61
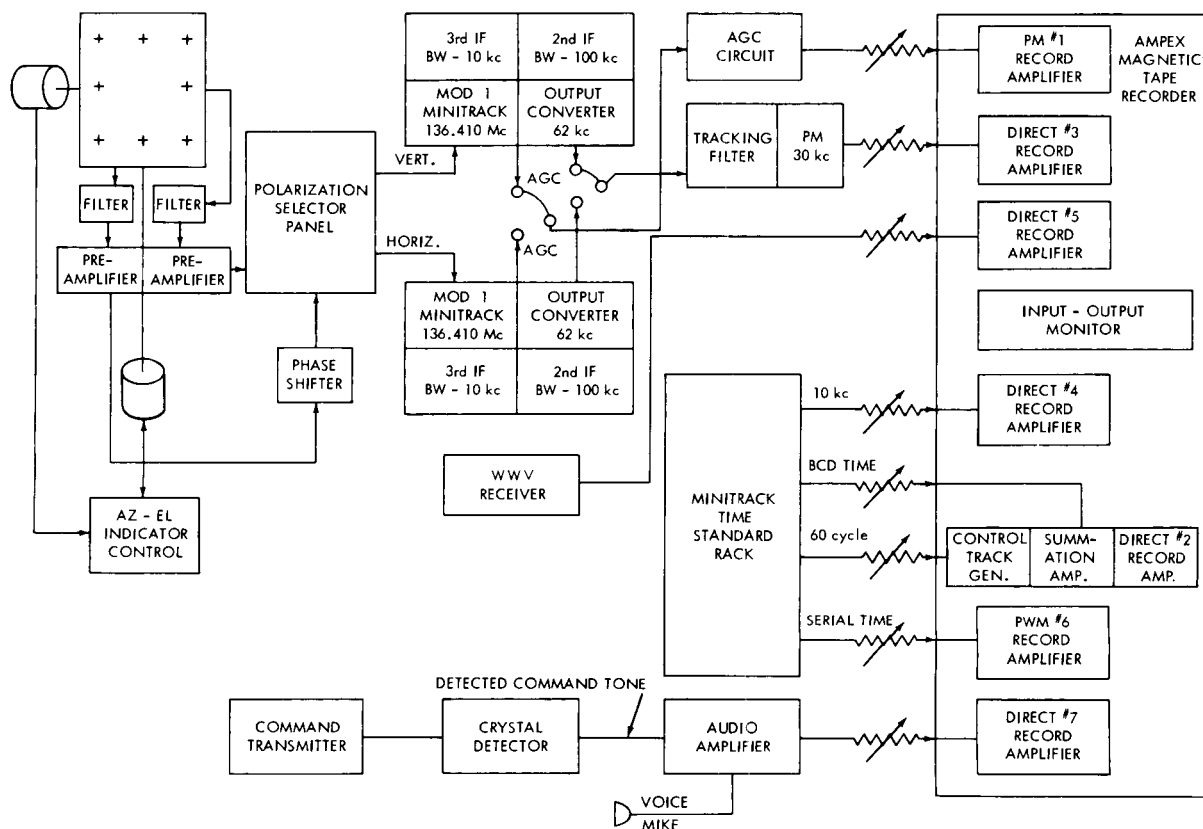
FIGURE 7-1. Data acquisition system.

Bandwidth (2nd IF)—100 kc

Output converter—62-kc center frequency

Output converter oscillator—3.312 Mc, ±20 cps

4. Tracking filter

Input—62-kc output of Mod I receiver having highest signal level

AGC—fast

Phase modulation output—detected

5 to 15 kc

Phase modulation filter—30 kc

Tracking loop bandwidth—Not less than 25 cps

5. Minitrack timing signals

Standard frequency—10 kc

Time—Serial and binary coded time

Precision clock drive—60 cps

6. Magnetic tape recorder track assignments—see table below

Track	Record amplifier	Source	Signal
1	FM	AGC circuit	AGC
2	Direct	Control track generator and data input (Minitrack)	60 cps, 70% AM on 18.24-kc carrier; BCD time
3	Direct	PM output of tracking filter	5 to 15 kc detected signal
4	Direct	Minitrack	10 kc standard
5	Direct	WWV receiver	WWV time
6	PWM	Minitrack	Serial coded time
7	Direct	Audio oscillator	Voice and command time

62

7. Magnetic tape recorder tape speeds
   FR-100—15 in./sec
   FR-600—7½ in./sec

The satellite telemetry acquisition requirements are such that real-time data are required as much as is possible and playback data are required once per orbit. There will be no problem in fulfilling the first of these requirements. The Spacecraft and Network Control Groups will schedule telemetry acquisition periods in accordance with the priority established for the Ariel I spacecraft, and real-time data will be obtained as often as is operationally possible.

The requirement that the satellite tape recorder be played back once per orbit may not be fulfilled 100 percent of the time. This is due primarily to the fact that each day there will be a 4- to 5-hour period during which no contact is available with the satellite. It is anticipated that these quiescent periods will be covered by the South Atlantic station but, since continuous contact with this station is not available, the effectiveness of this station's operation will not be known except on a post-facto basis. Another area of difficulty may be interference with other satellites. All efforts will be made to schedule interrogations on a non-interference basis, but there may be times when interference is unavoidable.

DATA HANDLING

General

Magnetic tapes of Ariel I telemetry data will be supplied the United Kingdom by the NASA Goddard Space Flight Center with the following general characteristics:

1. Two types of tapes will be supplied: high speed data tapes, and low speed data tapes.

2. Tapes will be digital and in standard IBM binary-coded decimal format.

3. Even parity and low density (200 characters/inch) will be used.

4. Each tape will have been checked for time consistency, and inconsistencies will be appropriately flagged on the tape. In addition, a print-out of the number of time inconsistencies and data word dropouts will be supplied with each tape.

5. Each tape will contain a number of files; the first record in each file will be an identification record.

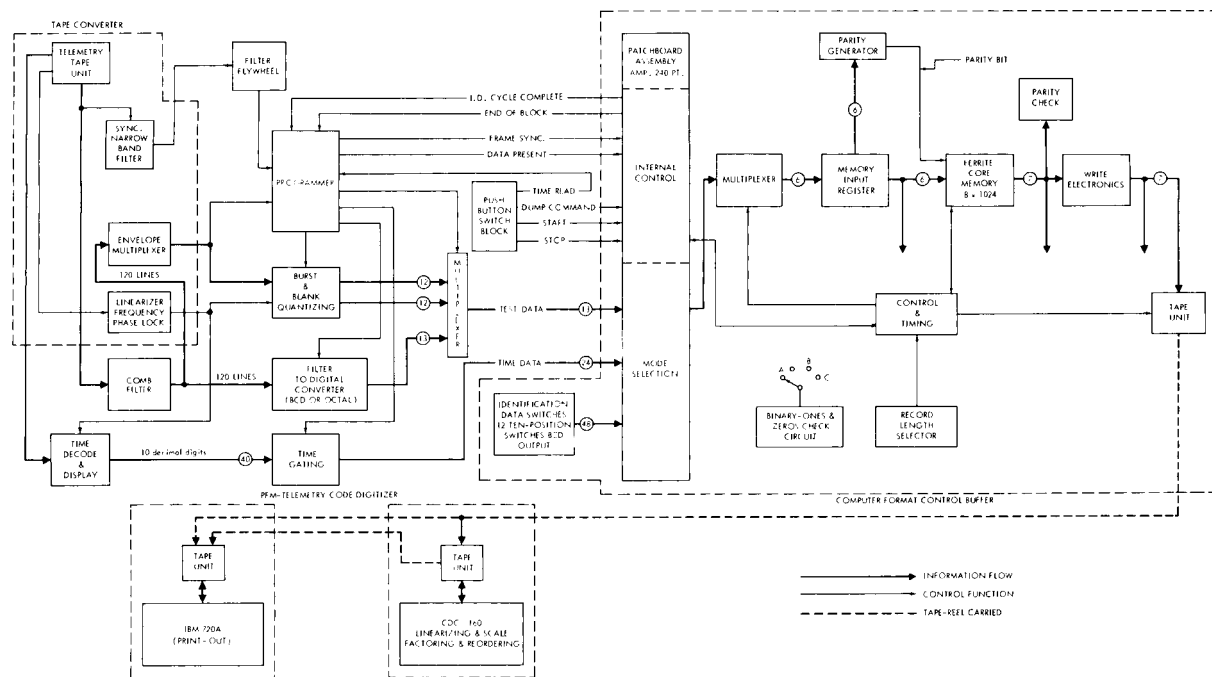The system that will be used for processing the data from Ariel I is shown in Figure 7-2

FIGURE 7-2. PFM-PWM to tape conversion system.

The equipment was designed to handle all telemetry formats of this general category (PFM). The elements of the system are the Tape Converter—Comb Filter, PFM Digitizer—Computer Format Control Buffer, High Speed Line Printer, and CDC-160 Data Processor. The output digital tapes will be used by the GSFC Computer Operations Branch personnel to merge the data with the orbital information in the IBM 7090 computer.

Tape Converter—Comb Filter

This portion of the system is designed to recover the telemetry signal in the presence of noise by utilizing the comb filter for signal-to-noise improvement and to recover the burst rate for use in synchronization. The comb filter has 120 filters equally spaced across the used frequency band with their response curves intersecting at the 3-decibel points. Integral logic permits determination of which filter is responding and allows electronic removal of all other filters. In this way sufficient resolution is obtained to permit the filter to function directly as the frequency measurement device. This design assumes that a single frequency exists in each burst. Some departure from this condition can be tolerated. However, experience on Explorer VIII shows that care must be taken to eliminate, or at least minimize, the switching transient effects on the oscillators in the payload encoder if the signal-to-noise improvement possible with the comb filter is to be utilized. This equipment will also provide a burst-blank envelope as well as a linearizing frequency and time code derived from the original telemetry tape.

PFM Digitizer—Computer Format Control Buffer

This equipment will utilize the outputs of the above equipment in such a manner as to establish synchronization, encode the 120 lines from the comb filter, and multiplex the frequency data with the time code. Time is stored from the time decoder when a frame sync occurs. The output of the Format Control Buffer is a digital magnetic tape in IBM binary-coded decimal format suitable for further processing by computer or off-line printer. The fre-

quency data will appear as a number between 0 and 119 in the case of analog channels, and as a number between 0 and 7 in the case of digitally encoded channels. In the latter case this permits retention of the original bit configuration so that a full digital word can be accumulated visually on print-out or by the computer.

High Speed Line Printer

The digital magnetic tapes prepared on the Format Control Buffer can be printed on this device. A full data print-out in terms of the telemetry and system units with 1 frame per line plus time of the sync pulse will result. Printing of selected sections of the full format can be provided after a simple operation in the off-line data processor.

CDC-160 Data Processor

The CDC-160 Data Processor is a small, transistorized, stored-program digital computer with magnetic tape and control equipment. The output magnetic tapes from the above equipment can be used as an input. Programs are available to decommutate, edit, accumulate, and record the data and provide digital magnetic tapes for further use as required.

DATA PROCESSING

Editing—Quick Look

The station telemetry tapes containing a 100-kilocycle standard frequency, Minitrack time code, telemetry signal, etc. will be received by the GSFC Data Systems Design Branch for editing and storage. Each tape will be reviewed for quality and quantity of usable data and will be checked against expected station performance. A summary of tapes by station will be maintained as a central input for station operation and as a guide for processing. It is anticipated that three categories of tapes will be stored: (1) unusable tapes resulting from inadequate signal-to-noise ratio, interference, or operator error; (2) questionable tapes requiring extra handling to recover the data; and (3) good tapes of sufficient quality to warrant immediate machine processing. The first class of tapes will be retained for archival purposes

Time Inconsistencies and Dropouts

The frame time advance will be checked, flagged if inconsistent, and these flags counted. The dropped-out data words will also be counted. Both counts will be accumulated and printed on a file basis.

1. *Inconsistent frame time advance:* The time of two successive frames will be differenced, and the difference compared to 320 ± 40 milliseconds. If the difference falls outside of this range, an asterisk (*) character will be inserted at the end of the frame. The reference value (320) and the tolerance (± 40) may have to be changed in the case of the recorded data because of tape recorder speed fluctuations.

2. *Dropout count:* When a data word drops out, three dash characters will appear. These characters will be counted and a sum, based on 3 character words, will be accumulated for each file. This sum will be printed, along with the sum of time-interval inconsistency flags.

Special Characters

The following gives the characters other than numerics that will be used:

Purpose	Character	Print	Bit Sequence C B A 8 4 2 1
Data dropout	Dash	—	0 1 0 0 0 0 0
Improper time advance	Asterisk	*	0 1 0 1 1 0 0

Samples of Ariel I data are shown in Figures 7–3 and 7–4.

Satellite No.

S			Year Data Received
'	1	2	Day of Year
5	9	6	Minitrack Station (Blossom Point)
1	6	J	Station Tape No.
	2	u n e	

Identification Label ⟶ 5 1 6 2 1 7 7 0 1 2 3 8

FRAME NO.	Z TIME Day	Z TIME Hr.Min	Z TIME Sec	CHANNEL NO. 1	2	3	4	5	6	7	8	9	10	11	12	13	14	15	16	
13	-07	1918	37.399	031	042	032	105	105	103	105	075	075	071	084	051	105	105	105	700	•
14	-07	1918	37.719	030	200	500	105	105	102	105	074	076	071	084	051	105	103	105	005	•
15	-07	1918	38.039	700	700	700	105	105	103	105	074	076	072	085	051	105	103	105	000	•
0	-07	1918	38.359	500	700	300	105	105	103	104	075	075	070	084	051	105	103	105	005	•
1	-07	1918	38.679	100	500	400	105	104	103	105	074	076	072	084	051	105	103	105	100	•
2	-07	1918	38.999	081	044	105	105	105	103	105	075	075	071	084	050	106	103	105	005	•
3	-07	1918	39.318	071	026	103	105	105	102	104	074	077	071	083	051	105	103	105	200	•
4	-07	1918	39.639	083	087	105	105	103	103	105	075	076	071	084	050	105	103	105	005	•
5	-07	1918	39.958	073	079	032	105	105	103	105	073	076	071	084	051	105	103	105	300	•
6	-07	1918	40.278	030	046	085	105	104	103	105	075	076	071	083	051	105	103	105	005	•
7	-07	1918	40.598	048	047	032	105	105	103	105	075	075	071	085	051	105	103	105	400	•
8	-07	1918	40.918	500	700	300	105	105	103	105	073	076	074	084	051	105	103	105	005	•
9	-07	1918	41.239	100	500	400	105	103	103	105	074	077	072	085	051	105	103	105	500	•
10	-07	1918	41.558	083	044	105	105	105	103	105	074	076	071	085	050	105	103	105	005	•
11	-07	1918	41.878	071	054	103	105	104	103	105	074	077	071	084	051	105	103	105	600	•
12	-07	1918	42.198	085	072	105	105	105	103	105	076	075	071	085	051	105	103	105	005	•
13	-07	1918	42.518	032	043	032	105	105	103	105	075	075	072	083	050	105	103	105	700	•
14	-07	1918	42.838	031	500	300	105	105	103	105	074	076	071	083	050	105	103	105	005	•
15	-07	1918	43.158	700	700	700	105	105	103	105	073	076	071	084	050	105	103	105	000	•
0	-07	1918	43.478	700	700	300	105	104	078	105	074	077	071	084	050	105	081	105	005	•
1	-07	1918	43.798	100	600	400	105	105	083	105	074	077	071	085	051	105	087	105	100	•
2	-07	1918	44.118	086	045	050	094	092	065	101	075	077	071	085	051	105	068	103	005	•
3	-07	1918	44.438	072	081	074	041	093	071	103	075	077	071	085	050	105	075	102	200	•

⋮ ⋮

Signifies playback of low speed recorded data
as a result of a station command.

⋮ ⋮

11	-07	1927	59.885	066	059	074	023	097	031	103	043	076	043	075	047	105	035	103	600	•
12	-07	1928	00.205	048	072	068	023	098	039	103	045	074	044	075	047	105	043	103	005	•
13	-07	1928	00.525	029	043	029	023	097	047	103	051	065	046	076	046	105	051	103	700	•
14	-07	1928	00.844	036	400	700	025	097	054	103	047	---	---	---	---	---	---	---	---	•
15	-07	1928	01.169	---	---	---	---	---	---	---	---	---	---	---	---	---	---	---	---	•
0	-07	1928	01.487	---	---	---	---	---	---	---	---	---	---	---	---	---	---	---	---	•
1	-07	1928	01.805	---	---	---.														
2	-07	1930	20.348	045	045	105	105	104	103	105	043	075	065	085	041	107	103	105	005	•

Indicates a time drop-out.
(Frame 1 to 2)

FIGURE 7–3. Sample of high speed (real-time) digitized data.

Figure 7–4. Sample of low speed digitized data (recorded 1/48*th* of high speed data).

69

REFERENCES

1. Bourdeau, R. E., Donley, J. L., Serbu, G. P., and Whipple, E. C., Jr., "Measurements of Sheath Currents and Equilibrium Potential on the Explorer VIII Satellite," *J. Astronautical Sci.* 8(3):65–73, Fall 1961.

2. Bourdeau, R. E., "Ionospheric Results with Sounding Rockets and the Explorer VIII Satellite," in *Space Research II:Proc. 2nd Internat. Space Sci. Sympos., Florence (Italy), April 1961*, ed. by H. C. van de Hulst, C. de Jager, and A. F. Moore, Amsterdam: North-Holland Publ. Co., 1961, pp. 554–573.

3. Serbu, G. P., Bourdeau, R. E., and Donley, J. L., "Electron Temperature Measurements on the Explorer VIII Satellite," *J. Geophys. Res.* 66(12): 4313–4315, Dec. 1961.

4. Bourdeau, R. E., Whipple, E. C., Jr., Donley, J. L., and Bauer, S. J., "Experimental Evidence for the Presence of Helium Ions Based on Explorer VIII Satellite Data," *J. Geophys. Res.* 67(2):467–475, Feb. 1962.

5. Bourdeau, R. E., and Bauer, S. J., "Structure of the Upper Atmosphere Deduced from Charged Particle Measurements on Rockets and the Explorer VIII Satellite," paper presented at 3rd Internat. Sci. Sympos., Washington, May 1962.

6. Krassovsky, V. I., "Exploration of the Upper Atmosphere with the Help of the Third Soviet Sputnik," *Proc. IRE* 41(2):289–296, Feb. 1959.

7. Pomerantz, M. A., Schwed, P., Hanson, H., and Benjamin, H., "Satellite-Borne Instrumentation for Observing Flux of Heavy Primary Cosmic Radiation," *J. Franklin Inst.* 271(275–291), Apr. 1, 1961.

8. Pomerantz, M. A., Agarwal, S. P., Schwed, P., and Hanson, H., "Satellite Determination of Heavy Primary Cosmic-Ray Spectrum," *Phys. Rev. Letters* 6:7(362), Apr. 1, 1961.

9. Pomerantz, M. A., and Witten, L., "Satellite Investigation of Time Variations of Heavy Nuclei on the Primary Cosmic Radiation," *Proc. Internat. Conf. on Cosmic Rays and the Earth Storm, Kyoto (Japan), September 1961.* II Main Sessions, Tokyo: Physical Society of Japan, 1962.

10. Friedman, H., Lichtman, S. W., and Byram, E. T., "Photon Counter Measurements of Solar X-Rays and Ultra-Violet Light," *Phys. Rev.* 83(5):1025 (1952).

11. Rense, W. A., "Intensity of Lyman-Alpha Line in the Solar Spectrum," *Phys. Rev.* 91(2):299 (1953).

12. Friedman, H., "Solar Radiation," *Astronautics* 7(8):14, Aug. 1962.

13. Cornille, H. J., Jr., "A Method of Accurately Reducing the Spin Rate of a Rotating Spacecraft," NASA TN D-1420, Oct. 1962.

14. Hord, W. H., "General Environmental Test Specification and Test Procedures for Design Qualification & Flight Acceptance Testing of Delta Launched Satellite," NASA/GSFC/TE internal publication, Sept. 1961.

15. Hord, W. H., "Environmental Test Specifications for Design Qualification and Flight Acceptance Tests of the International Satellite," NASA/GSFC/TE internal publication, 6 Dec. 1961.

16. Hord, W. H., "Test Plan—Structural Test ETU #1 S-51 Satellite," NASA/GSFC/TE internal publication, Apr. 1961.

17. Hord, W. H., "Environmental Exposures and Tests for Subassemblies of International Ionosphere Satellite S-51," NASA/GSFC/TE internal publication, Feb. 1961.

ADDITIONAL BIBLIOGRAPHY

DESIGN AND DEVELOPMENT REPORTS

1. Fedor, J. V., "Analytical Theory of the Stretch Yo-Yo for De-Spin of Satellites," NASA Technical Note D-1676, April 1963.
2. Eng, T. L., "Energy Absorber for the Ariel I Instrument Booms," NASA Technical Note D-1857, 1963 (In press).
3. Conn, J. H., and Sutton, J. F., "Report of Environmental Vibration Test—Structural Model No. 1, International Ionosphere Satellite, S-51," Goddard Space Flight Center 321.2(JC) S-51-11, June 1961.
4. Forsythe, R. W., "A Method for Simulating Zero Gravity Erection of Satellite Appendages," NASA Technical Note D-1852, 1963 (In press).
5. Forsythe, R. W., "Analysis of Dissimilar Satellite Appendages During Erection," NASA Technical Note D-1688, 1963 (In press).

PUBLICATION STATUS AS OF FEB. 1, 1963, FOR THE EXPERIMENTAL RESULTS OF MEASUREMENTS MADE BY ARIEL I

1. Pounds, K., and Willmore, A. P., "X-Ray Measurements on the Ariel Satellite," *Proc. of the International Conference on the Ionosphere* (In press July 1962).
2. Willmore, A. P., Boyd, R. L. F., and Bowen, P. J., "Some Preliminary Results of the Plasma Probe Experiments on the Ariel Satellite," *Proc. of the International Conference on the Ionosphere* (In press July 1962).
3. Sayers, J., Rothwell, P., and Wager, J. H., "Evidence for a Further Ionospheric Ledge Above the F_2 Region," Research Note No. 6210, University of Birmingham, August 24, 1962; also published in *Nature Magazine*, Sept. 22, 1962.

APPENDIX A

Physical Measurements of Ariel I

The weights, centers of gravity and moments of inertia are given in the following itemization:

SATELLITE ONLY*

Weight (lb)_____ 135. 82

All components folded:

Center of gravity, forward of separation plane (in.)_____ 5. 961
Moment of inertia (slug-ft²)
I_{xx}_____ 5. 25
I_{zz} (Roll axis)_____ 1. 99
I_{yy}_____ 4. 75

All components extended:

Center of gravity, forward of separation plane (in.)_____ 8. 125
Moment of inertia (slug-ft²)
x-x axis_____ 5. 130
Roll axis_____ 5. 484
y-y axis_____ 4. 030

FOLDED ARIEL I PAYLOAD†

Weight (lb)
Orbiting satellite_____ 133. 8
De-spin weights_____ 2. 0
Separation and release system (with tiedowns)_____ 21. 3
Dutchman and vibration experiment ‡_____ 20. 6
TOTAL payload weight not furnished by Delta vehicle_____ 177. 7
Center of gravity, forward of separation plane (in.)_____ 1. 42

Moment of inertia (slug-ft²)
Pitch axis_____ 9. 277
Roll axis_____ 2. 610

SEPARATION UNIT AND DUTCHMAN†

Weight (lb)_____ 35. 56
Center of gravity, aft of separation plane (in.)_____ 8. 53
Moment of inertia (slug-ft²)
Pitch axis_____ 0. 294
Roll axis_____ 0. 451

ANTENNAS AND HARNESS (VIBRATION EXPERIMENT)†

Weight (lb)_____ 3. 58
Center of gravity, aft of separation plane (in.)_____ 44. 94
Moment of inertia (slug-ft²)
Pitch axis_____ 0. 0705
Roll axis_____ 0. 0831

TIE DOWNS†

Weight (lb)_____ 2. 66
Center of gravity, aft of separation plane (in.)_____ 32. 30
Moment of inertia (slug-ft²)
Pitch axis_____ 0. 016
Roll axis_____ 0. 080

---

* Refer to Figures A1 and A2.
† Refer to Figure A3.
‡ Includes U.K.-designed contamination experiment and solar aspect sensor, and telemetering antennas.
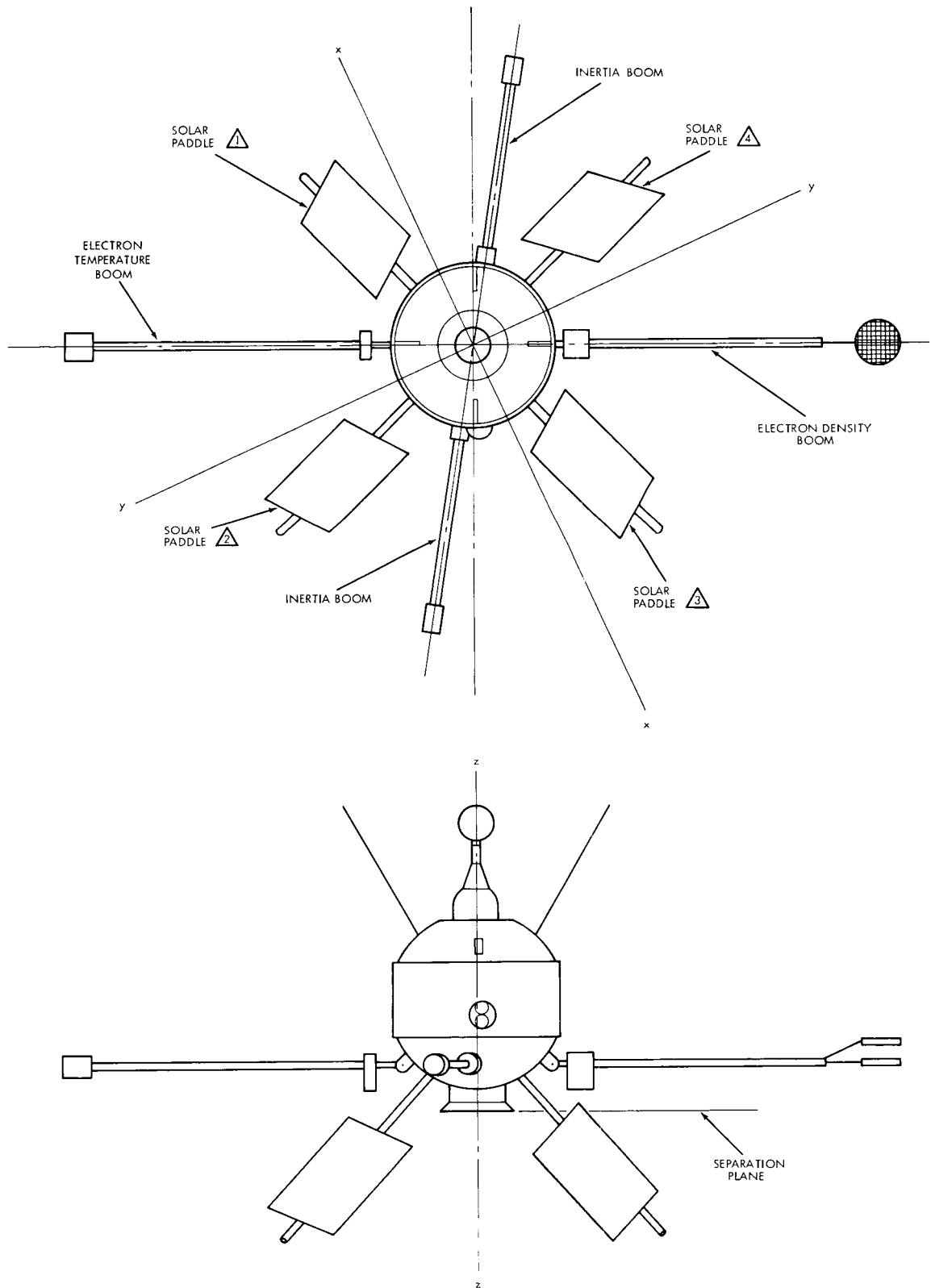
FIGURE A1. Payload axes.

74
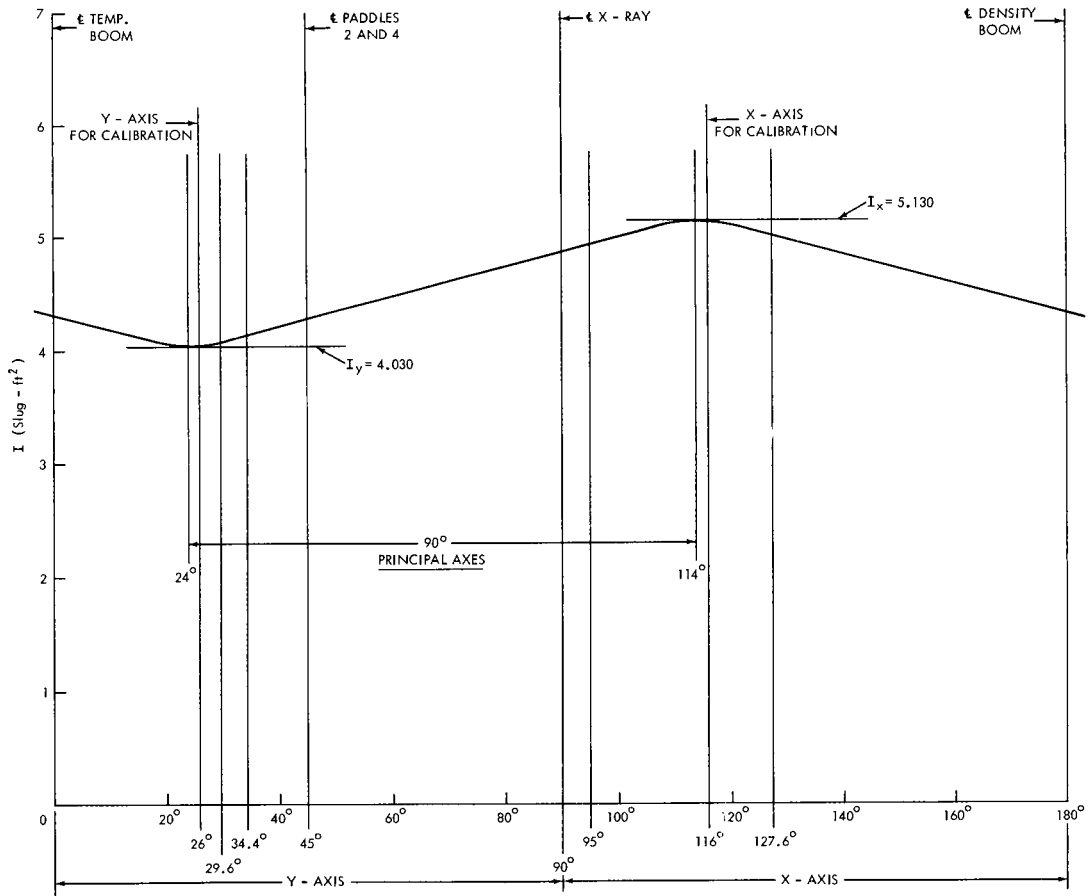
FIGURE A2. Principal moments of inertia vs. payload axes, all components extended.
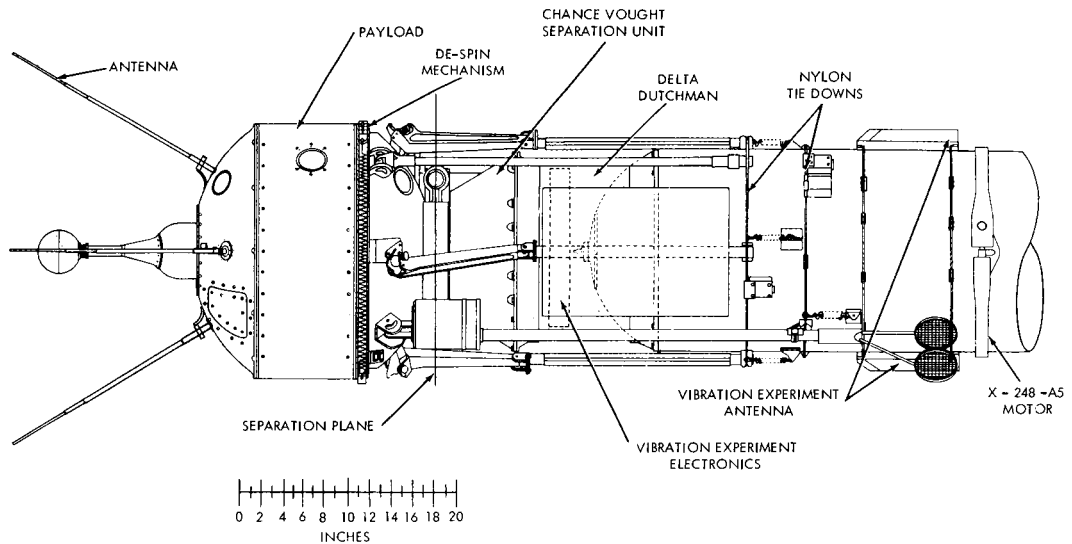
FIGURE A3. Ariel I nomenclature diagram.

TABLE A1
Detailed Weight Breakdown of Ariel I

Item	Remarks	Weight (lb)	Item	Remarks	Weight (lb)
Upper dome	Includes thermal and RF coating	6. 53	University College London Experiments—Continued		
Mid-skin	Includes thermal and RF coating	6. 80	UCL electronics container 2	Includes 10 U.K. cards	6. 76
Lower dome	Includes thermal grating only	1. 52	Imperial College Experiment		
Shelf and base assembly	Shelf, struts, base, fasteners	12. 63			
Paddle arms and hinges (4)	Includes interface fasteners	4. 36	Cosmic ray analyzer	Includes electronics	5. 70
Inertia booms and hinges (2)	Includes interface fasteners	3. 85	University of Birmingham Experiment		
Experiment boom hinges	Includes interface fasteners	0. 87			
Escapement assembly	Includes nylon guides	1. 54	Electron density boom	----------------	5. 50
De-spin housing	Includes guillotines	1. 76	Electronics container	----------------	2. 79
De-spin weights, Spring antennas (4)	Excluded from orbit weight	2. 00 / 0. 80	GSFC Non-Structure Components		
Separation ring adapter	Includes interface fasteners	0. 51	Tape recorder	----------------	3. 66
Battery containers	Includes spacers	3. 05	Tape recorder dc control	----------------	0. 39
Dynamic balance	----------------	1. 93	Encoder card UCL no. 1	In UCL container 1	0. 49
Tape recorder and electron temperature supports	----------------	1. 07	Encoder card UCL no. 2	In UCL container 2	0. 56
			Cosmic ray encoder card	Including container	0. 96
Turn-on plug and housing	----------------	0. 14	Electronic pack A	2 encoder cards, encoder clock 2 converter cards, lid	5. 87
Harness bracketry	Includes clamps fasteners	1. 34	Electronic pack B	2 programmer, 2 converter, 1 undervoltage detector, transmitter, and command receiver cards, lid	6. 93
Component bracketry	Non-structure components	0. 91			
Internal thermal equalization	Coatings and heat sinks	0. 97			
University College London Experiments					
			Battery selector	----------------	0. 50
Lyman-alpha detectors (3)	----------------	1. 62	1-Year timers (2)	----------------	0. 72
X-ray counters (2)	----------------	0. 64	Solar paddles (4)	Including spars	8. 78
Solar aspect sensor	----------------	0. 43	Battery packs (2)	Including potting	12. 08
Ion mass spectrometer	Includes 4-inch extension tube	0. 54	Solar shunt regulator	----------------	0. 24
Electron temperature sensor	----------------	0. 37	Harness network	Top dome, main assemble below shelf assembly	6. 54
Electron temperature boom	Includes balance weights	5. 50			
UCL electronics container 1	Includes 4 U.K. cards	5. 67	TOTAL ARIEL I WEIGHT_____		135. 82